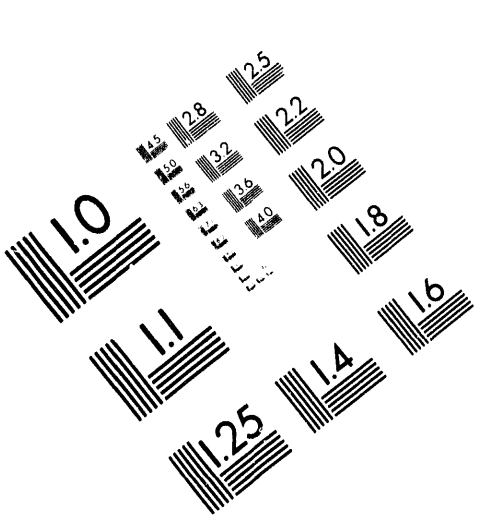

Association for Information and Image Management

1100 Wayne Avenue, Suite 1100
Silver Spring, Maryland 20910

301/587-8202

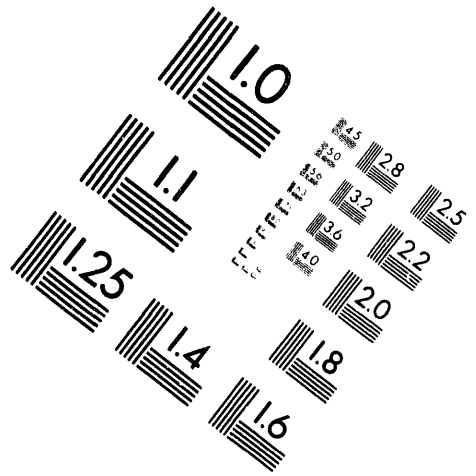

Centimeter

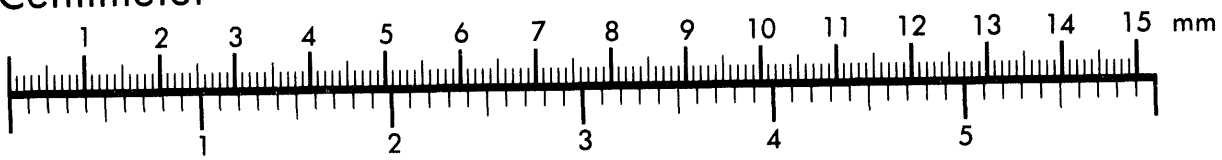

Inches

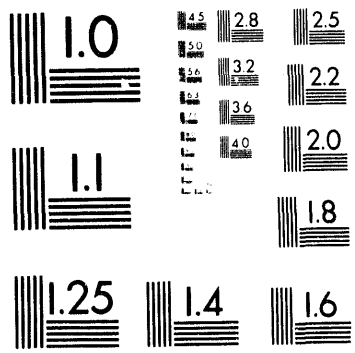

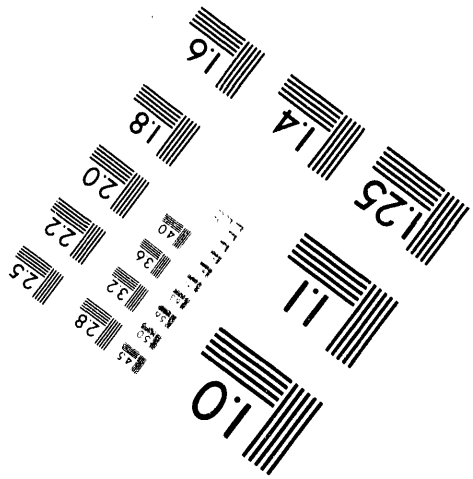

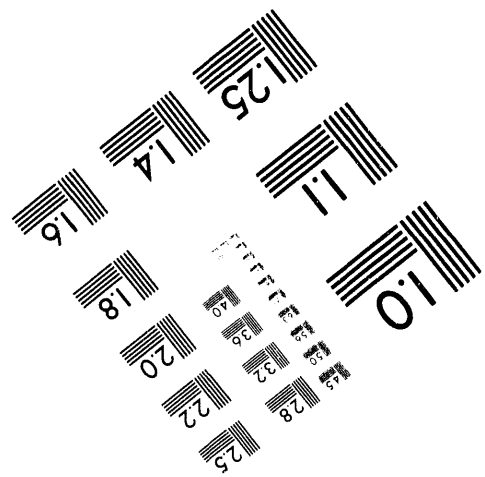

MANUFACTURED TO AIIM STANDARDS
BY APPLIED IMAGE, INC.

1 of 2

SAND91-1208
Unlimited Release
Printed August 1994

Distribution
Category UC-523

TEST RESULTS ON DIRECT CONTAINMENT HEATING BY HIGH-PRESSURE MELT EJECTION INTO THE SURTSEY VESSEL: THE TDS TEST SERIES

Michael D. Allen
Thomas K. Blanchat
Martin M. Pilch

Severe Accident Phenomenology
Sandia National Laboratories
Albuquerque, NM 87185

ABSTRACT

The Technology Development and Scoping (TDS) test series was conducted to test and develop instrumentation and procedures for performing steam-driven, high-pressure melt ejection (HPME) experiments at the Surtsey Test Facility to investigate direct containment heating (DCH). Seven experiments, designated TDS-1 through TDS-7, were performed in this test series. These experiments were conducted using similar initial conditions; the primary variable was the initial pressure in the Surtsey vessel. All experiments in this test series were performed with a steam driving gas pressure of $\simeq 4$ MPa, 80 kg of alumina/iron/chromium thermite melt simulant, an initial hole diameter of 4.8 cm (which ablated to a final hole diameter of $\simeq 6$ cm), and a $1/10^{th}$ linear scale model of the Surry reactor cavity. The Surtsey vessel was purged with argon (<0.25 mol.% O_2) to limit the recombination of hydrogen and oxygen, and gas grab samples were taken to measure the amount of hydrogen produced.

ACKNOWLEDGMENTS

The authors express their gratitude to Robert T. Nichols, who was the test director for this test series, to Michael Oliver, who was the electronics and instrumentation engineer, and to James Ross and Tim Covert, who were the mechanical technicians. The authors appreciate the technical review of this report provided by Dr. David C. Williams and Christine M. Erickson.

This work was funded by the Accident Evaluation Branch of the United States Nuclear Regulatory Commission.

TABLE OF CONTENTS

Section		Page
1.0	INTRODUCTION	1
2.0	EXPERIMENT DESCRIPTION	1
2.1	Experiment Apparatus	1
2.1.1	Boiler	2
2.1.2	Steam Accumulator Tank	2
2.1.3	Burst Diaphragm	2
2.1.4	Melt Generator	3
2.1.5	Cavity	3
2.2	Instrumentation	3
2.2.1	Pressure Measurements	3
2.2.2	Temperature Measurements	4
2.2.3	Gas Analyses	5
2.2.4	Posttest Debris Recovery	5
2.2.5	Debris Velocity Measurements	5
2.2.6	Data Acquisition System	6
2.3	Initial Conditions	6
2.4	Pressurization Sequence	8
3.0	EXPERIMENTAL RESULTS	8
3.1	Pressure Results	10
3.2	Temperature Results	12
3.3	Gas Analyses	13
3.4	Debris Characterization	13
3.5	Debris Velocity Measurements	14
4.0	SUMMARY OF RESULTS	14
5.0	REFERENCES	107

LIST OF TABLES

Table		Page
1.	TDS Instrumentation Location and Purpose	16
2.	Initial Conditions for the TDS Experiments	19
3.	Gas Measurements for the TDS Experiments	20
4.	Debris Dispersal Summary for the TDS Experiments	21
5.	Summary of the Results for the TDS Experiments	22

LIST OF FIGURES

Figure		Page
1.	Schematic diagram of the Surtsey vessel showing the experimental apparatus used to produce a HPME	23
2.	Schematic diagram of the experimental apparatus used to produce a HPME into the Surtsey vessel	24
3.	Exploded view of the burst diaphragm assembly used in the TDS test	25
4.	Cross-sectional view of the burst diaphragm assembly used in the TDS tests	26
5.	Side view of the 1:10 linear scale model of the Surry reactor cavity used in the TDS tests	27
6.	Exploded view of the 1:10 linear scale model of the Surry reactor cavity used in the TDS tests	28
7.	Pyrometer locations in TDS-1 through TDS-6	29
8.	Pyrometer locations in TDS-7	30
9.	Locations of photodiodes and breakwires with respect to the Surry cavity model in the TDS tests	31
10.	Blowdown history of the TDS-1 experiment	32
11.	Blowdown history of the TDS-2 experiment	33
12.	Blowdown history of the TDS-3 experiment	34
13.	Blowdown history of the TDS-4 experiment	35
14.	Blowdown history of the TDS-5 experiment	36
15.	Blowdown history of the TDS-6 experiment	37
16.	Blowdown history of the TDS-7 experiment	38
17.	Steam blowdown time for the TDS-1 experiment	39

LIST OF FIGURES (continued)

Figure		Page
18.	Steam blowdown time for the TDS-2 experiment	40
19.	Steam blowdown time for the TDS-3 experiment	41
20.	Steam blowdown time for the TDS-4 experiment	42
21.	Steam blowdown time for the TDS-5 experiment	43
22.	Steam blowdown time for the TDS-6 experiment	44
23.	Steam blowdown time for the TDS-7 experiment	45
24.	Steam temperatures measured in the steam accumulator tank with type-K thermocouples in the TDS-1 experiment	46
25.	Steam temperatures measured in the steam accumulator tank with type-K thermocouples in the TDS-2 experiment	47
26.	Steam temperatures measured in the steam accumulator tank with type-K thermocouples in the TDS-3 experiment	48
27.	Steam temperatures measured in the steam accumulator tank with type-K thermocouples in the TDS-4 experiment	49
28.	Steam temperatures measured in the steam accumulator tank with type-K thermocouples in the TDS-5 experiment	50
29.	Steam temperatures measured in the steam accumulator tank with type-K thermocouples in the TDS-6 experiment	51
30.	Steam temperatures measured in the steam accumulator tank with type-K thermocouples in the TDS-7 experiment	52
31.	Surtsey vessel pressure versus time measured at level 1 in the TDS-1 experiment	53
32.	Surtsey vessel pressure versus time measured at level 3 in the TDS-1 experiment	54

LIST OF FIGURES (continued)

Figure		Page
33.	Surtsey vessel pressure versus time measured at level 5 in the TDS-1 experiment	55
34.	Surtsey vessel pressure versus time measured at level 1 in the TDS-2 experiment	56
35.	Surtsey vessel pressure versus time measured at level 3 in the TDS-2 experiment	57
36.	Surtsey vessel pressure versus time measured at level 5 in the TDS-2 experiment	58
37.	Surtsey vessel pressure versus time measured at level 1 in the TDS-3 experiment	59
38.	Surtsey vessel pressure versus time measured at level 3 in the TDS-3 experiment	60
39.	Surtsey vessel pressure versus time measured at level 5 in the TDS-3 experiment	61
40.	Surtsey vessel pressure versus time measured at level 1 in the TDS-4 experiment	62
41.	Surtsey vessel pressure versus time measured at level 3 in the TDS-4 experiment	63
42.	Surtsey vessel pressure versus time measured at level 5 in the TDS-4 experiment	64
43.	Surtsey vessel pressure versus time measured at level 1 in the TDS-5 experiment	65
44.	Surtsey vessel pressure versus time measured at level 3 in the TDS-5 experiment	66
45.	Surtsey vessel pressure versus time measured at level 5 in the TDS-5 experiment	67

LIST OF FIGURES (continued)

Figure		Page
46.	Surtsey vessel pressure versus time measured at level 1 in the TDS-6 experiment	68
47.	Surtsey vessel pressure versus time measured at level 3 in the TDS-6 experiment	69
48.	Surtsey vessel pressure versus time measured at level 5 in the TDS-6 experiment	70
49.	Surtsey vessel pressure versus time measured at level 1 in the TDS-7 experiment	71
50.	Surtsey vessel pressure versus time measured at level 3 in the TDS-7 experiment	72
51.	Surtsey vessel pressure versus time measured at level 5 in the TDS-7 experiment	73
52.	Comparison of the Surtsey vessel pressures measured in TDS-1 and TDS-2	74
53.	Comparison of the Surtsey vessel pressures measured in TDS-3 and TDS-5	75
54.	Comparison of the Surtsey vessel pressures measured in TDS-6 and TDS-7	76
55.	Comparison of the Surtsey vessel pressures measured in the TDS tests having an initial vessel pressure of 0.156 MPa	77
56.	Cavity pressure and Surtsey vessel pressure versus time for the TDS-1 experiment	78
57.	Cavity pressure and Surtsey vessel pressure versus time for the TDS-2 experiment	79
58.	Cavity pressure and Surtsey vessel pressure versus time for the TDS-3 experiment	80
59.	Cavity pressure and Surtsey vessel pressure versus time for the TDS-4 experiment	81

LIST OF FIGURES (continued)

Figure		Page
60.	Cavity pressure and Surtsey vessel pressure versus time for the TDS-5 experiment	82
61.	Cavity pressure and Surtsey vessel pressure versus time for the TDS-6 experiment	83
62.	Cavity pressure and Surtsey vessel pressure versus time for the TDS-7 experiment	84
63.	Gas temperatures measured in Surtsey with aspirated thermocouples in the TDS-1 experiment	85
64.	Gas temperatures measured in Surtsey with aspirated thermocouples in the TDS-2 experiment	86
65.	Gas temperatures measured in Surtsey with aspirated thermocouples in the TDS-3 experiment	87
66.	Gas temperatures measured in Surtsey with aspirated thermocouples in the TDS-4 experiment	88
67.	Gas temperatures measured in Surtsey with aspirated thermocouples in the TDS-5 experiment	89
68.	Gas temperatures measured in Surtsey with aspirated thermocouples in the TDS-6 experiment	90
69.	Gas temperatures measured in Surtsey with aspirated thermocouples in the TDS-7 experiment	91
70.	Debris temperature at the chute exit measured with a type 11x20 optical pyrometer in the TDS-1 experiment	92
71.	Debris temperature at the chute exit measured with a two-color pyrometer in the TDS-1 experiment	93
72.	Debris temperature at the chute exit measured with a type 11x20 optical pyrometer in the TDS-2 experiment	94

LIST OF FIGURES (continued)

Figure		Page
73.	Debris temperature at the chute exit measured with a two-color pyrometer in the TDS-2 experiment	95
74.	Debris temperature at the chute exit measured with a type 11x20 optical pyrometer in the TDS-3 experiment	96
75.	Debris temperature at the chute exit measured with a type 11x20 optical pyrometer in the TDS-4 experiment	97
76.	Debris temperature at the chute exit measured with a type 11x20 optical pyrometer in the TDS-5 experiment	98
77.	Debris temperature at the chute exit measured with a two-color pyrometer in the TDS-5 experiment	99
78.	Debris temperature at the chute exit measured with a type 11x20 optical pyrometer in the TDS-6 experiment	100
79.	Debris temperature at the chute exit measured with a type 11x20 optical pyrometer in the TDS-7 experiment	101
80.	Debris temperature at the chute exit measured with a two-color pyrometer in the TDS-7 experiment	102
81.	Debris temperature at the chute exit measured with a type 11x30 optical pyrometer in the TDS-7 experiment	103
82.	Posttest sieve analysis of debris recovered from the bottom head of the Surtsey vessel in the TDS experiments	104
83.	Comparison of the sieve mass median diameter for debris recovered from the bottom head of the Surtsey vessel in the TDS experiments	105
84.	Breakwire signals used to measure debris velocity in the TDS-7 test	106

1.0 INTRODUCTION

In a pressurized water reactor (PWR) core-melt accident the bottom head of the reactor pressure vessel (RPV) may fail while the primary system is pressurized. The blowdown of the reactor coolant system (RCS) may then entrain molten core debris in high-velocity steam and eject fragmented particles from the cavity into the reactor containment building (RCB). This sequence of events is called a high-pressure melt ejection (HPME). Three mechanisms may cause a rapid increase in the pressure and temperature of the RCB: (1) efficient debris-to-gas heat transfer, (2) exothermic metal/oxygen and metal/steam reactions, and (3) hydrogen combustion. These processes are collectively referred to as direct containment heating (DCH). Understanding factors that enhance or mitigate DCH is necessary because the load imposed on the RCB may threaten its integrity.

Scaled experiments that simulate hypothetical HPME accidents in a nuclear power plant (NPP) are performed at the Surtsey Test Facility at Sandia National Laboratories (SNL) for the U.S. Nuclear Regulatory Commission. These experiments investigate the phenomena associated with DCH. High-temperature, chemically reactive melt is ejected by high-pressure steam into a 1:10 linear scale model of a reactor cavity. Debris is entrained by the steam blowdown into the Surtsey vessel, where specific DCH phenomena can be studied.

This report describes the Technology Development and Scoping (TDS) test series. There were seven experiments performed in this test series, designated TDS-1 through TDS-7. Parameters common to all the TDS tests were: (1) the melt simulant was 80 kg of alumina/iron/chromium thermite; (2) steam at about 4 MPa was used as the blowdown gas; (3) the atmosphere of the Surtsey vessel was inerted with argon in order to allow measurement of hydrogen production from steam/metal reactions during the entrainment phase. The melt simulant was ejected into a 1:10 linear scale model of the Surry reactor cavity and was dispersed upward into the open Surtsey vessel so that the first surface encountered by most of the material was the upper head of the Surtsey vessel. The primary parameter varied in the TDS tests was the initial pressure in the Surtsey vessel. Three initial absolute pressures were used: (1) 0.08 MPa in TDS-3 and TDS-5, (2) 0.16 MPa in TDS-1, TDS-2, TDS-6, and TDS-7, and (3) 0.23 MPa in TDS-4.

2.0 EXPERIMENT DESCRIPTION

A schematic diagram of the Surtsey vessel showing the experimental apparatus used in the TDS tests is shown in Figure 1. All of the tables and figures in this report are at the end of the text. The circled numbers in the figures that show the experimental apparatus indicate the locations of the instrumentation and correspond to the list of instrumentation in Table 1.

2.1 Experimental Apparatus

Figure 2 shows a larger schematic diagram of the experimental apparatus used in the TDS tests. This apparatus is similar to the one used in the HIPS-10S experiment [Allen et al. 1990]. The basic components of the system were the boiler, which supplied superheated steam to the steam accumulator tank; the burst diaphragm, which acted as a fast opening valve that separated the steam and thermite until a few seconds prior to the melt ejection; the melt generator, which

housed a steel-lined MgO crucible that contained the melt simulant; and a 1:10 linear scale model of the Surry reactor cavity without scale models of the instrument guide tubes. A more complete description of each of the components is given below.

2.1.1 Boiler

Superheated steam was supplied to the steam accumulator tank using a 75 kW self-contained electric boiler (Hydro Steam Industries, Springfield, VA, model number STR 1638). It is capable of producing 91 kg of steam per hour at 7.8 MPa. The steam pressure in the boiler was regulated by a proportional controller to within 0.3 MPa of the set point pressure.

2.1.2 Steam Accumulator Tank

The steam accumulator tank was a 2-m-long, schedule 140 pipe section fitted with blind flanges on both ends so that it had an internal volume of 0.267 m^3. The total interior volume of the steam accumulation system, including the 10-cm-diameter pipe to the burst diaphragm, was 0.29 m^3. This volume is approximately 1:10 linear scale of the reactor coolant system (RCS) in most PWRs. It is slightly overscaled compared to the RCS volume in the Surry plant, which is 275.3 m^3 including the pressurizer volume.

The steam accumulator tank was heated around its circumference with six 3-kW band heaters. Each flange at the end of the accumulator was heated with eight 1.2-kW calrod heaters. The entire accumulator was wrapped with fiberfrax insulation. The heaters were used to maintain the interior walls of the accumulator at temperatures greater than the saturation temperature of steam at 4.1 MPa (T_{sat} = 524 K). This prevented condensation of steam on the interior walls of the accumulator tank.

There were vent valves located on the accumulator tank and the 10-cm-diameter pipe (Figure 2). These valves were initially open so that steam could be flowed through the accumulator and 10-cm-diameter pipe to purge them of air prior to each experiment. This purging process minimized air contamination in the steam driving gas. The vent valves were closed to pressurize the steam accumulator tank.

2.1.3 Burst Diaphragm

An exploded view and a cross-sectional view of the burst diaphragm (Fike Metal Products, Blue Springs, MO) are shown in Figures 3 and 4, respectively. The complete double disk holder assembly consists of two rupture disks installed in a permanent holder made of three separate components: the base, midflange, and holddown (Figure 3). The burst diaphragm was designed for ease of installation and maintenance, with preassembly and leak testing of the unit on a workbench before insertion between companion flanges (Figure 4). The burst diaphragm was designed to rupture when the differential pressure across the diaphragms exceeded 2.68 MPa at 583 K. The pressure in the space between the rupture disks was continuously monitored with a model XTM-190 Kulite pressure transducer, and the output was continuously displayed in the experiment control room.

2.1.4 Melt Generator

The melt generator, shown in Figure 5, housed a crucible that contained the thermite melt simulant. The inner liner of the crucible was made from 14 gauge mild steel rolled to an inner diameter of approximately 25.9 cm. This was placed inside a nominal 30.5-cm diameter schedule 20 pipe section that was 76.2 cm long. The annulus between the outer pipe section and the inner liner was filled with a wet (5% H_2O) ram MgO insulating material. The end of the cylinder was closed by welding a 5.1-cm thick steel plate to the outer shell. The bottom plate was tapped and fitted with a 4.8-cm fusible brass plug. Melt ejection occurred when the thermite melted through this plug. A hole was drilled and tapped in the side of the crucible at 66 cm from the top. A type-K thermocouple was inserted through this hole into the thermite and was fixed in place using a standard bored-through Swagelok fitting. A signal from this thermocouple was used to fail the burst diaphragms, which brought steam into contact with molten thermite in the melt generator.

2.1.5 Cavity

A side view of the 1:10 linear scale model of the Surry reactor cavity is shown in Figure 5. There was a 0.81-m long transition piece that attached the model of the reactor cavity to the Surtsey vessel. The transition piece was constructed of steel with the inner walls lined with concrete. Steel I-beams were welded around the perimeter to reinforce the transition piece.

Figure 6 shows an exploded view of the Surry cavity model with dimensions. The model was constructed of reinforced steel with concrete inner walls. The floor was lined with a 1.9-cm thick steel plate. There was a 45.7-cm-diameter pipe section with 1.4-cm-thick walls with an archway cut into it that simulated the reactor pressure vessel (RPV) support skirt. The ceiling of the cavity was steel. The walls of the simulated in-core instrument tunnel and cofferdam exit were concrete. Simulated in-core instrument guide tubes were not used in the TDS test series.

The side of the cavity had nine tapped ports for instrumentation (Figure 6). In the TDS experiments one port was used for a pressure transducer and another port was used to purge the cavity with argon prior to the experiment.

2.2 Instrumentation

Table 1 is a list of the instrumentation used in the TDS experiments. This table gives the channel number from the data acquisition system (Section 2.2.6), location, and purpose of each device. In addition, the locations of most of the instruments are shown in the schematic diagrams of the experimental setup, i.e., Figures 1 and 2.

2.2.1 Pressure Measurements

The instruments that measured pressures in the accumulator tank (channels 31 and 32), between the rupture disks of the burst diaphragm (channel 33), and in the crucible (channels 34 and 35) were Kulite model XTM-190 pressure transducers (Kulite Semiconductor Products Inc., Ridgefield, NJ). The pressure in the cavity (channel 36) was measured with a Precise Sensor model 141-1 pressure transducer (Precise Sensors, Monrovia, CA). This device was a metal

diaphragm strain gauge-type transducer with a range of 0 to 1.4 MPa. The pressure transducers were factory calibrated by the manufacturer and are recalibrated at regular intervals against standards traceable to the National Institute of Standards and Technology (NIST) by the Sandia Calibrations Laboratory. The data acquisition system records data from the pressure transducers at a rate of 1400 data points per second during the HPME transient.

2.2.2 Temperature Measurements

Temperatures in the TDS tests were measured with type-K thermocouples. The location and purpose of each of these thermocouples are given in Table 1. The locations of these thermocouples are also shown in the schematic diagram of the experimental apparatus in Figure 2. These thermocouples are calibrated at regular intervals against NIST traceable standards by the Sandia Calibrations Laboratory.

Three aspirated thermocouple assemblies measured gas temperatures in the Surtsey vessel following the HPME transient. An aspirated thermocouple assembly consisted of three bare, type-K thermocouples mounted in an anodized aluminum tube. These assemblies were installed through instrumentation ports at levels 1, 3, and 5 (Figure 1). Each tube had a remotely actuated, solenoid-operated valve that was opened immediately after the HPME transient before the vessel pressure started to rise. Opening the solenoid valve caused hot gas in the vessel to flow through the tube containing the thermocouples. This configuration allowed the tubes surrounding the thermocouples to shield the bare junctions from direct radiant heat.

In TDS-1 through TDS-6, two pyrometers were used to measure the temperature of the ejected debris. A two-color pyrometer (Modline R Series, Model Number R-35C10, Ircon Inc., Stokie, IL) and an optical pyrometer (Series 1100, Type 11x20, Ircon Inc., Stokie, IL) were focused at the instrument tunnel chute exit inside the Surtsey vessel. The exact locations of these pyrometers with respect to the chute exit are shown in Figure 7. The two-color pyrometer had a temperature range of 1773 to 3773 K and a calibrated accuracy of 1% of the full-scale temperature; the response time of the two-color pyrometer was 0.1 s at the sensing head. The response time of the Ircon Series 1100 pyrometer was 1.5 ms to 95% of the full range; it was capable of measuring temperatures between 1973 and 3073 K with a specified accuracy of 1% of the full-scale temperature. In a transient event such as a HPME experiment, the pyrometer accuracy is expected to be no better than ± 50 K. These pyrometers were factory calibrated and were also recalibrated by the Sandia Calibrations Laboratory. Data points from the thermocouples and the pyrometers were recorded by the data acquisition system at a rate of 10 per second prior to thermite ignition, and then just prior to thermite ignition the data acquisition system was switched to the fast mode, in which data points were recorded at a rate of 1400 per second.

In TDS-7, three pyrometers were used to measure the temperature of the debris ejected from the cavity. In addition to the two used in the earlier test, another optical pyrometer (Series 1100, Type 11x30, Ircon, Inc., Stokie, IL) was used. The exact locations of these pyrometers with respect to the chute exit are shown in Figure 8.

2.2.3 Gas Analyses

The Surtsey vessel was inerted with argon (>99 mol.% Ar) in the TDS test series to prevent metal/oxygen reactions and to preserve the hydrogen produced by metal/steam reactions. Seven pre-evacuated 500-cm^3 gas grab samples were drawn from the vessel: a background sample at level 4 (Figure 1) just prior to ignition of the thermite; three 10-s gas grab samples at levels 2, 4, and 6 were taken at 2 minutes after the HPME; and three 10-s gas grab samples at levels 2, 4, and 6 were taken approximately 30 minutes after the HPME.

For the 10-s gas grab samples, the pressure in the sample bottles became positive with respect to ambient pressure and almost equal to the pressure in the vessel; thus, any leakage would have been out of the bottle. Had leakage into the bottle occurred, high nitrogen concentrations would have appeared in the gas sample. The gas samples were analyzed using gas mass spectroscopy by Battelle, Pacific Northwest Laboratory in Richland, WA. Results of the analyses from the TDS test series and premixed blind samples have demonstrated excellent accuracy, reliability, and reproducibility.

2.2.4 Posttest Debris Recovery

After each experiment, debris was manually recovered so that the total mass dispersed into the Surtsey vessel and the fraction at specific locations could be determined. The following measurements were made: (1) mass that adhered to the upper head of the Surtsey vessel, (2) mass that adhered to the walls of the Surtsey vessel, (3) mass on the lower head of the Surtsey vessel, (4) mass in the vertical chute between the incore instrument tunnel and the Surtsey vessel, and (5) mass recovered from the cavity and the incore instrument tunnel. With the long cylindrical melt generator used in the TDS tests, as opposed to the hemispherical design used in the later experiments [Allen et al. 1992c-h; Allen et al. 1993; Allen et al. 1994; Blanchat et al. 1994], virtually all of the thermite was ejected from the melt generator into the cavity. A posttest sieve analysis of debris recovered from the bottom head of Surtsey was performed to determine the sieve mass median particle diameter and geometric standard deviation. A standard set of 35 sieves was used with openings between 9.5 mm and 0.038 mm.

2.2.5 Debris Velocity Measurements

Photodiodes were used at the locations shown in Figure 9 (channels 1 through 8) in TDS-3 through TDS-7 to measure the debris velocity. The photodiodes were collimated and were focused horizontally across the Surtsey vessel to signal luminous debris moving upward in the vessel. Though this system worked when tested with a bright light moving upward in the vessel, it did not accurately measure debris velocity in any of the TDS tests.

Since the photodiode array was unsuccessful at measuring debris velocities, an array of breakwires (channels 11 through 16 in Figure 9) were placed horizontally across the center of the Surtsey vessel at six levels. When the debris front severed a breakwire, the data acquisition system recorded a timing signal. In HPME experiments, low momentum debris tends to be pushed out of the cavity during the single phase ejection before steam blowthrough; this debris sometimes failed the breakwires low in the vessel and thus gave erroneous signals. The signals

from the breakwires higher in the vessel were uniform and gave consistent debris velocity measurements.

2.2.6 Data Acquisition System

The data acquisition system is based on a Hewlett Packard model 1000 series A-600 minicomputer. Four analog-to-digital converters are located within the chassis of the computer with each converter multiplexing 40 analog channels; thus, this system has the capability to record 160 analog data channels. In each TDS experiment, 10 data points per second were sampled prior to thermite ignition. At thermite ignition, the data acquisition system was switched into the fast data acquisition mode so that 1400 data points per second were sampled during the HPME transient.

2.3 Initial Conditions

The initial conditions for the TDS experiments are summarized in Table 2. Table 2 lists the initial pressure and temperature of the steam in the accumulator tank prior to the failure of the burst diaphragm for each of the TDS experiments. Using the volume of the steam accumulator system (0.29 m^3) and standard steam tables, the number of g·moles of steam driving gas was calculated for each of the TDS tests and these values are listed in Table 2. The pressure of the steam driving gas at melt plug failure is also given in Table 2.

The initial conditions of the Surtsey atmosphere are also listed in Table 2. The initial Surtsey pressure, average temperature, and freeboard volume (103 m^3) were used in the ideal gas law to calculate the initial number of g·moles in Surtsey for each of the TDS tests. The initial gas concentrations in mole percent obtained from gas analyses of a single gas grab sample are also listed in Table 2. The primary parameter varied in the TDS tests was the initial pressure in the Surtsey vessel.

Table 2 shows the initial and final hole size in the bottom of the melt generator. The base of the melt generator was a 5.1-cm thick steel plate that was tapped for a 4.8-cm diameter brass plug (295 g). The thermite melt simulant melted the brass plug virtually immediately and ablated the steel plate during the single phase thermite ejection to a final diameter of approximately 6 cm. The final hole sizes in TDS-4, TDS-5, TDS-6, and TDS-7, were measured using a planimeter.

The TDS tests were the first DCH experiments in Surtsey to use steam as the driving gas and to include chromium in the thermite melt simulant. Previous Surtsey DCH experiments had used dry bottled nitrogen as the driving gas. The melt simulant in previous experiments was composed of a mixture of iron oxides (primarily Fe_3O_4) and aluminum powders (without chromium). The idealized metallothermitic reaction between these constituents is shown below:

$$3Fe_3O_4 + 8Al \rightarrow 9Fe + 4Al_2O_3$$

This reaction achieves temperatures similar to those predicted in severe reactor accidents (2500 K). If this debris were forcibly ejected by steam, the molten iron would react with steam according to the reaction:

$$Fe(\ell) + H_2O \rightarrow FeO(\ell) + H_2$$

This reaction will progress to the right until the iron is consumed or until the equilibrium hydrogen-to-steam partial pressure ratio is reached. The equilibrium hydrogen-to-steam partial pressure ratio for situations in which the FeO product of reaction does not dissolve in other oxides such as Al_2O_3 at 1500 to 2500 K is about 2. That is, a limit to the reaction of steam with the molten iron is encountered when only about two-thirds of the steam in the vicinity of the melt has been converted into hydrogen.

This thermodynamic limit to steam reaction with iron does not represent the situation with core debris well. In reactor core debris, highly reducing materials such as zirconium metal and chromium metal will be present. When zirconium is present, a thermodynamic limit to the reaction of steam will not be encountered until the hydrogen-to-steam partial pressure ratios are on the order of 10^4 or 10^5. In reality, this means nearly all of the steam in the vicinity of a metal droplet can react to form hydrogen at least until the zirconium is consumed.

To improve the representation of core debris, chromium metal was added to the iron oxide/aluminum thermite melt used in the earlier DCH tests [Allen et al. 1991a]. The amount of chromium added to the melt was selected so that it would be about 18 wt.% of the metal phase. The chromium does not participate in the reactions used to form the melt. The reaction

$$Cr_2O_3 + 2Al \rightarrow 2Cr + Al_2O_3$$

$$\Delta G_f(1500\ K) = -98.5\ kcal/mole$$

is strongly favored. That is, Al reacts with Cr_2O_3 rather that Cr reacting with Al_2O_3. Therefore, the chromium metal acted as an inert diluent in the reaction mixture used to form the melt simulant in the TDS tests.

When the melt is expelled with steam, the chromium in the melt can react with steam to form hydrogen:

$$2Cr(\ell) + 3H_2O \rightarrow Cr_2O_3 + 3H_2$$

This reaction will proceed to the right until the hydrogen-to-steam partial pressure ratio is on the order of 100 (377 at 1500 K and 23 at 2000 K). That is, as with core debris containing zirconium, no thermodynamic limit to the reaction with steam is encountered until nearly all of the steam has reacted or the chromium has been consumed.

Another advantage of including chromium in the melt is that it makes steam reactions with the metal phase exothermic, as they are with the metallic phases of actual core debris:

$$Zr + 2H_2O \rightarrow ZrO_2 + 2H_2 \quad \Delta H(1500\ K) = -1.5\ kcal/g\ Zr$$

$$2Cr + 3H_2O \rightarrow Cr_2O_3 + 3H_2 \quad \Delta H(1500\ K) = -0.8\ kcal/g\ Cr$$

The reaction of iron with steam at 1500 K is actually slightly endothermic:

$$Fe + H_2O \rightarrow FeO + H_2 \quad \Delta H(1500\ K) = +0.02\ kcal/g\ Fe$$

If iron was the only metal phase present, the reaction of the iron would contribute to the cooling of the dispersed melt and possibly enhanced cavity retention; whereas with actual core debris the metal reactions with steam help to keep the dispersed debris hot.

The initial charge used in the TDS experiments was prepared by mixing stoichiometric amounts of iron oxide (assumed to be Fe_3O_4) and aluminum powders with chromium granules. The masses of each constituent of the thermite melt simulant are given in Table 2.

The addition of chromium to the thermite raises the possibility that the inert material will quench the reaction temperature sufficiently to preclude a self-sustaining propagation of the reaction. Bogolyubov [1980] states that a minimum heat release of 2.3 MJ/kg is required for an aluminothermic system to be self-propagating. This empirically based criterion is based on a large number of experiments with 0.5 kg of thermite. Physically this criterion seems to correspond to a heat release sufficient to produce fully molten alumina.

The DCH-3,4 experiments [Allen et al. 1991a] used thermitic melts that were nearly identical to the current melt, only without the chromium. The specific heat content of those melts is estimated to be about 3.0 MJ/kg, based upon the measured peak temperatures of 2600 K. The addition of chromium to the melt is expected to further reduce the heat content to 2.8 MJ/kg, which is still above Bogolyubov's criterion of 2.3 MJ/kg for a self-propagating reaction.

2.4 Pressurization Sequence

The TDS experiments were performed using the following pressurization sequence. Initially, the space inside the crucible was at atmospheric pressure. When it was time to perform the experiment, the space between the rupture disks in the burst diaphragm assembly was pressurized with argon to $\simeq$2.1 MPa by opening a remotely operated valve. Then, a valve between the boiler and the accumulator was remotely opened to allow the accumulator tank to pressurize with steam to 4.2 MPa. Thus, when this pressurization was complete, the accumulator tank was at $\simeq$4.2 MPa, the space between the rupture disks of the burst diaphragm was at $\simeq$2.1 MPa, and the space inside the 10-cm-diameter steel pipe from the burst diaphragm to the crucible was at atmospheric pressure. Using this pressurization scheme, the differential pressure did not exceed 2.68 MPa, and the burst diaphragm remained intact until actuators for the burst diaphragm valves received a signal from the type-K thermocouple embedded in the thermite about 7.5 cm above the brass melt plug. The signal vented the space between the rupture disks to a 2-liter gas cylinder. This created a pressure differential across the burst diaphragm greater than 2.68 MPa, and quickly failed the burst diaphragm, bringing the high-pressure steam into contact with the molten thermite.

3.0 EXPERIMENTAL RESULTS

The TDS series was conducted to test and develop instrumentation and procedures for performing HPME/DCH experiments in the Surtsey Test Facility. Seven experiments,

designated TDS-1 through TDS-7, were performed. These experiments were conducted using similar initial conditions, except for the initial pressure in the Surtsey vessel. All experiments in this test series were performed with a steam driving gas pressure of approximately 4 MPa, 80 kg of alumina/iron/chromium thermite melt simulant, an initial hole diameter of 4.8 cm (which ablated to a final hole diameter of $\simeq$6 cm), a 1/10th linear scale model of the Surry reactor cavity (Figures 5 and 6), and the Surtsey vessel was purged with argon (<0.25 mol.% O_2). The initial pressures in the Surtsey vessel in each of the TDS tests are listed in Table 2.

There was one significant modification made in the configuration of the apparatus during this test series. In the first five tests there was a 2.5-cm gap between the top of the reactor support skirt and the ceiling of the scaled reactor cavity (Figure 5). The flow path for gas and entrained debris was primarily through the archway; however, there was also a flow path over the top of the reactor support skirt, around the annulus between the reactor support skirt and the concrete biological shield walls of the cavity, and around the outer edges of the archway into the scaled in-core instrument tunnel. For TDS-6 and TDS-7, the reactor support skirt was lengthened so that the support skirt was sealed against the ceiling of the cavity; thus the only flow path was through the archway in the support skirt. This change made a significant difference in the fraction of the debris dispersed into the Surtsey vessel, which resulted in a measurable difference in the debris dispersal and the pressure response.

The TDS test series was performed with the melt generator and cavity outside of the Surtsey vessel (Figure 1), as opposed to the configuration used in the DCH-1 through DCH-4 experiments [Allen et al. 1991a], in which the apparatus was inside the vessel. The steam-driven high-pressure melt ejections in the TDS test series were generated with the setup shown in Figure 2. Superheated steam was generated with an electric boiler. The steam accumulator tank (internal volume = 0.29 m^3) was pressurized to $\simeq$4.25 MPa by remotely opening the valve between the boiler and accumulator. The space between the rupture disks of the burst diaphragm was concurrently pressurized with argon to 2.1 MPa. The free gas volume between the burst diaphragm and the thermite was initially at ambient pressure. The thermite powder was remotely ignited with a pyrofuse. The burn time between ignition and melt ejection was usually between 25 and 28 seconds.

During this period, the gas in the crucible and in the 10-cm piping above the melt generator was heated by the molten thermite and rapidly expanded. If the pressure in this space exceeded 1.5 MPa, the crucible vent opened and gas was vented to maintain the pressure in this space at less than 1.5 MPa. Venting only occurred in TDS-5 and TDS-7. The intention of this design was to have the pressure difference between the steam accumulator tank and the crucible space greater than 2.6 MPa so that the burst diaphragm would fail at the appropriate time.

After the thermite was ignited, the burn front propagated downward. A type-K thermocouple, which was embedded in the thermite 7.5 cm above the brass melt plug in the base of the melt generator, sensed the melt front. The type-K thermocouple sent a signal that locked the vent valve closed, and after 0.5 s delay, opened the valve between the burst diaphragm and the 2-liter bottle (Figure 2). Relieving the pressure in the space between the rupture disks of the burst diaphragm immediately failed it and exposed the molten thermite to superheated steam. Within 2 to 5 seconds the brass plug in the base of the melt generator melted and initiated the steam-driven HPME. This sequence of events was followed in all of the TDS tests except

TDS-1; in TDS-1 the burst diaphragm was intentionally failed after all of the thermite had flowed into the cavity. This apparently had no major effect on the experiment results since the results of TDS-1 were virtually identical to the results of the TDS-2, which was conducted using the same initial conditions as TDS-1 except that high-pressure steam was in contact with the molten thermite 2 s before the beginning of the HPME.

3.1 Pressure Results

The results of the TDS test series are reported in the tables and figures following the text. The first set of figures, Figures 10 through 16, show the blowdown histories for TDS-1 through TDS-7, respectively. The measured pressures in the accumulator tank, between the rupture disks of the burst diaphragm, and in the gas space in the crucible are plotted versus experiment time. In all of the plots shown in this report, zero time corresponds to the initiation of the HPME, which was measured by a photodiode under the brass melt plug that was triggered by melt plug failure and debris ejection into the cavity. Figures 10 through 16 are plotted using the same scales to make comparisons easier. The steam accumulator tank was at a constant pressure of approximately 4.3 MPa until burst diaphragm failure. The pressure in the space between the rupture disks of the burst diaphragm was constant at about 2.2 MPa. The pressure in the crucible above the molten thermite gradually increased; in TDS-5 and TDS-7 it reached 1.5 MPa and briefly vented. Though these curves are similar, insight can be gained by studying each of the blowdown curves individually.

In the TDS-1 test, burst diaphragm failure was intentionally initiated by the operator after all of the molten thermite had flowed out of the melt generator. Figure 10 shows that after the brass melt plug failed at time t = 0 s, molten thermite flowed out of the hole between 0 and 0.7 s. Then gas, initially at about 1 MPa, flowed out of the ablated hole in the base of the melt generator at an experiment time between 0.7 and 1.1 s. At approximately 1.25 s, the operator failed the burst diaphragm, causing the pressure in the accumulator, burst diaphragm, and crucible to equilibrate.

Figures 11, 12, and 13 are the blowdown histories for TDS-2, -3, and -4, respectively. These curves are typical blowdown histories of experiments with no crucible venting or any other anomaly. The superheated steam was in contact with molten thermite for 2 s in TDS-2, for almost 6 s in TDS-3, and for about 4.5 s in TDS-4.

Figure 14 is the blowdown history for TDS-5. In this experiment the crucible pressure reached $\simeq$ 1.6 MPa at t = -3.7 s and the crucible vent opened briefly to relieve the pressure. In TDS-5 the crucible vent only opened once. At t = -2.8 s the burst diaphragm failed and at t = -2.5 s steam came into contact with the molten thermite.

Figure 15 is the blowdown history for the TDS-6 experiment. This curve appears different from the others, but the differences should have had no effect on the results measured in the Surtsey vessel, e.g., pressure increase and hydrogen generated. In this test the crucible pressure reached the value at which it should have vented; however, at about the same time, the type-K thermocouple sensed the melt front and locked the crucible vent closed. During the 0.5 s delay before the burst diaphragm failed, the pressure in the crucible continued to increase until the pressure difference between the steam accumulator tank and the crucible was not great enough

to fail the burst diaphragm. The rupture disk between the burst diaphragm and accumulator failed, but the rupture disk between the crucible and the burst diaphragm remained intact; consequently, the pressure in the crucible space continued to increase until the brass melt plug failed. As molten thermite flowed out of the melt generator, the free gas volume expanded and thus the pressure in the crucible space decreased to a value at which the pressure difference was great enough to fail the remaining rupture disk. The steam came into contact with the molten thermite almost exactly at the time gas blow through began. As pointed out previously, this blowdown history should have no impact on the quantities measured in the Surtsey vessel.

Figure 16 shows the blowdown history for the TDS-7 experiment. The crucible vent opened four times (only two are shown in Figure 16). The burst diaphragm failed at t = -4 s, which brought steam into contact with molten thermite at about t = -3.7 s. Other than the crucible venting four times, this is a fairly typical blowdown curve for the TDS tests.

Figures 17 through 23 show the absolute pressure in the steam accumulator tank in MPa versus experiment time for TDS-1 through TDS-7, respectively. Each of these figures is plotted on the same scale: absolute pressure from 0 to 5 MPa versus experiment time from -0.5 to 2.5 s. These curves indicate that the steam blowdown is virtually complete at t = 1.5 s in the TDS tests, except for TDS-1 which started late, but had an elapsed blowdown time similar to the other tests.

Figures 24 through 30 show the temperature of the steam driving gas plotted against experiment time for TDS-1 through TDS-7, respectively. The initial gas temperatures in the steam accumulator tank listed in Table 2 are taken from these figures. The values listed in Table 2 are an average of the temperatures from channels 91 and 92 at time t = 0 s.

Figures 31 through 51 show the Surtsey vessel pressures measured in TDS-1 through TDS-7. For each test, there are three pressure curves: one from channel 21 at level 1, one from channel 23 at level 3, and one from channel 25 at level 5. These plots indicate that the pressures measured in individual experiments varied by less than 2 kPa. The initial pressures in the Surtsey vessel were varied for these experiments and are listed in Table 2 for TDS-1 through TDS-7. The pressure results in Figures 31 through 51 indicate that the increase in the Surtsey vessel pressure due to HPME shows a weak positive dependence on the initial vessel pressure. This is apparently because heat transfer coefficients tend to increase with density and consequently debris/gas heat transfer also increases with density.

Figure 52 compares the increase in the Surtsey vessel pressure for the TDS-1 and the TDS-2, which were conducted with the same initial conditions. The increases in Surtsey vessel pressure for TDS-1 and TDS-2 are in excellent agreement, which indicates that it makes no apparent difference, within certain limits, when steam comes into contact with the melt.

Figure 53 compares the increases in the Surtsey vessel pressure due to the HPME for TDS-3 and TDS-5, which were performed with virtually the same initial pressure in the Surtsey vessel, i.e., 0.8 MPa. These results are not in particularly good agreement. The peak pressure in Surtsey was 44 kPa higher in TDS-3 compared to TDS-5. There are two explanations that may have contributed to this difference. First, the accumulator tank was significantly hotter in TDS-5 (731 K) and in TDS-3 (549 K). Consequently, at the same accumulator pressure there were

fewer moles of steam driving gas in TDS-5 than in TDS-3 (Table 2). Thus, TDS-5 had less heat transfer fluid, i.e., the blowdown steam to carry heat from the debris into the Surtsey vessel and less debris entrainment into the Surtsey vessel (Section 3.4). Second, the initial atmosphere contained 0.25 mol.% O_2 in TDS-3 and 0.0 mol.% O_2 in TDS-5. There was probably some hydrogen combustion in TDS-3 that caused a higher pressure increase than in TDS-5.

Figure 54 compares the increases in the Surtsey vessel pressure due to the HPME in TDS-6 and TDS-7, which were performed with similar initial conditions. These experiments, performed as replicates to show reproducibility, are in good agreement; there is about 16 kPa difference in the peak pressures.

Figure 55 compares the increases in the Surtsey vessel pressure for TDS-1, TDS-2, TDS-6, and TDS-7, which were all performed with similar initial conditions and an initial pressure in the vessel of approximately 0.156 MPa. However, TDS-6 and TDS-7 were conducted with no gap between the reactor support skirt and the ceiling of the cavity. Both TDS-6 and TDS-7 had a higher fraction of debris dispersed into the vessel, and thus a larger pressure increase in the vessel.

The debris entrainment interval is best determined by comparing cavity pressure to vessel pressure. Figures 56 through 62 show the cavity pressure and vessel pressure plotted against experiment time for TDS-1 through TDS-7, respectively. Each of these curves is plotted using the same scales to make comparisons easier. There is a small pressure peak in the cavity just after the HPME began at time t = 0 s. This narrow peak was caused by gas expansion as hot thermite first entered the cavity. The second broad peak, usually beginning at about t = 0.35 s and lasting 0.6 to 0.7 s, was due to thermite entrainment from the cavity floor by the high-velocity steam blowdown. The debris ejection interval is marked on these figures.

3.2 Temperature Results

Figures 63 through 69 show the gas temperatures measured at the wall of the Surtsey vessel with aspirated thermocouples for TDS-1 through TDS-7, respectively. Based on later experiments [Allen et al. 1994; Blanchat et al. 1994], it was concluded that aspirated thermocouples are not the best way to measure bulk gas temperatures in these types of experiments. The data are presented here for completeness, however. Generally, the aspirated thermocouple at level 1 measured the lowest gas temperatures. The highest temperatures were measured at either level 3 or 5 at times between 2 and 4 seconds. Occasionally, a hot debris particle was drawn into the aspirated thermocouple and deposited on the bare thermocouple wire. This apparently caused the level 3 thermocouple to fail in TDS-4, TDS-6, and TDS-7. It appears that the solenoid valves on the downstream end of the aspirated thermocouples did not open in TDS-3 so there was no gas flow past the thermocouples.

Debris temperature at the chute exit was measured using a two-color pyrometer and an optical pyrometer in the TDS test. A second optical pyrometer in a different arrangement was added in TDS-7. Figures 70 through 81 show the pyrometer results for the TDS tests. In each of these figures, there is a horizontal dotted line across the plot at a reference temperature of 2300 K. A reference temperature of 1973 K is shown for the optical pyrometers, and a reference temperature of 1773 K is shown for the two-color pyrometer. These reference

temperatures correspond to a pyrometer output of 2 mV and are the lowest values for which the pyrometers were calibrated. Consequently, any signals received that were less than 2 mV were plotted at 273 K in Figures 70 through 81.

There was not a clear difference in the temperatures measured with the optical pyrometers among the TDS tests. The mean peak temperatures were between 2200 K and 2400 K, with an average of about 2300 K. The temperatures measured with the two-color pyrometers were 200 to 300 K lower than the temperatures measured with the optical pyrometers on the same experiments. It was concluded that the optical pyrometers were giving accurate temperatures of debris exiting the scaled reactor cavity and that the response time of the two-color pyrometer was too slow for these types of experiments.

3.3 Gas Analyses

Hydrogen was sampled using 500-cm^3 evacuated grab sample bottles in the TDS experiments. In each experiment a background gas grab sample was taken at level 4 of the Surtsey vessel just prior to thermite ignition. At two minutes after the photodiode below the brass melt plug signaled melt ejection, a timing circuit opened gas grab sample bottles at levels 2, 4, and 6 for 10 seconds. Gas grab sample bottles at levels 2, 4, and 6 were manually opened approximately 30 minutes after melt ejection. The contents of these bottles were analyzed by gas mass spectroscopy for H_2, Ar, N_2, O_2, and CO_2.

Background gas concentration measurements for the TDS tests are given in Table 2. The background argon concentration ranged between 98.7 mol.% and 99.6 mol.%, and the background oxygen concentration ranged between 0.0 mol.% and 0.25 mol.%. The background hydrogen concentration should have been zero; it is believed that the hydrogen measurement for TDS-7 (0.18 mol.%) was due to an error in the gas mass spectroscopy measurement.

The posttest gas concentration measurements for the TDS tests are given in Table 3. Gas measurements were not attempted in TDS-1. The values given in Table 3 are the final gas concentrations in Surtsey in mole percent averaged over the three samples taken at 2 minutes and the three samples taken at 30 minutes (minus any samples that had defective valve seats and obviously leaked). The two-minute gas grab samples at three different levels indicated that the Surtsey vessel atmosphere was well mixed after two minutes. The gas concentrations did not show a change between the two-minute and thirty-minute samples.

The posttest gas concentrations were used to calculate the total number of moles of hydrogen produced during the HPME, i.e., initial vessel moles times posttest hydrogen fraction. The amount of hydrogen produced in the TDS tests was between 150 and 173 g·moles, except for TDS-3 (209 g·moles). It is unclear why the TDS-3 test produced more hydrogen than the others.

3.4 Debris Characterization

The percentage of debris dispersed into the vessel was determined by a meticulous debris recovery procedure. The results of this procedure are reported in Table 4. For the first five TDS tests, in which there was a gap between the RPV skirt and cavity ceiling, the percent

dispersed into the vessel was between 52.4% and 61.5%. The percentage dispersed into the vessel in TDS-6 was 73.9% and in TDS-7 was 69.4%. The total debris mass recovered for each of the TDS tests is about 20% greater than the mass of the initial thermite charge (80 kg). The additional mass is the result of oxidation of metallic debris by steam, ablation of concrete in the cavity, and melting of the inner steel liner in the crucible and of the brass melt plug.

Figures 82 and 83 show the results of the sieve analyses of debris recovered from the bottom head of the Surtsey vessel for TDS-4, TDS-5, TDS-6, and TDS-7. The debris consisted of spherical particles with rough surfaces that were usually partially hollow. Figure 82 shows that the particle size distributions for these four tests were lognormally distributed and were in good agreement. The sieve mass median diameter ranged from 0.67 mm to 0.9 mm with a geometric standard deviation of about 4.

3.5 Debris Velocity Measurements

The photodiode array was never successfully used to accurately measure the debris velocity in the TDS tests. The photodiodes seemed to randomly trigger as the HPME progressed. The velocity of the debris plume was measured using a breakwire array in TDS-5, TDS-6, and TDS-7. The average debris velocity along the vertical axis of the Surtsey vessel was 36 m/s in TDS-5, 34 m/s in TDS-6, and 35 m/s in TDS-7. Figure 84 shows the breakwire signals that were used to measure the debris velocity in the TDS-7 test. The time between the breakwire signals was relatively constant between level 1 and level 6, which are shown in Figure 9. Thus, the debris velocity in TDS-7 was relatively constant as it moved upward in the Surtsey vessel.

4.0 SUMMARY OF RESULTS

It was important in the DCH issue resolution process to develop hardware, techniques, procedures, and instrumentation for reliably performing high-quality DCH experiments at 3 to 4 week intervals. Previous DCH experiments [Allen et al. 1991a] using similar melt simulants, but using nitrogen gas as a surrogate for steam, were conducted at about 9-month intervals. The TDS test series demonstrated that steam-driven, high-pressure melt ejection experiments with an alumina/iron/chromium melt simulant could be successfully performed at 3-week intervals. Originally, the TDS tests were not going to be documented; however, because the data from these tests are being used to assess models, it was decided to publish the results of these tests.

Table 5 gives a summary of the results of the TDS test series. The only parameter intentionally varied in these tests was the initial pressure in the Surtsey vessel. Three initial pressures were used: 0.08 MPa in TDS-3 and TDS-5, 0.16 MPa in TDS-1, TDS-2, TDS-6, and TDS-7, and 0.23 MPa in TDS-4. This test series indicated that the peak pressure increase showed a weak positive dependence on the initial vessel pressure.

These experiments were used to test various types of instrumentation to investigate DCH phenomena. For example, our initial idea of using a photodiode array to measure debris velocity was not successful. After several attempts, we used a simple breakwire array and accurately measured the velocity of the leading edge of the debris plume.

In some of the tests, additional instrumentation that is not discussed in this report was added to test its feasibility. Some examples include (1) an eddy current coil around the exit chute to measure the debris ejection interval, (2) acoustic sensors on the upper and lower heads to measure debris velocity, (3) radiometers to measure heat flux to the vessel wall, and (4) a gas chromatography/mass spectroscopy unit for measuring single-location, on-line hydrogen concentration. All of this instrumentation was eventually abandoned because it was not producing useful data and the cost of developing the instrumentation and experimental technique was prohibitive.

Table 1. TDS Instrumentation Location and Purpose

Channel	Instrument	Location	Purpose
1	Photodiode array	Cavity 1	Measure debris velocity
2	Photodiode array	Cavity 2	Measure debris velocity
3	Photodiode array	Level 1	Measure debris velocity
4	Photodiode array	Level 2	Measure debris velocity
5	Photodiode array	Level 3	Measure debris velocity
6	Photodiode array	Level 4	Measure debris velocity
7	Photodiode array	Level 5	Measure debris velocity
8	Photodiode array	Level 6	Measure debris velocity
10	Type-K thermocouple	Crucible	Activate valves
11	Breakwire	Level 1	Measure debris velocity
12	Breakwire	Level 2	Measure debris velocity
13	Breakwire	Level 3	Measure debris velocity
14	Breakwire	Level 4	Measure debris velocity
15	Breakwire	Level 5	Measure debris velocity
16	Breakwire	Level 6	Measure debris velocity
18	Photodiode	Crucible plug	Signal initiation of HPME
19	Photodiode	Cavity exit	Detect cavity ejection
20	Two-color pyrometer	Cavity exit	Measure debris temperature
21	Breakwire	Top	Measure debris velocity
22	Breakwire	Chute exit	Measure debris velocity
29	Optical pyrometer	Chute exit	Measure debris temperature
30	Optical pyrometer	Chute exit	Measure debris temperature
31	Pressure transducer	Accumulator	Measure steam pressure
32	Pressure transducer	Accumulator	Measure steam pressure
33	Pressure transducer	Burst diaphragm	Measure gas pressure
34	Pressure transducer	Crucible	Measure gas pressure

Table 1. TDS Instrumentation Location and Purpose

Channel	Instrument	Location	Purpose
35	Pressure transducer	Crucible	Measure gas pressure
36	Pressure transducer	Cavity	Measure gas pressure
44	Thermocouple	Level 1	Measure gas temperature
45	Thermocouple	Level 1	Measure gas temperature
46	Thermocouple	Level 1	Measure gas temperature
50	Thermocouple	Level 3	Measure gas temperature
51	Thermocouple	Level 3	Measure gas temperature
52	Thermocouple	Level 3	Measure gas temperature
56	Thermocouple	Level 5	Measure gas temperature
57	Thermocouple	Level 5	Measure gas temperature
58	Thermocouple	Level 5	Measure gas temperature
59	Ignitor	Crucible	Thermite ignition
61	Pressure transducer	Level 1	Measure gas pressure
62	Pressure transducer	Level 1	Measure gas pressure
63	Pressure transducer	Level 3	Measure gas pressure
64	Pressure transducer	Level 3	Measure gas pressure
65	Pressure transducer	Level 5	Measure gas pressure
66	Pressure transducer	Level 5	Measure gas pressure
77	Thermocouple	Crucible	Measure gas temperature
78	Thermocouple	Tee on crucible	Measure gas temperature
80	Thermocouple	Crucible vent	Measure gas temperature
81	Thermocouple	Accumulator	Measure wall temperature
82	Thermocouple	Accumulator	Measure wall temperature
83	Thermocouple	Accumulator	Measure wall temperature
84	Thermocouple	Accumulator	Measure wall temperature
85	Thermocouple	Accumulator	Measure wall temperature

Table 1. TDS Instrumentation Location and Purpose

Channel	Instrument	Location	Purpose
86	Thermocouple	Accumulator	Measure wall temperature
87	Thermocouple	Accumulator	Measure wall temperature
88	Thermocouple	Accumulator	Measure wall temperature
90	Thermocouple	Accumulator	Measure wall temperature
91	Thermocouple	Accumulator	Measure steam temperature
92	Thermocouple	Accumulator	Measure steam temperature
93	Thermocouple	10-cm pipe	Measure steam temperature
L2	Gas grab sample	Surtsey level 2	Measure gas composition prior to and after HPME
L4	Gas grab sample	Surtsey level 4	Measure gas composition prior to and after HPME
L6	Gas grab sample	Surtsey level 6	Measure gas composition prior to and after HPME

Table 2
Initial Conditions for the TDS Experiments

		TDS-1	TDS-2	TDS-3	TDS-4	TDS-5	TDS-6	TDS-7
Accumulator steam pressure (MPa)		4.30	4.25	4.20	4.25	4.28	4.26	4.23
Accumulator steam temperature (K)		572	596	549	541	731	602	578
Steam driving gas (g • moles)		292	271	307	303	209	267	283
Steam driving pressure (MPa)		4.00	3.65	3.80	4.00	3.80	4.10	3.99
Initial Surtsey pressure (MPa)		0.158	0.160	0.080	0.229	0.082	0.160	0.156
Surtsey temperature (K)		300	302	291	288	278	278	286
Surtsey gas moles (g • moles)		6525	6564	3406	9851	3654	7130	6757
Gas composition in Surtsey (mol. %)	Ar	99.61	99.14	98.72	99.59	99.44	99.30	99.10
	N_2	0.36	0.66	0.96	0.32	0.30	0.54	0.58
	O_2	0.02	0.18	0.25	0.08	0.00	0.14	0.13
	CO	nm	nm	nm	nm	nm	0.00	0.00
	CO_2	nm	0.00	0.00	0.00	0.00	0.00	0.00
	H_2	0.00	0.00	0.01	0.00	0.00	0.00	0.18
Initial hole diameter (cm)		4.80	4.80	4.80	4.80	4.80	4.80	4.80
Final hole diameter (cm)		~6 (nm)	~6 (nm)	~6 (nm)	6.04	6.00	5.87	6.00
Thermite composition iron oxide (kg) aluminum (kg) chromium (kg) Thermite charge (kg)		54.44 16.91 8.65 80.00						
Surtsey freeboard volume (m^3)		103						

nm - not measured

Table 3
Gas Measurements for the TDS Experiments

		TDS-1	TDS-2	TDS-3	TDS-4	TDS-5	TDS-6	TDS-7
Final gas composition in Surtsey (mol. %)	Ar	nm	95.61	92.49	97.86	94.61	96.88	96.53
	N_2	nm	1.45	1.13	0.44	0.90	0.40	0.90
	O_2	nm	0.21	0.02	0.04	0.24	0.04	0.14
	CO	nm	nm	nm	nm	nm	0.22	0.17
	CO_2	nm	0.11	0.17	0.07	0.00	0.05	0.05
	H_2	nm	2.60	6.14	1.52	4.20	2.42	2.22
Posttest H_2 (g · moles)		nm	171	209	150	153	173	150

nm - not measured

Table 4
Debris Dispersal Summary for the TDS Experiments

	TDS-1	TDS-2	TDS-3	TDS-4	TDS-5	TDS-6	TDS-7
Upper head (kg) (a)	28.77	20.52	22.13	15.43	16.40	27.10	30.12
Walls (kg) (b)		2.22	4.09	4.15	3.45	4.09	4.00
Lower head (kg) (c)	31.63	27.23	27.38	27.56	26.77	35.04	32.97
Chute (kg)	7.99	5.96	33.81	8.08	7.58	5.41	6.43
Cavity (kg)	29.76	30.65		36.52	32.77	17.93	23.15
Total (kg) (d) (see footnote)	98.15	86.58	87.41	91.74	86.97	89.57	96.67
Percent dispersed (a+b+c)/d*100	61.5	57.8	61.3	51.4	53.6	73.9	69.4

The total debris mass recovered posttest is usually about 20% greater than the mass of the initial thermite charge (80 kg) because of the additional mass from oxidation of metallic debris by steam, ablation of concrete in the cavity, and melting of the inner crucible liner and brass melt plug.

Table 5
Summary of the Results for the TDS Experiments

	TDS-1	TDS-2	TDS-3	TDS-4	TDS-5	TDS-6	TDS-7
Initial vessel pressure (MPa)	0.158	0.160	0.080	0.229	0.082	0.160	0.156
Steam driving pressure (MPa)	4.00	3.65	3.80	4.00	3.80	4.10	3.99
Steam driving gas (g • moles)	292	271	307	303	209	267	283
Final hole size (cm)	~6 (nm)	~6 (nm)	~6 (nm)	6.04	6.00	5.87	6.00
H_2 produced (g • moles)	nm	171	209	150	153	173	150
Debris dispersal (%)	61.5	57.8	61.3	51.4	53.6	73.9	69.4
ΔP due to HPME (MPa)	0.296	0.286	0.262	0.329	0.218	0.328	0.312

nm - not measured

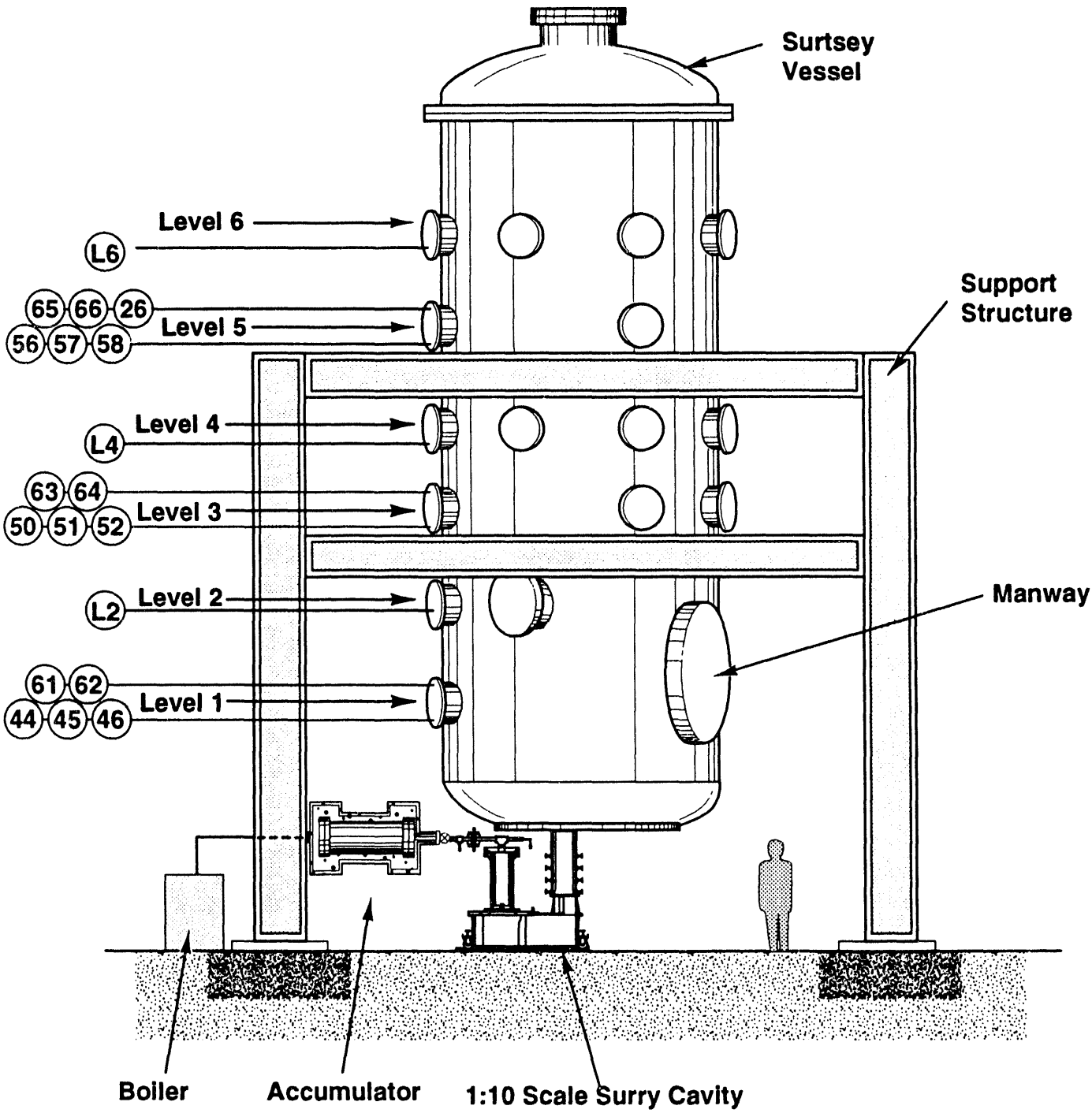

Figure 1. Schematic diagram of the Surtsey vessel showing the experimental apparatus used to produce a HPME. The circled numbers show the locations of the instrumentation and correspond to the list of instrumentation channels in Table 1.

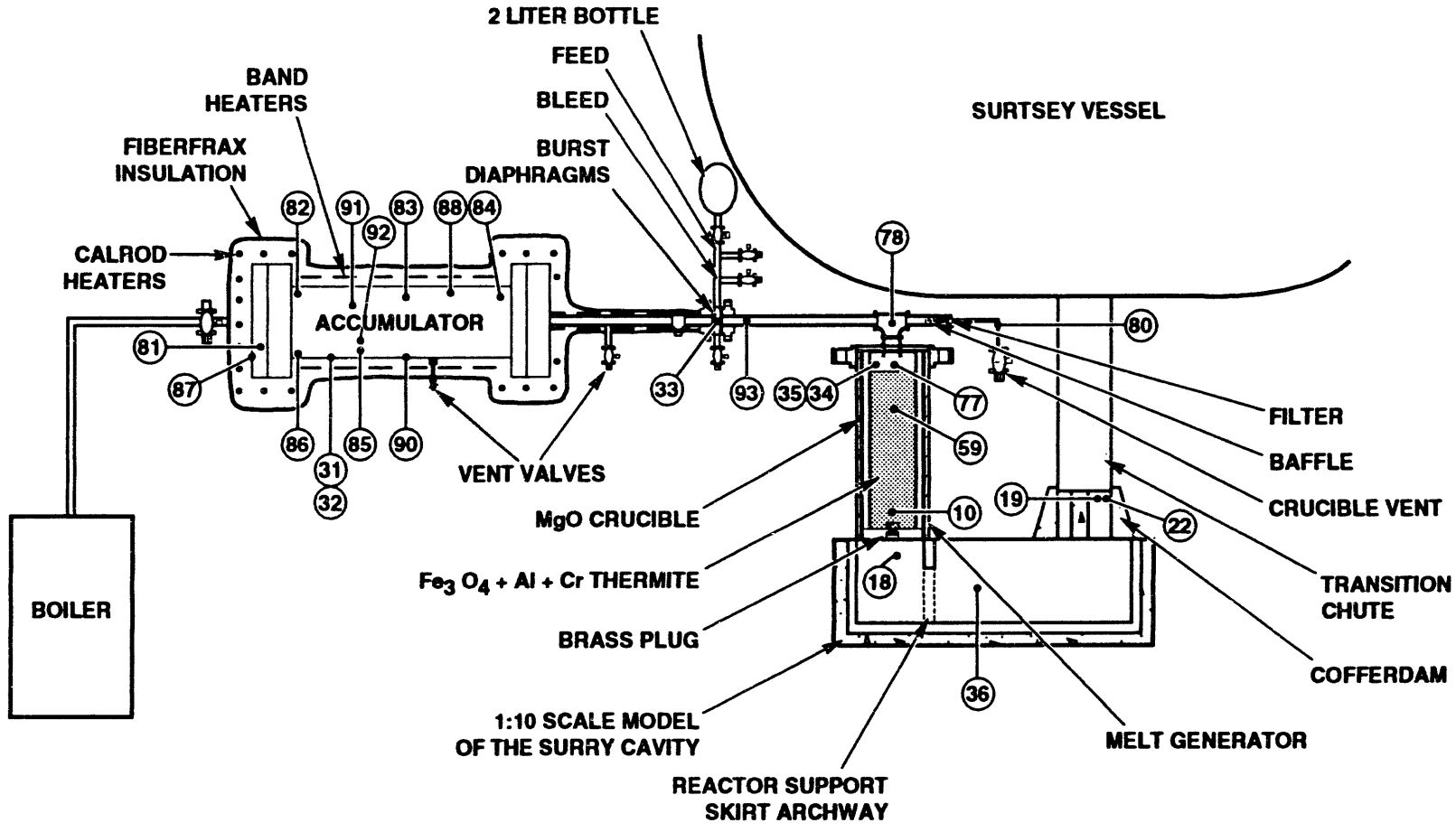

Figure 2. Schematic diagram of the experimental apparatus used to produce a HPME into the Surtsey vessel. The circled numbers show the locations of the instrumentation and correspond to the list of instrumentation channels in Table 1.

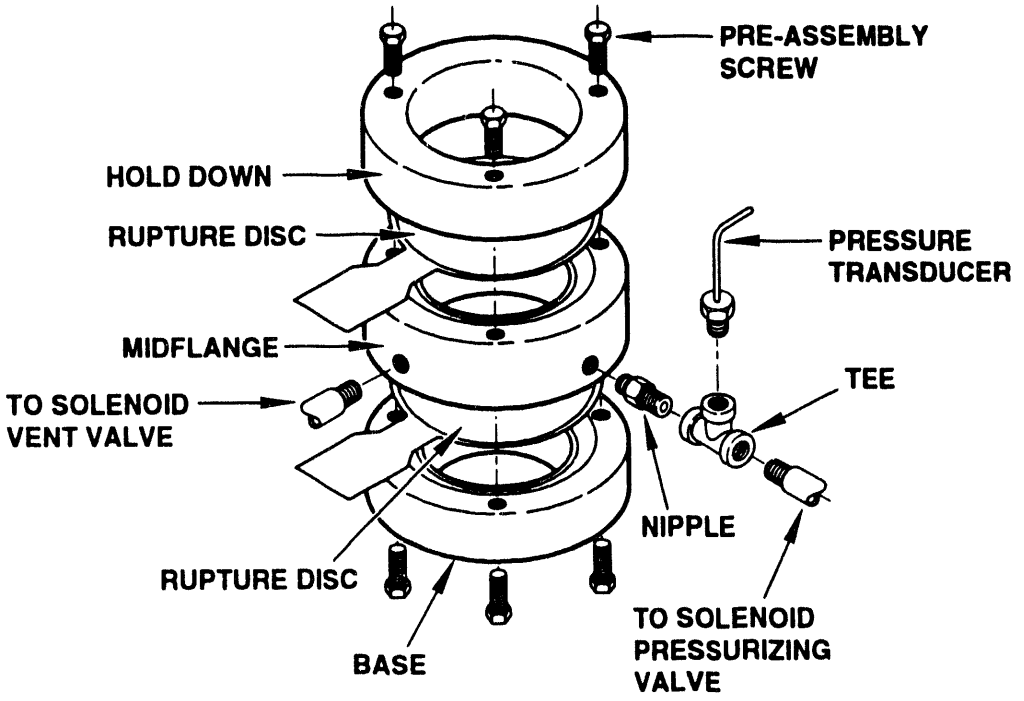

Figure 3. Exploded view of the burst diaphragm assembly used in the TDS tests.

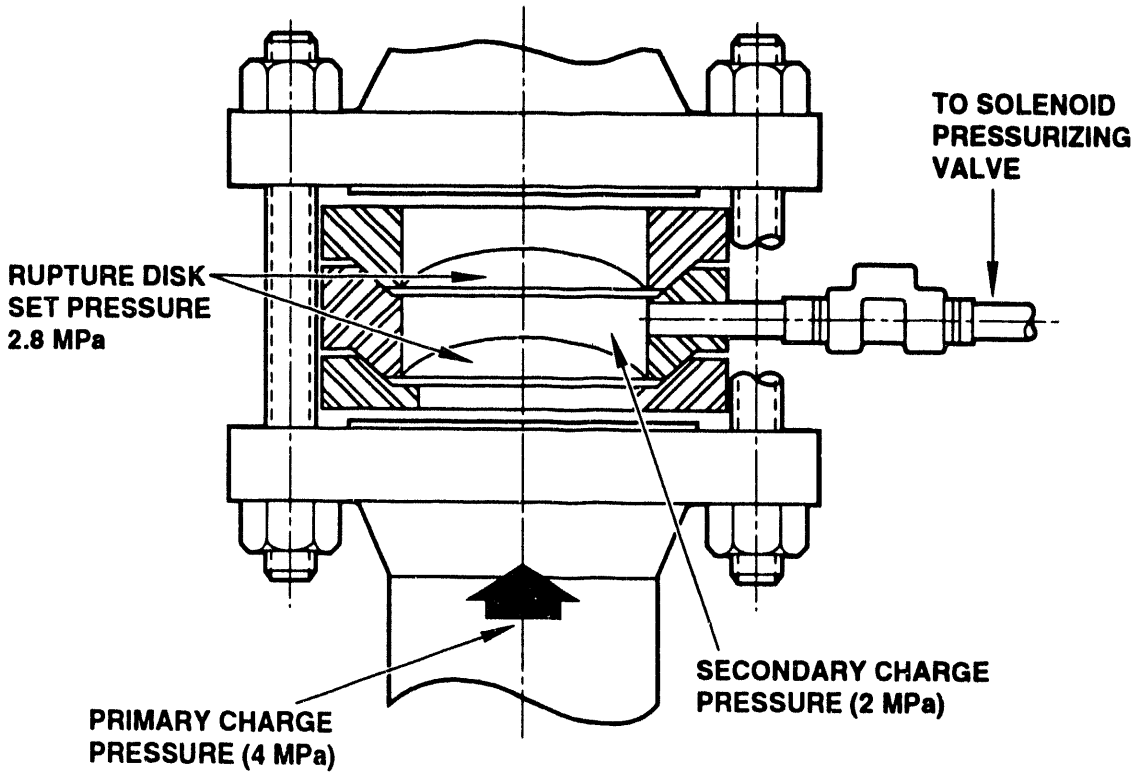

Figure 4. Cross-sectional view of the burst diaphragm assembly used in the TDS tests.

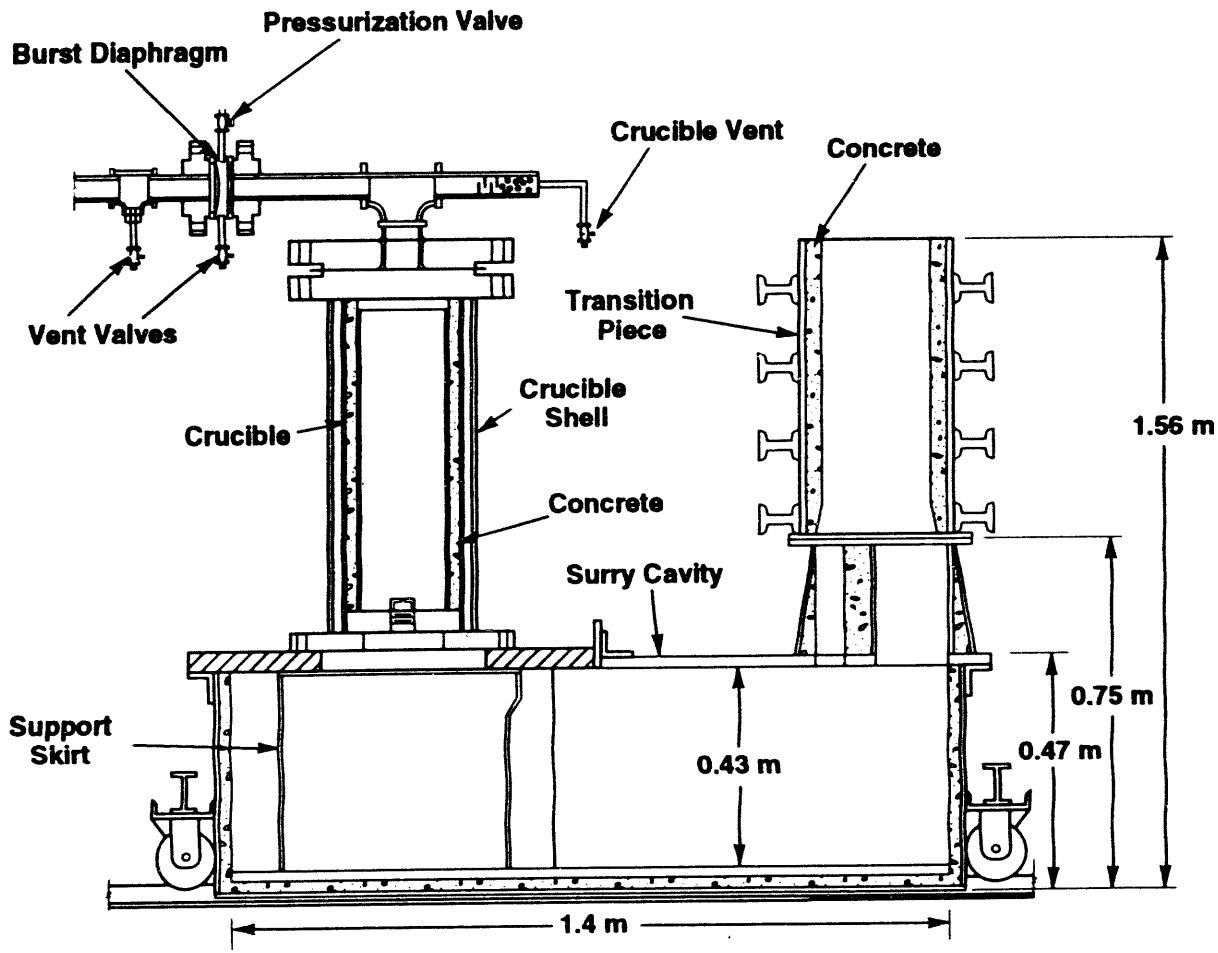

Figure 5. Side view of the 1:10 linear scale model of the Surry reactor cavity used in the TDS tests.

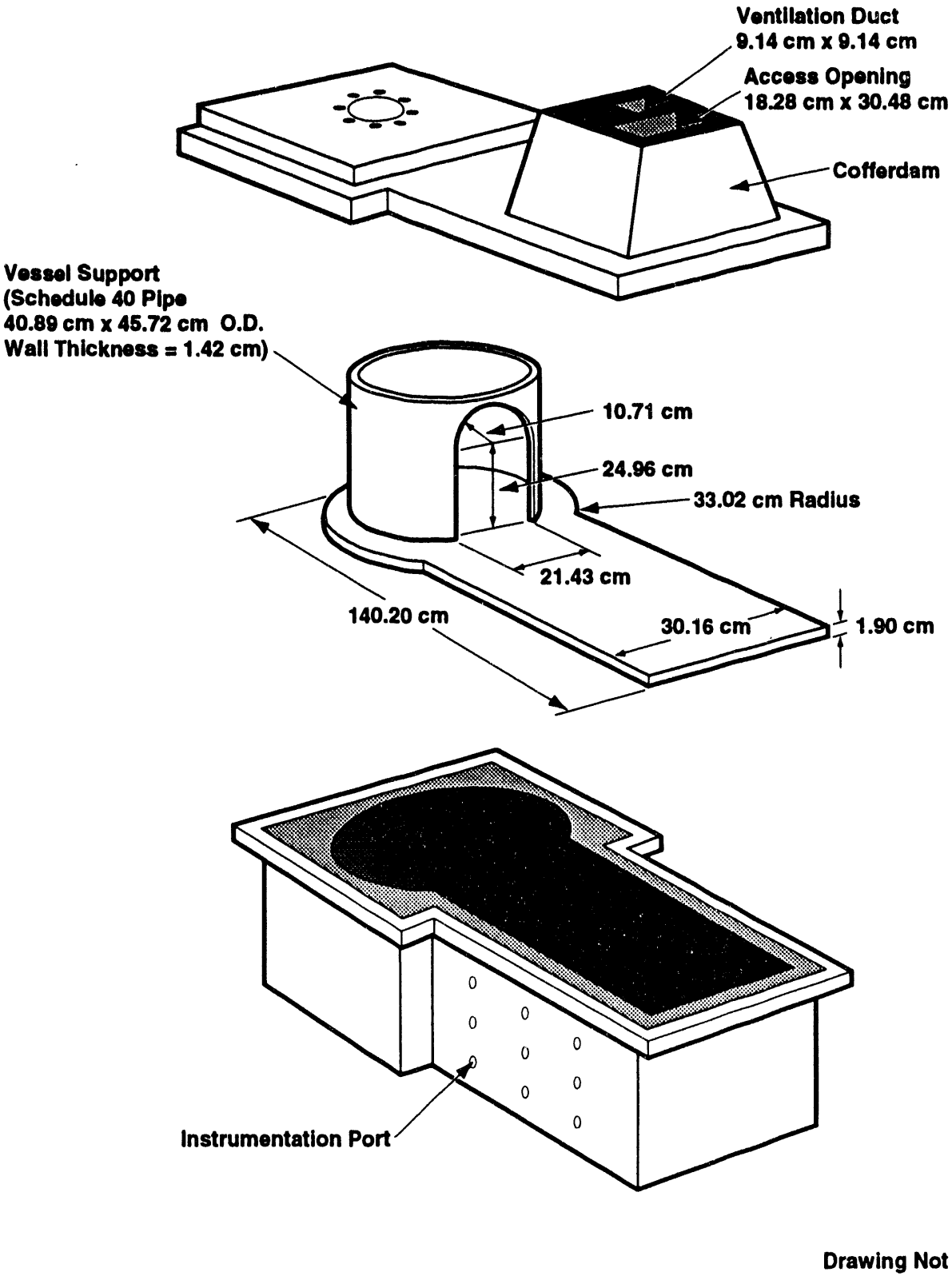

Figure 6. Exploded view of the 1:10 linear scale model of the Surry reactor cavity used in the TDS tests.

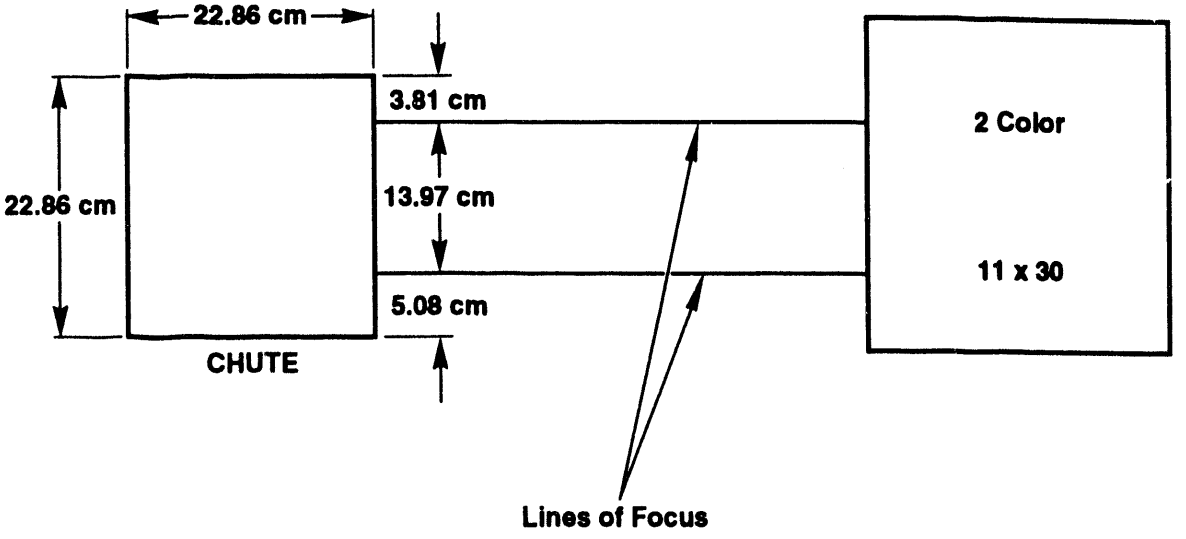

Top - View

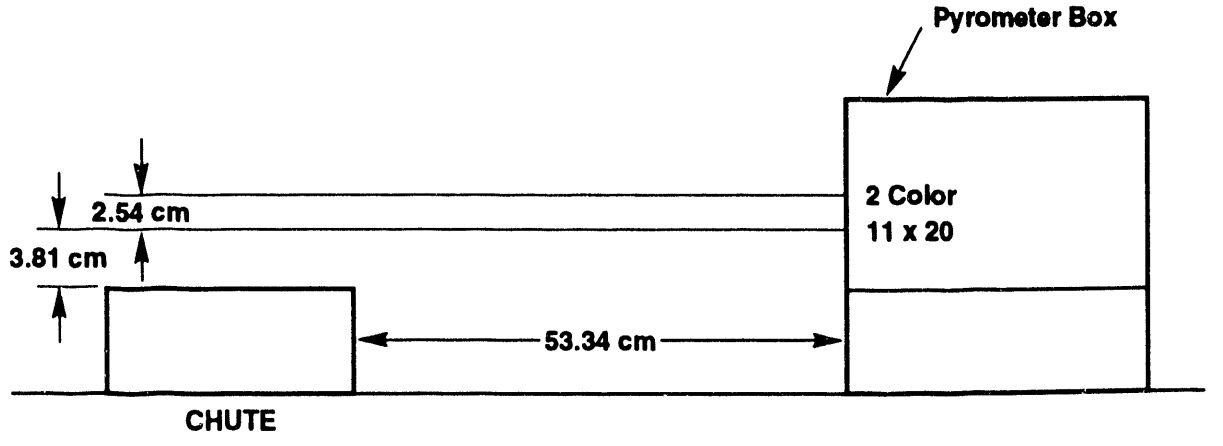

Side - View

Figure 7. Pyrometer locations in TDS-1 through TDS-6.

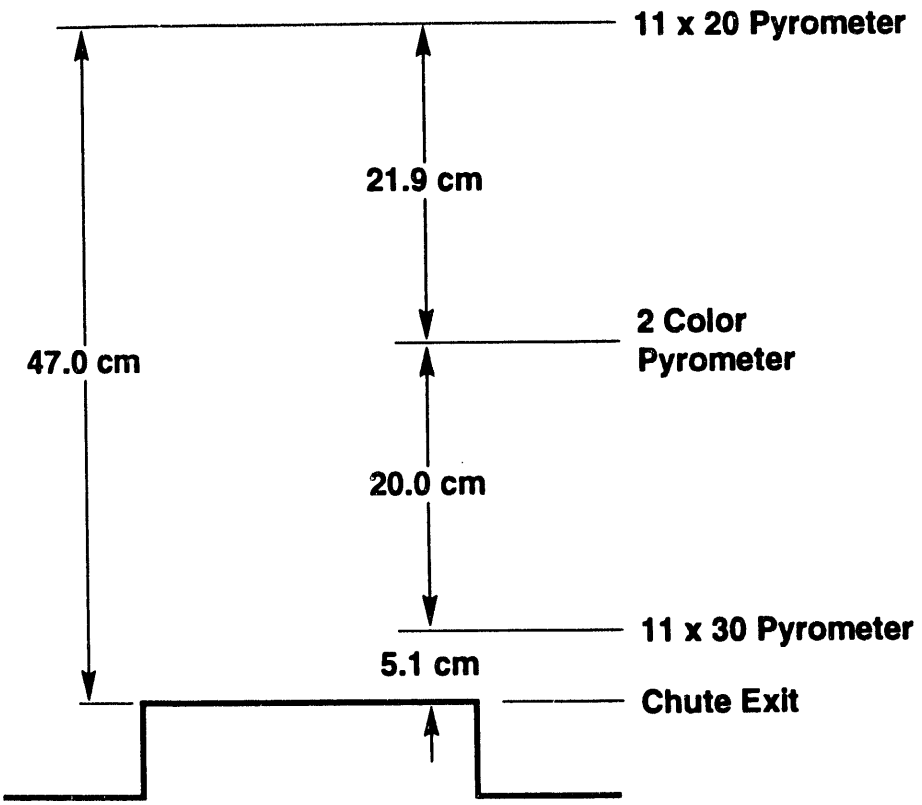

Side - View

Figure 8. Pyrometer locations in TDS-7.

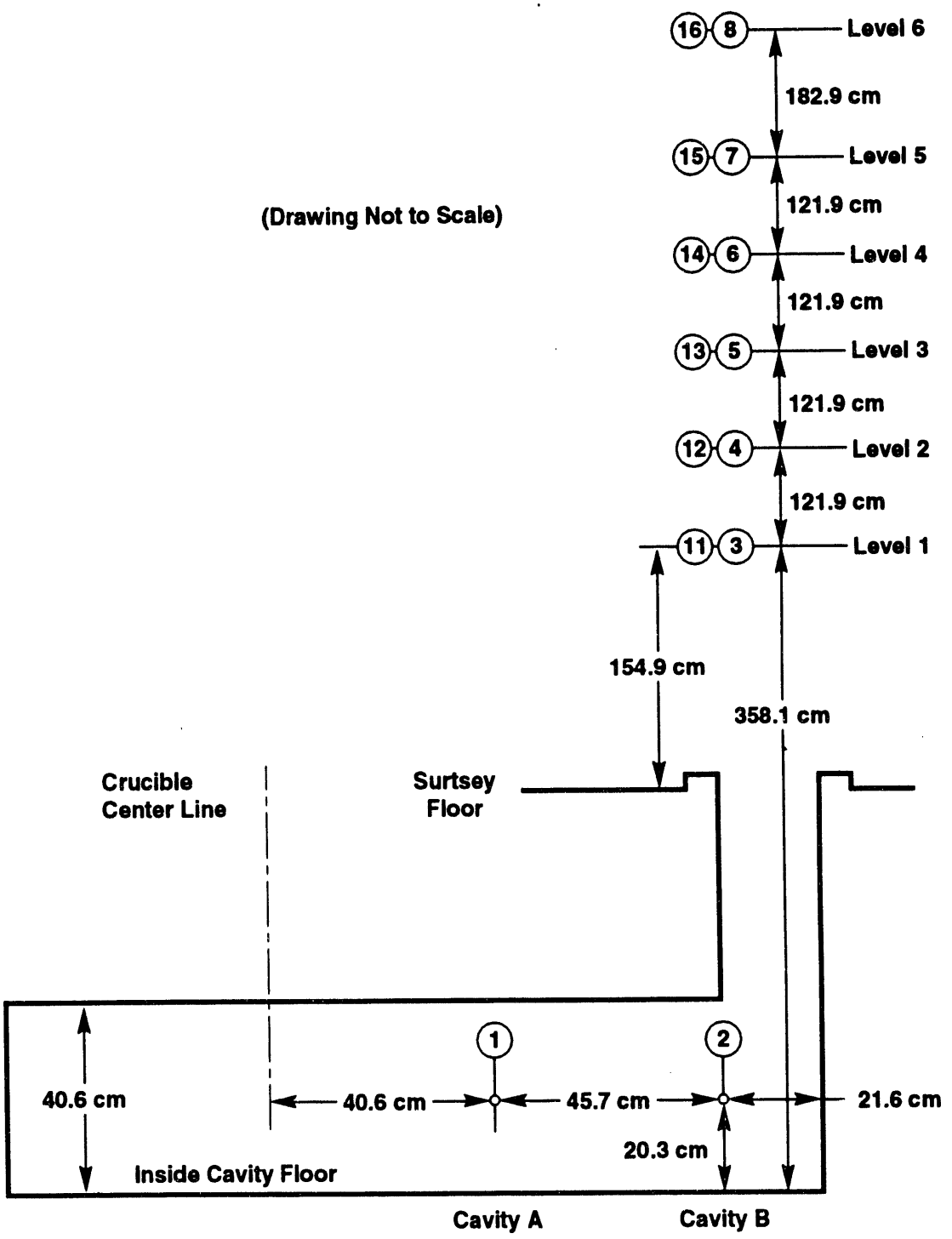

Figure 9. Locations of photodiodes and breakwires with respect to the Surry cavity model in the TDS tests.

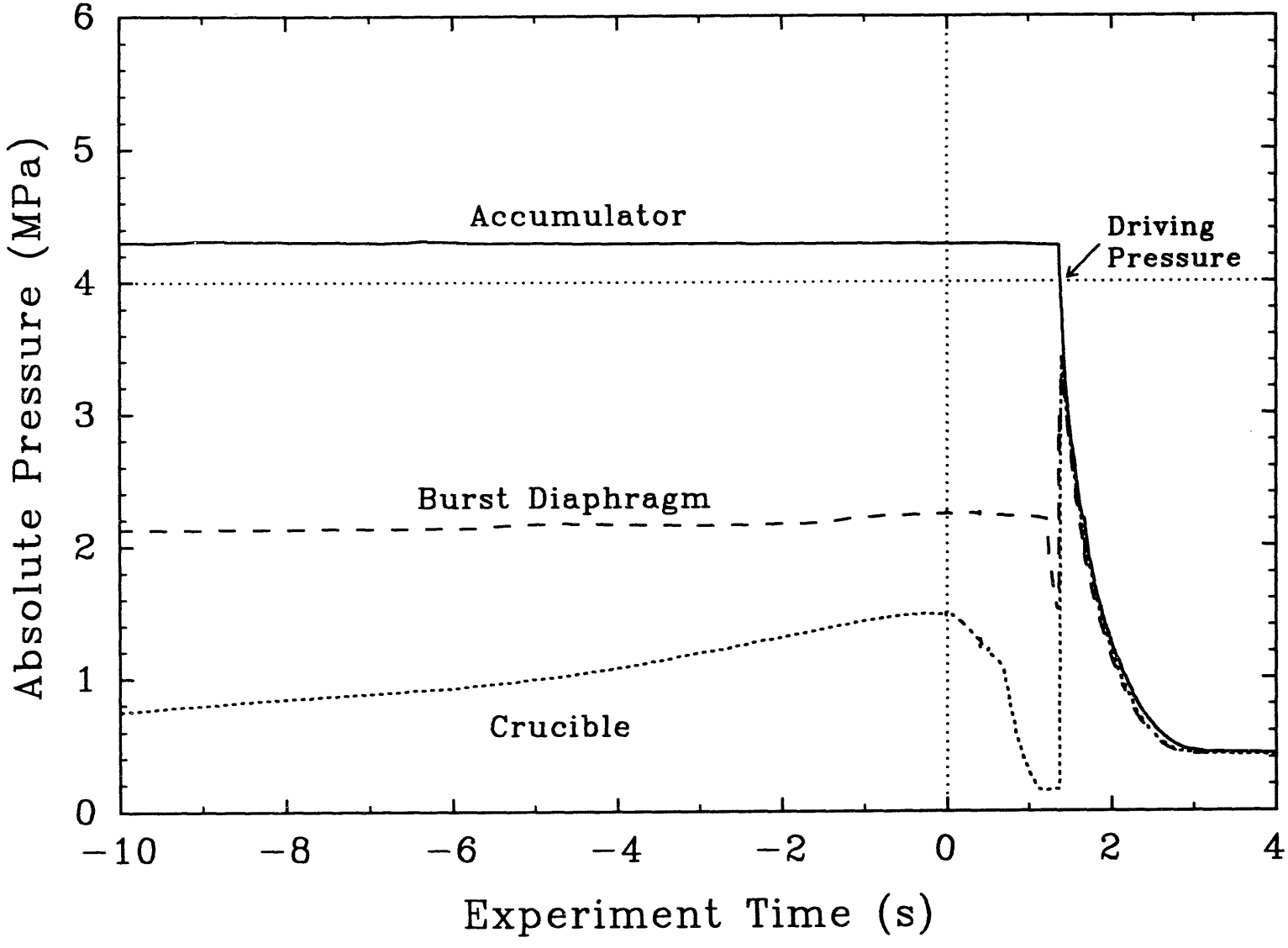

Figure 10. Blowdown history of the TDS−1 experiment.

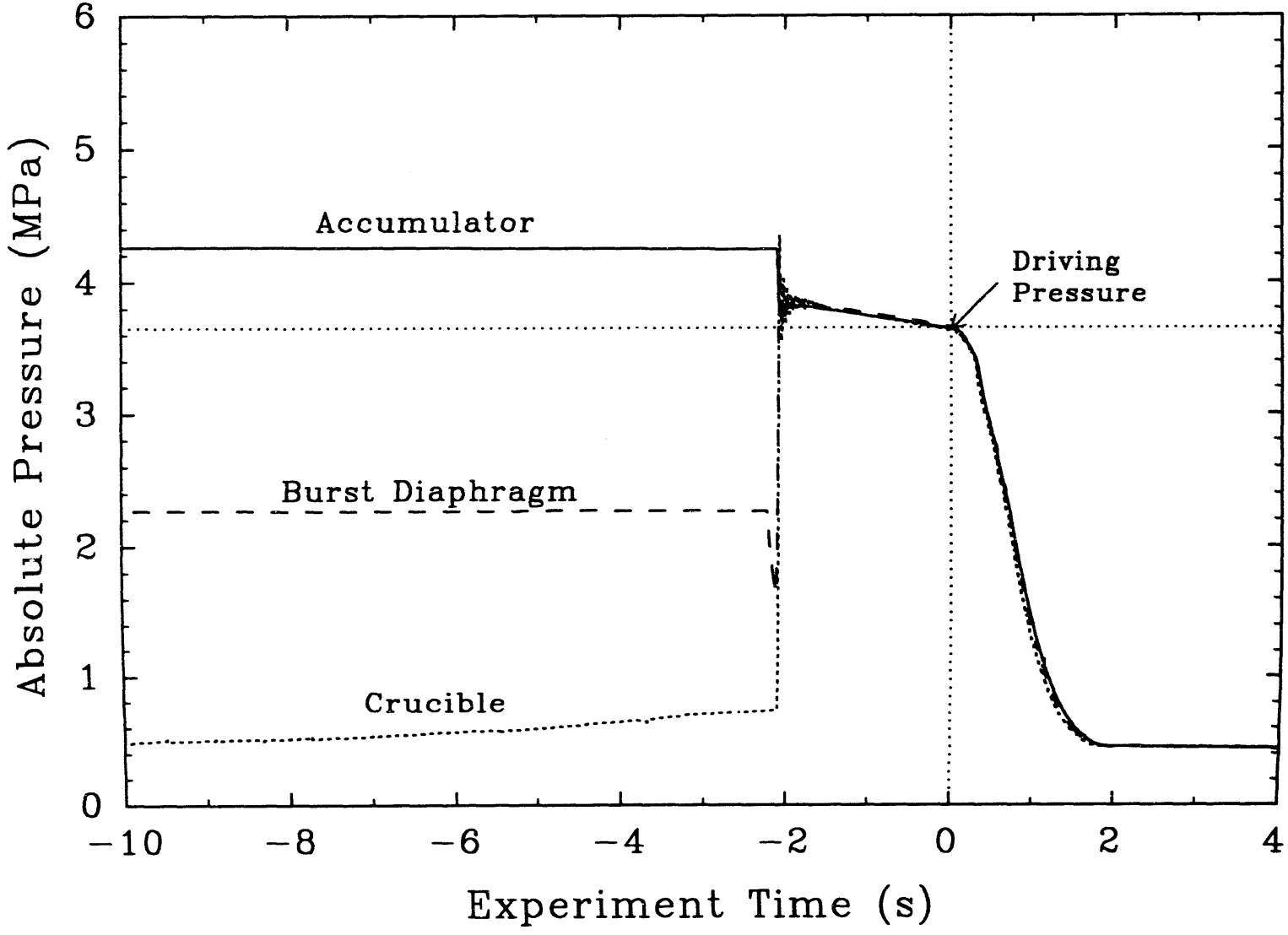

Figure 11. Blowdown history of the TDS−2 experiment.

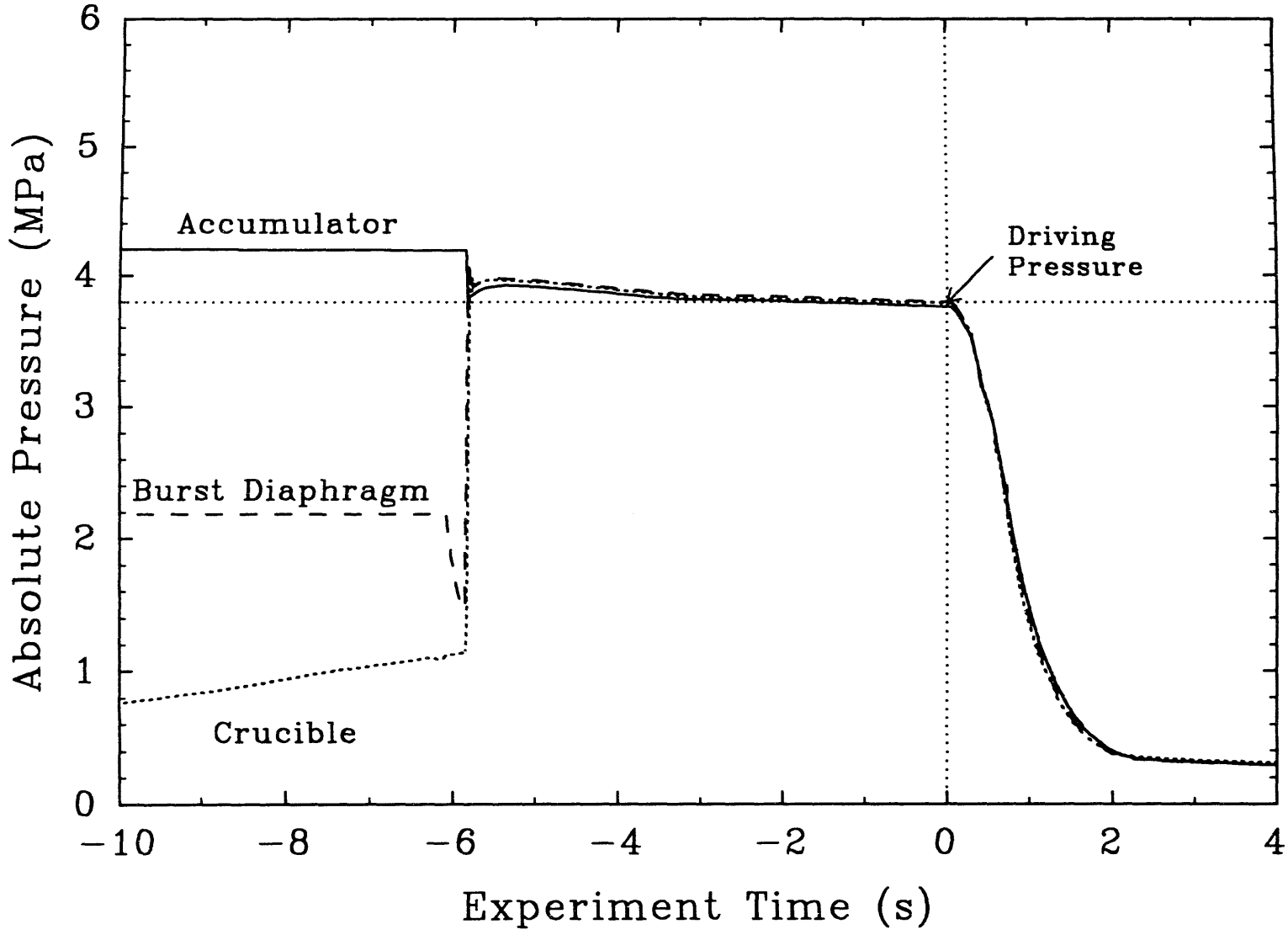

Figure 12. Blowdown history of the TDS−3 experiment.

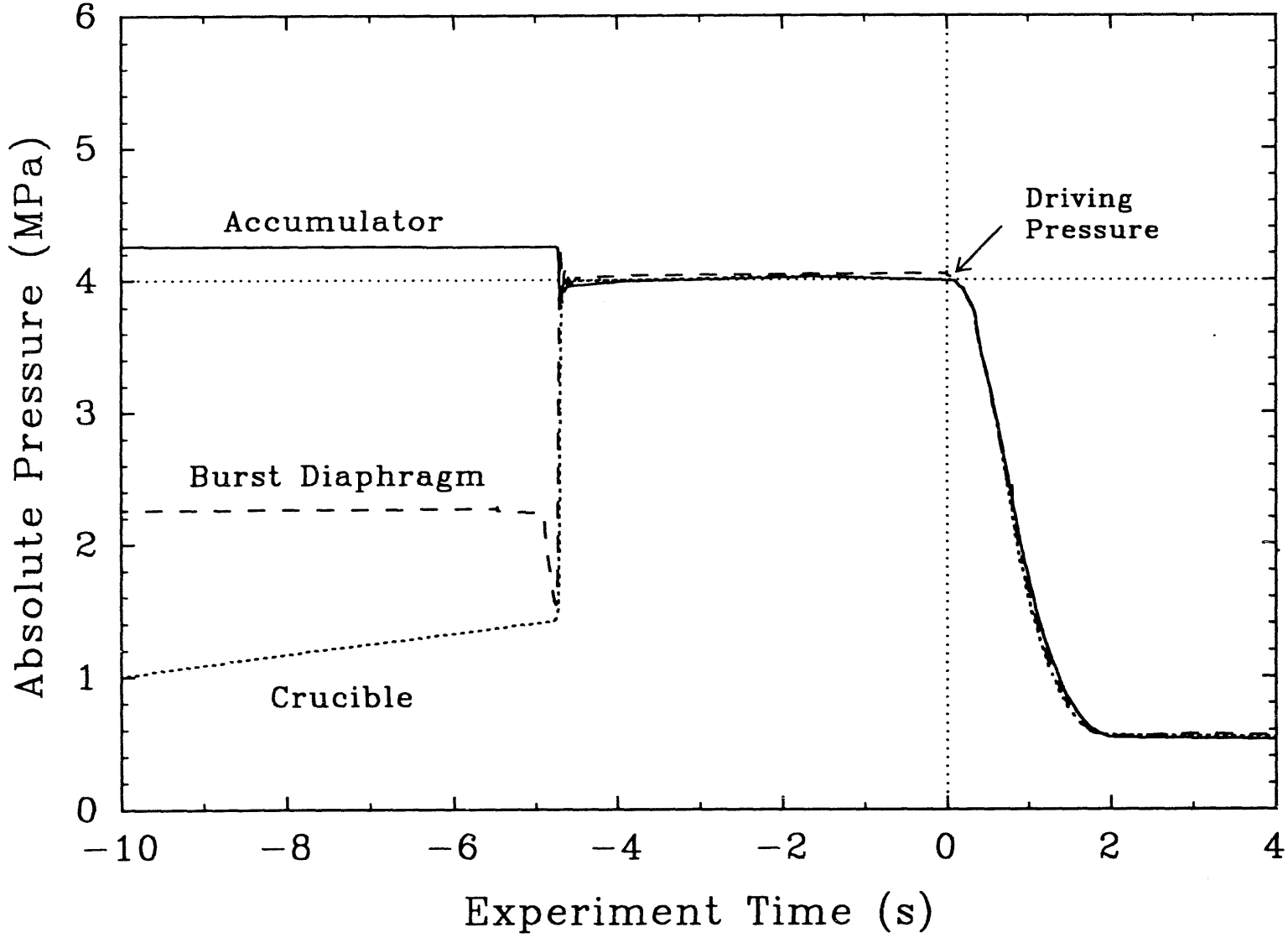

Figure 13. Blowdown history of the TDS−4 experiment.

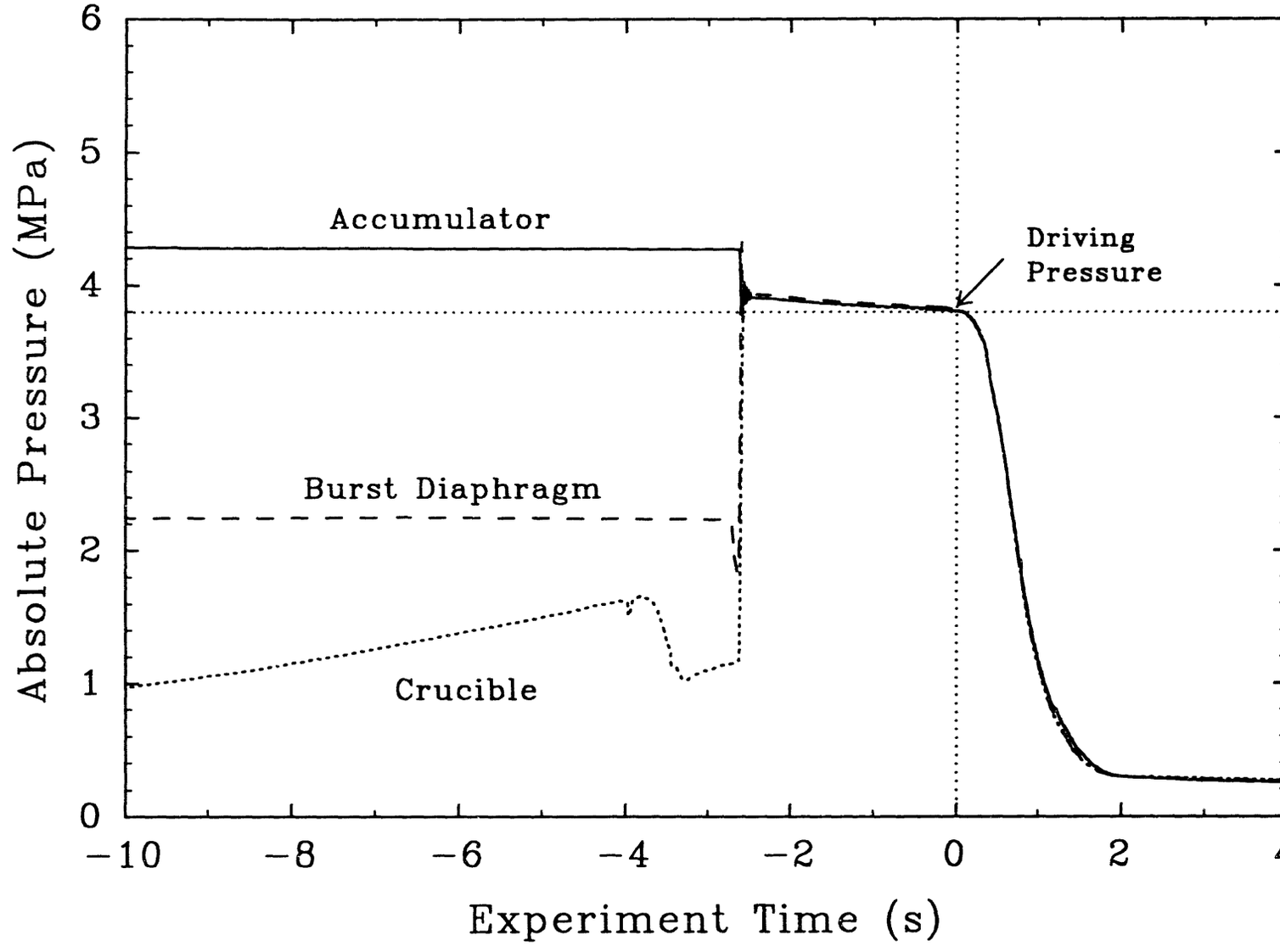

Figure 14. Blowdown history of the TDS−5 experiment.

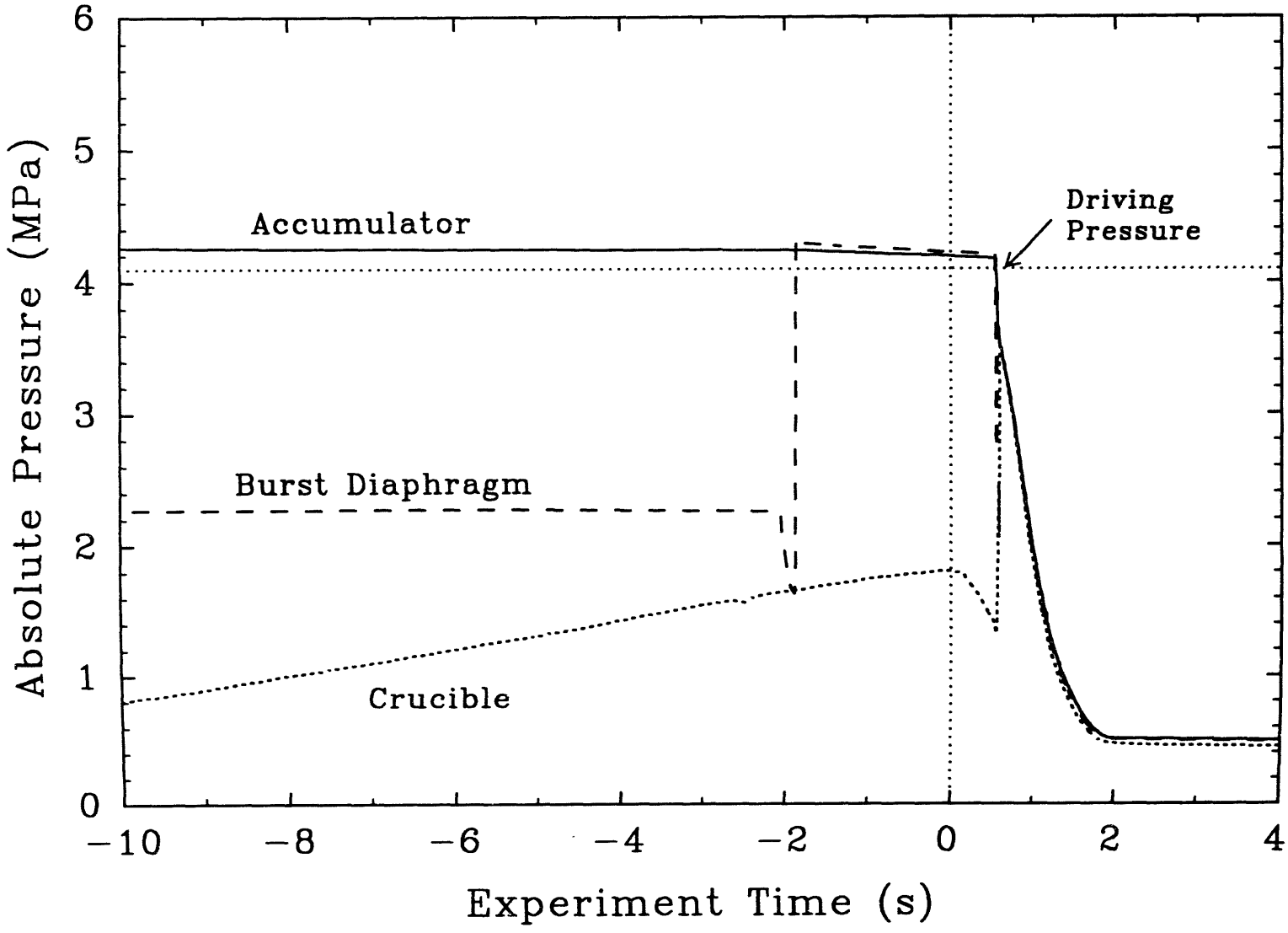

Figure 15. Blowdown history of the TDS−6 experiment.

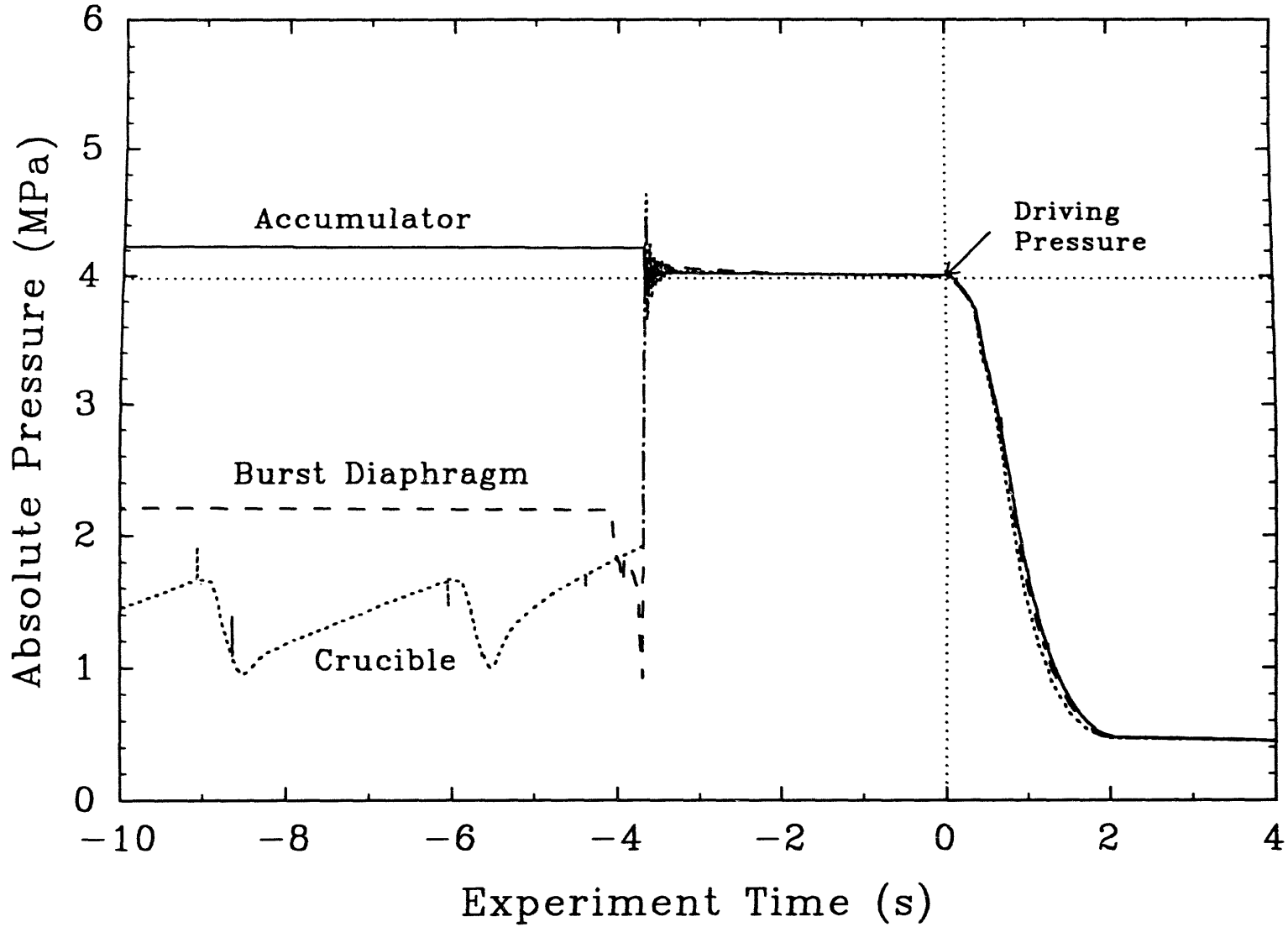

Figure 16. Blowdown history of the TDS−7 experiment.

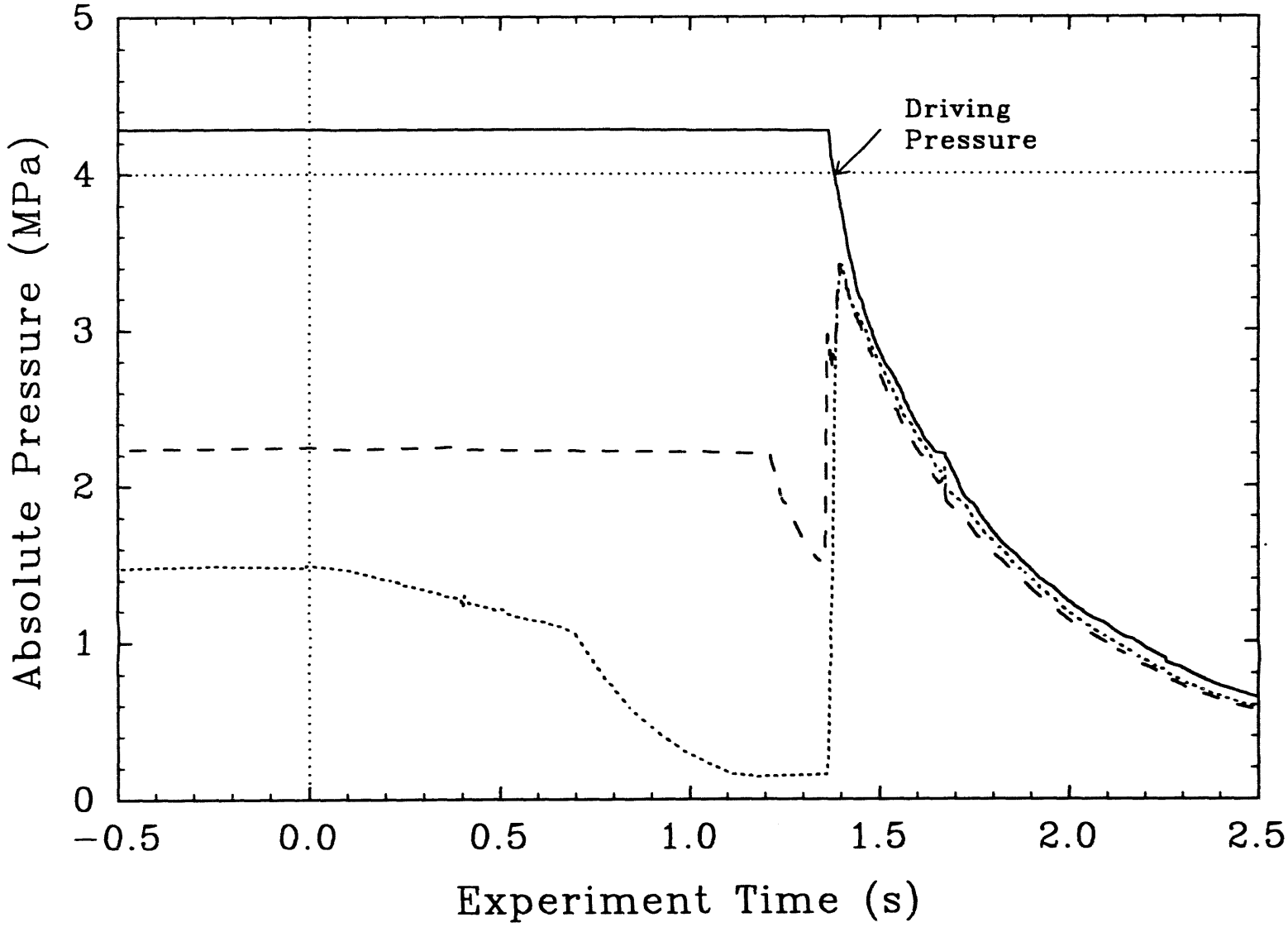

Figure 17. Steam blowdown time for the TDS−1 experiment.

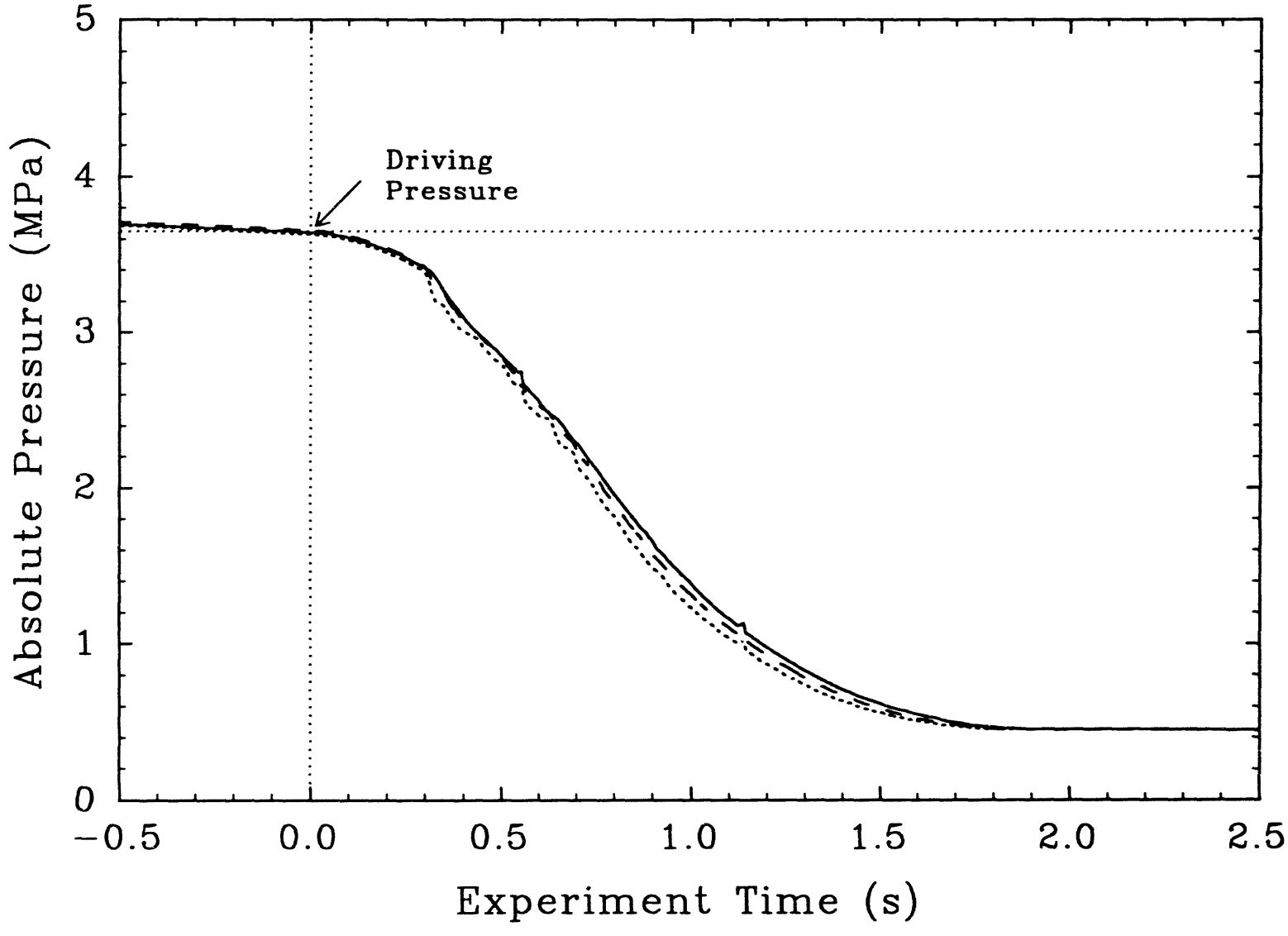

Figure 18. Steam blowdown time for the TDS-2 experiment.

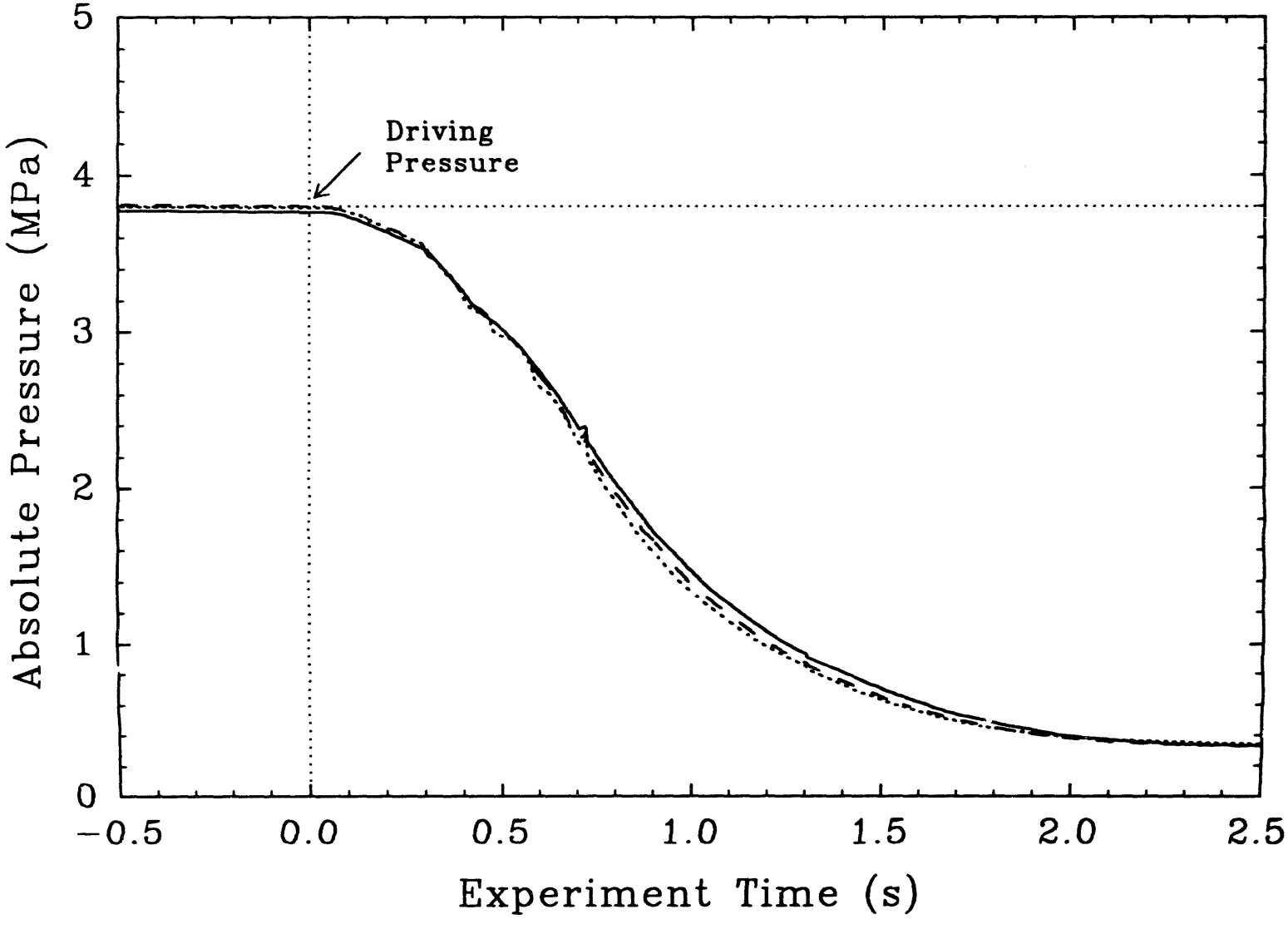

Figure 19. Steam blowdown time for the TDS−3 experiment.

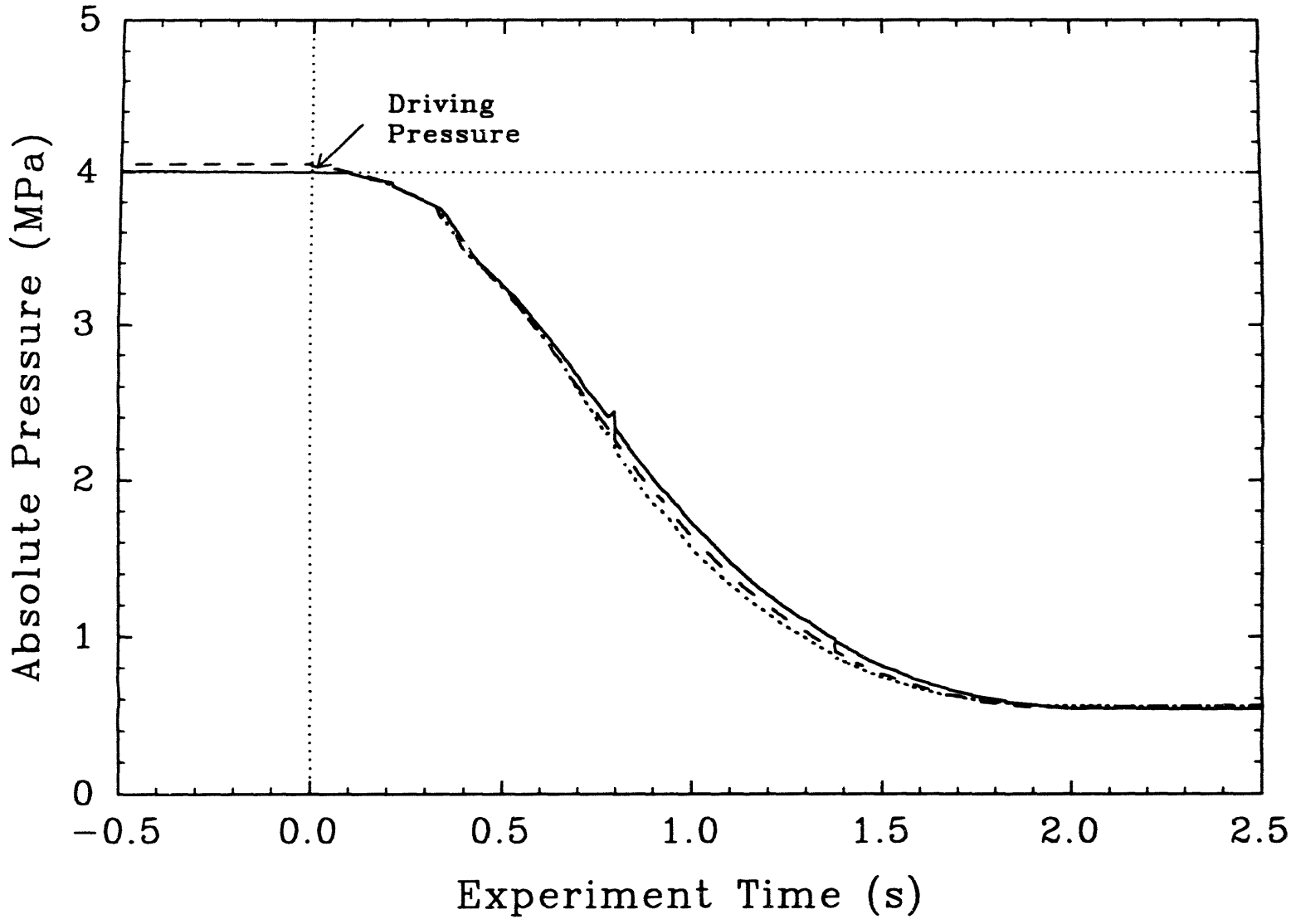

Figure 20. Steam blowdown time for the TDS−4 experiment.

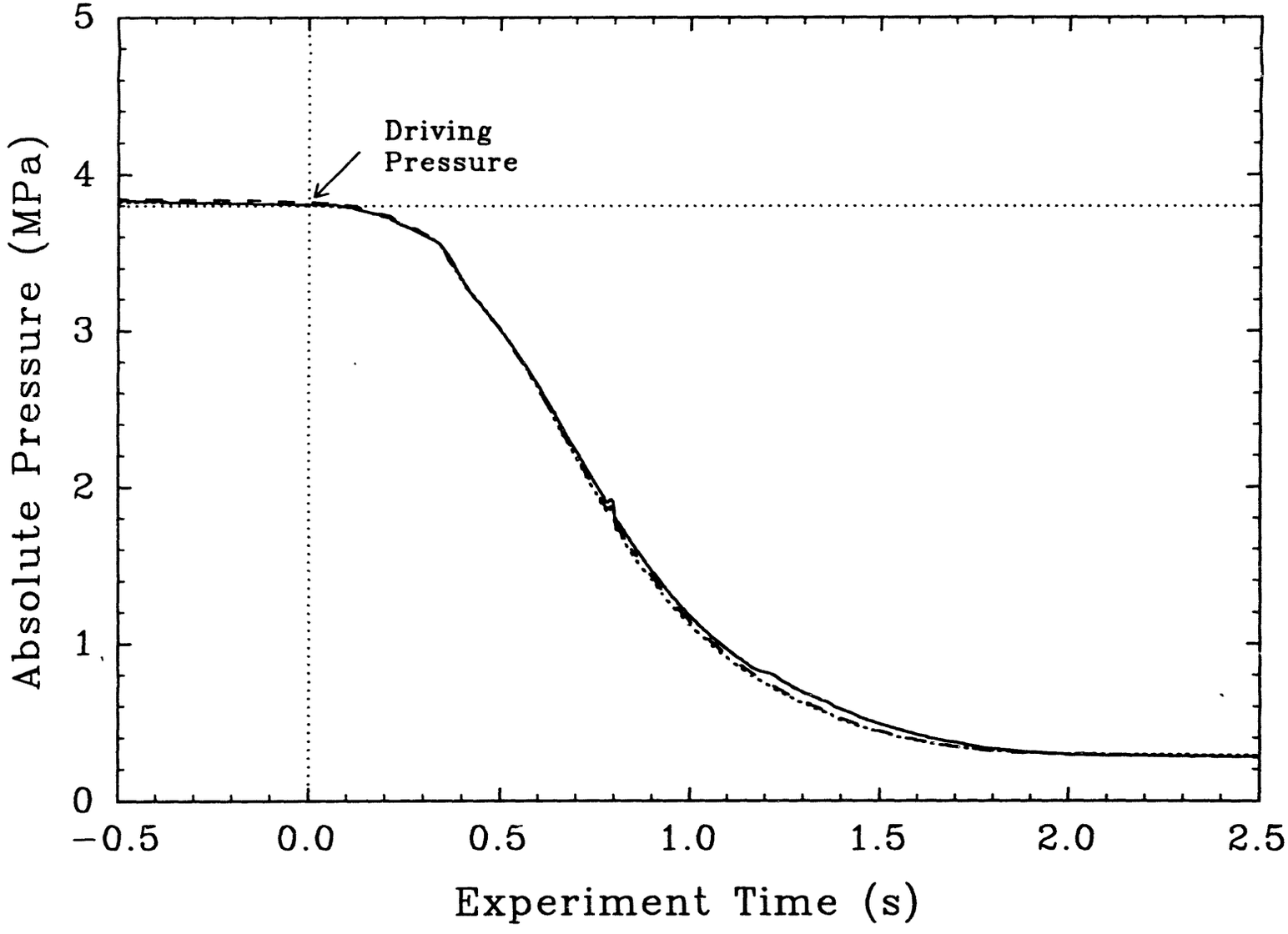

Figure 21. Steam blowdown time for the TDS−5 experiment.

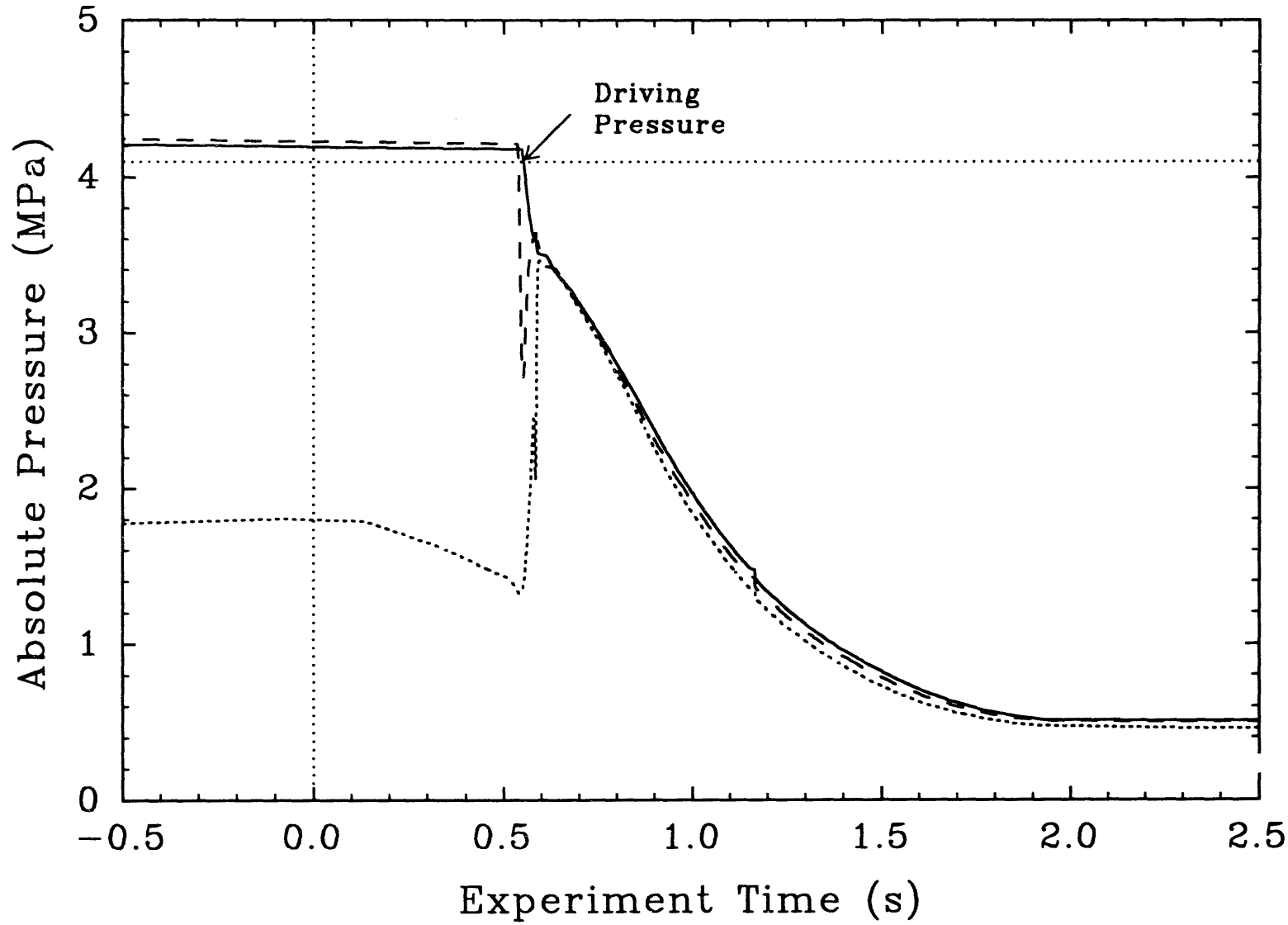

Figure 22. Steam blowdown time for the TDS−6 experiment.

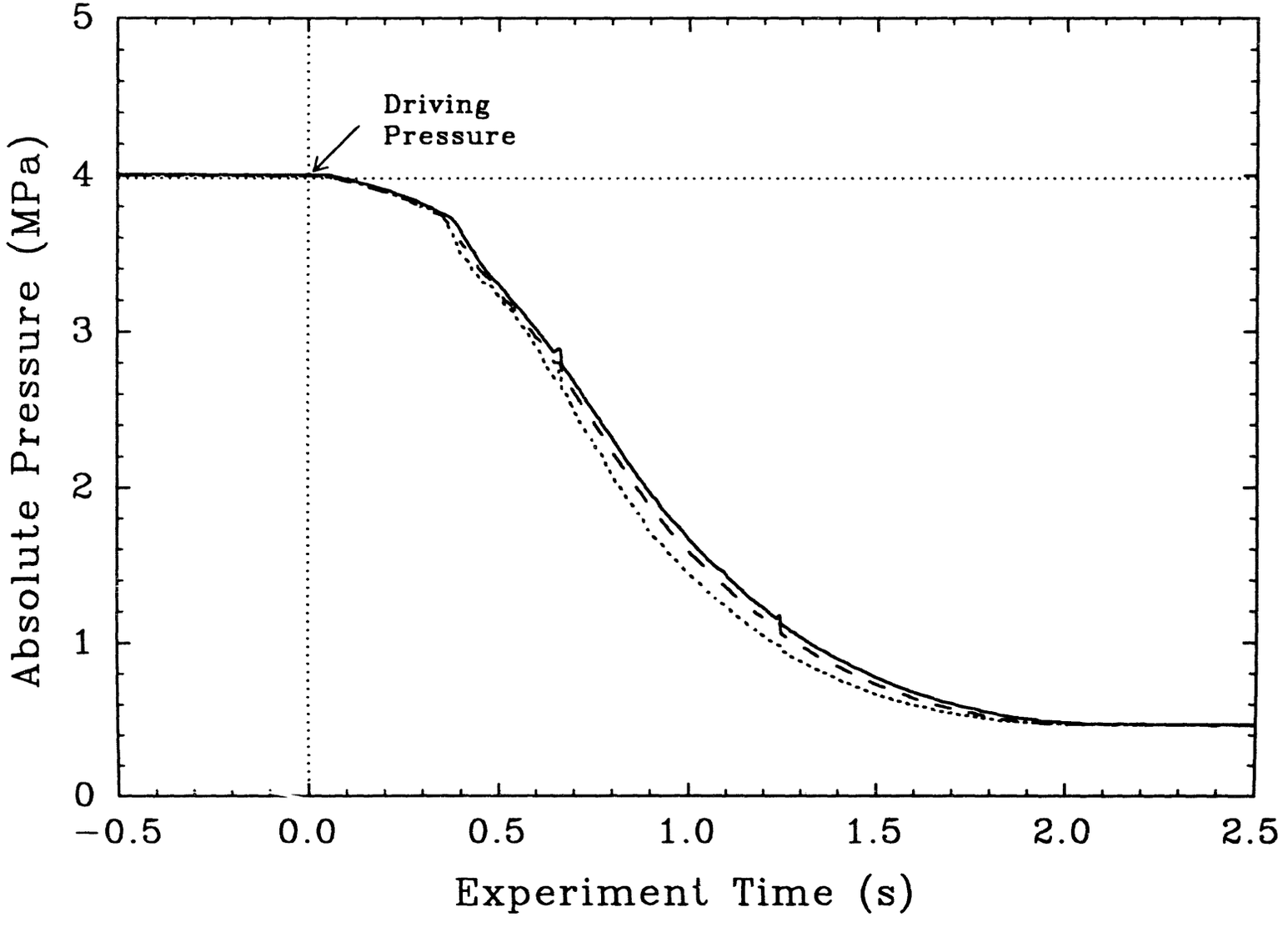

Figure 23. Steam blowdown time for the TDS−7 experiment.

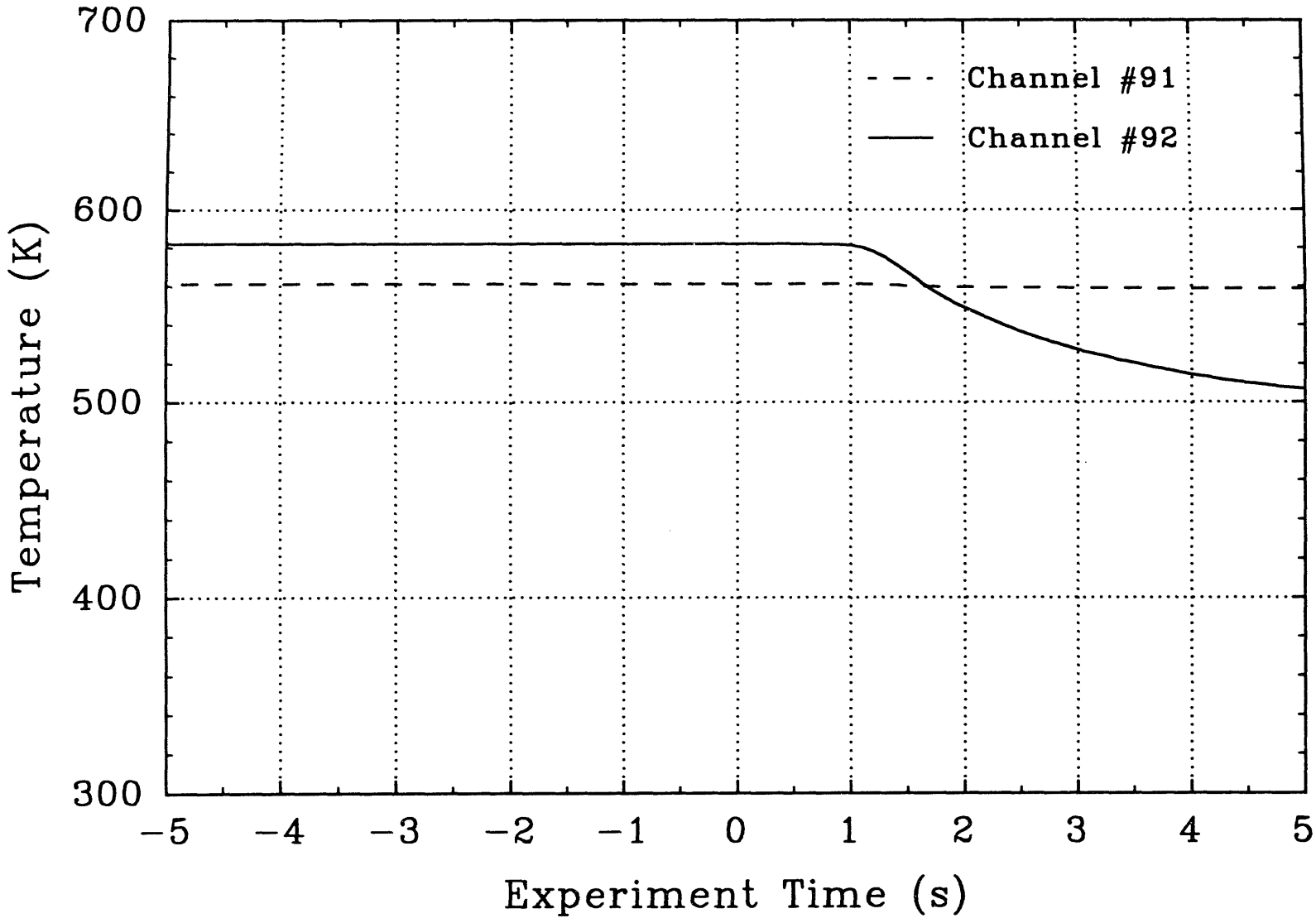

Figure 24. Steam temperatures measured in the steam accumulator tank with type-K thermocouples in the TDS-1 experiment.

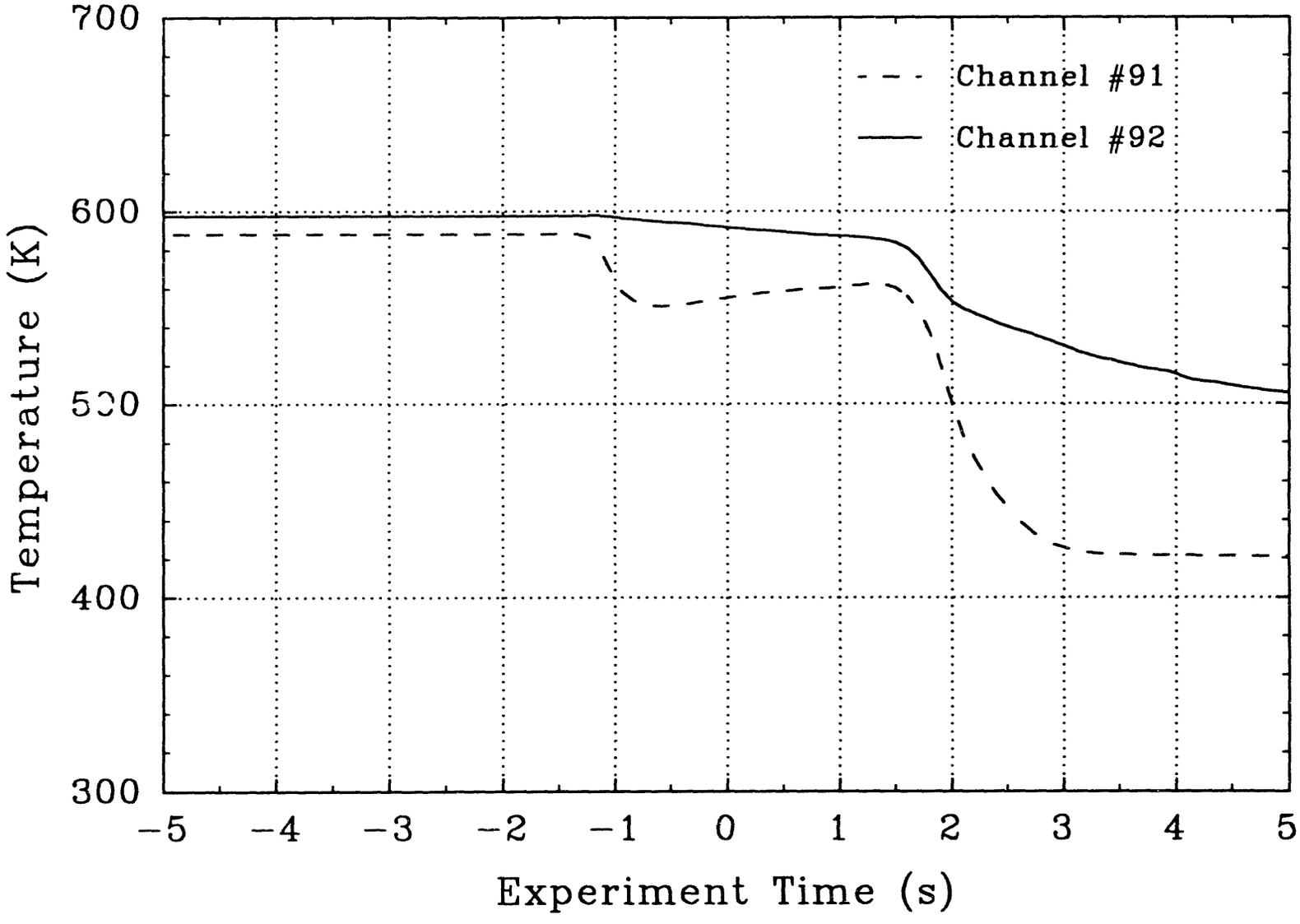

Figure 25. Steam temperatures measured in the steam accumulator tank with type-K thermocouples in the TDS-2 experiment.

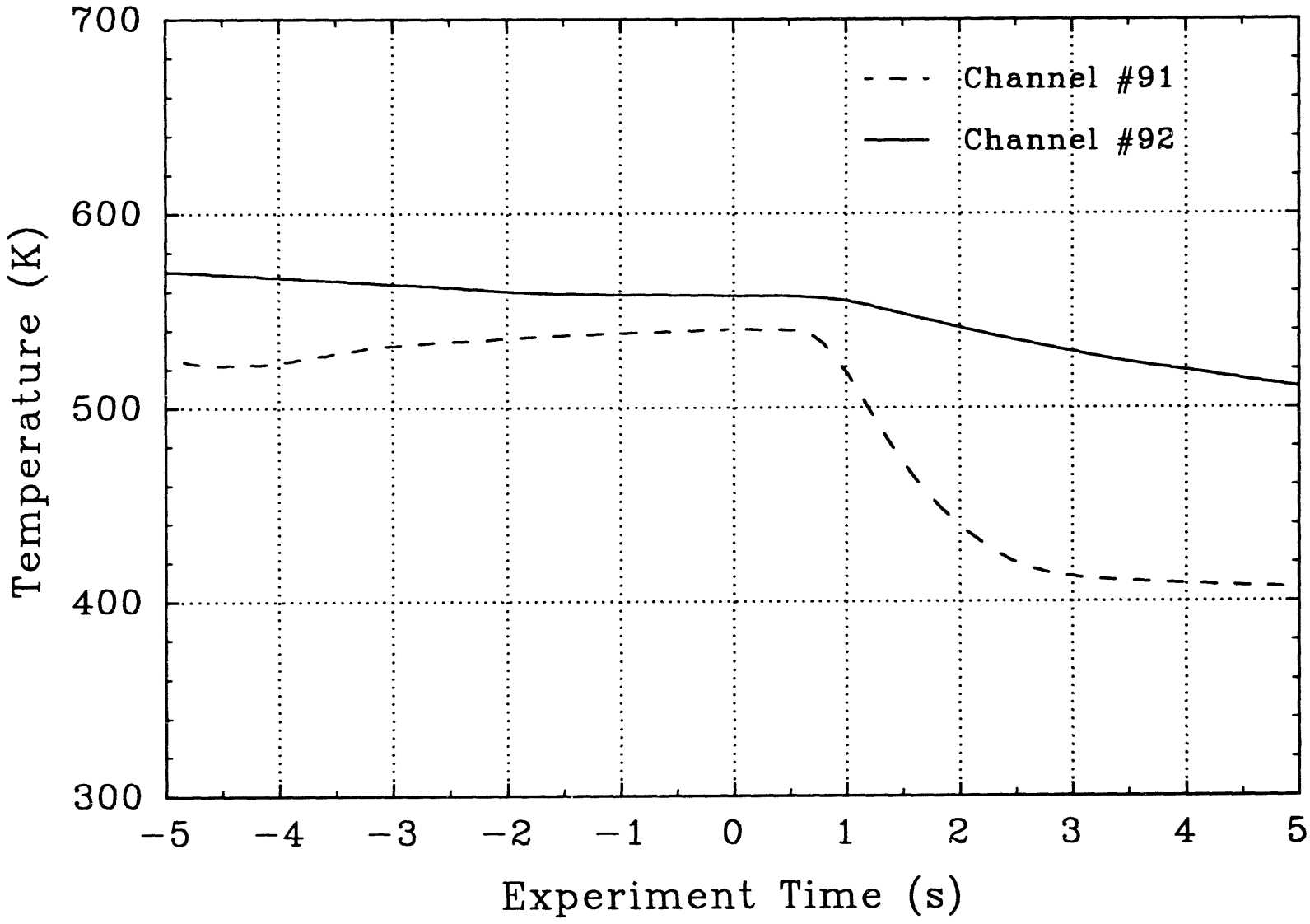

Figure 26. Steam temperatures measured in the steam accumulator tank with type−K thermocouples in the TDS−3 experiment.

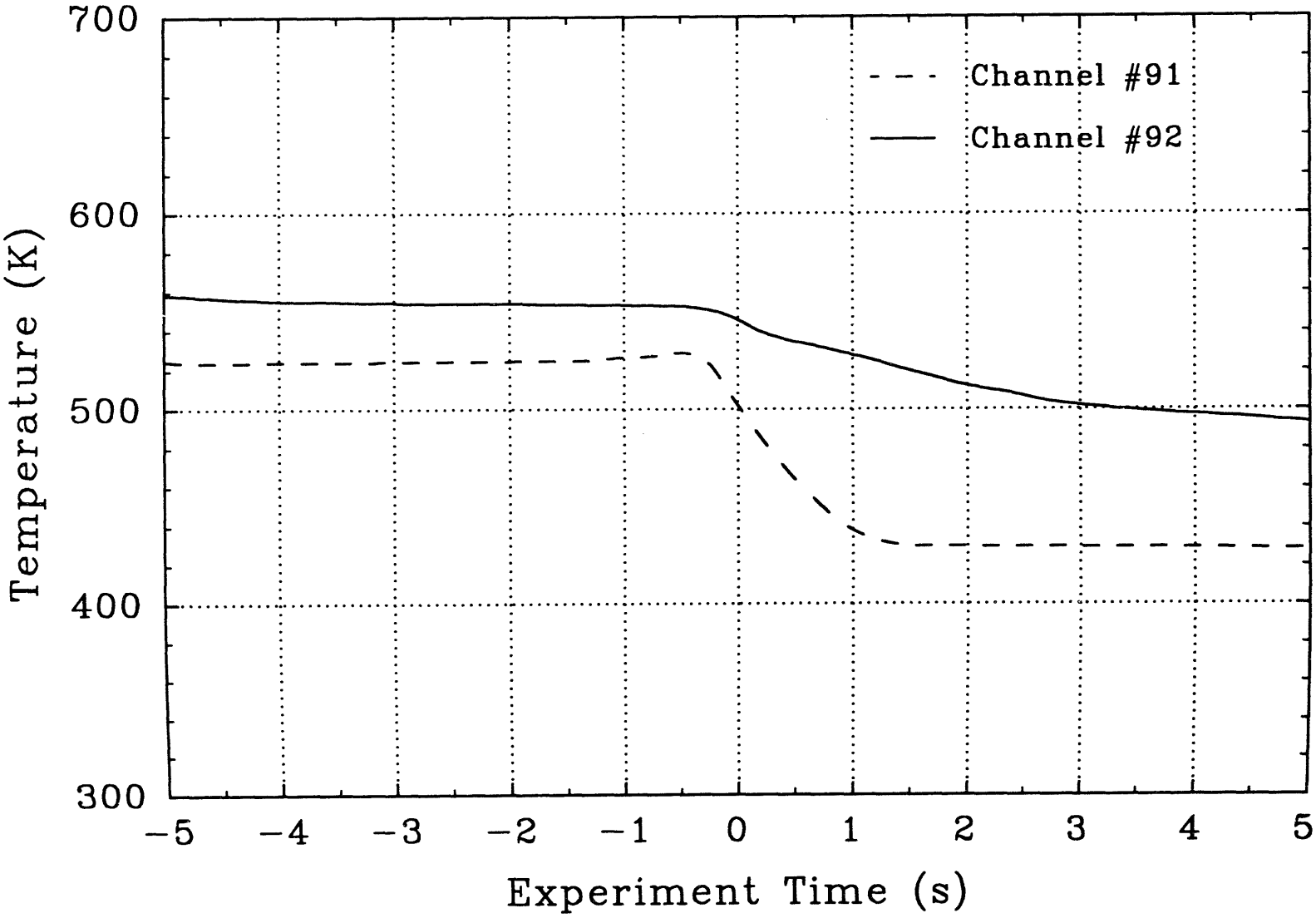

Figure 27. Steam temperatures measured in the steam accumulator tank with type-K thermocouples in the TDS-4 experiment.

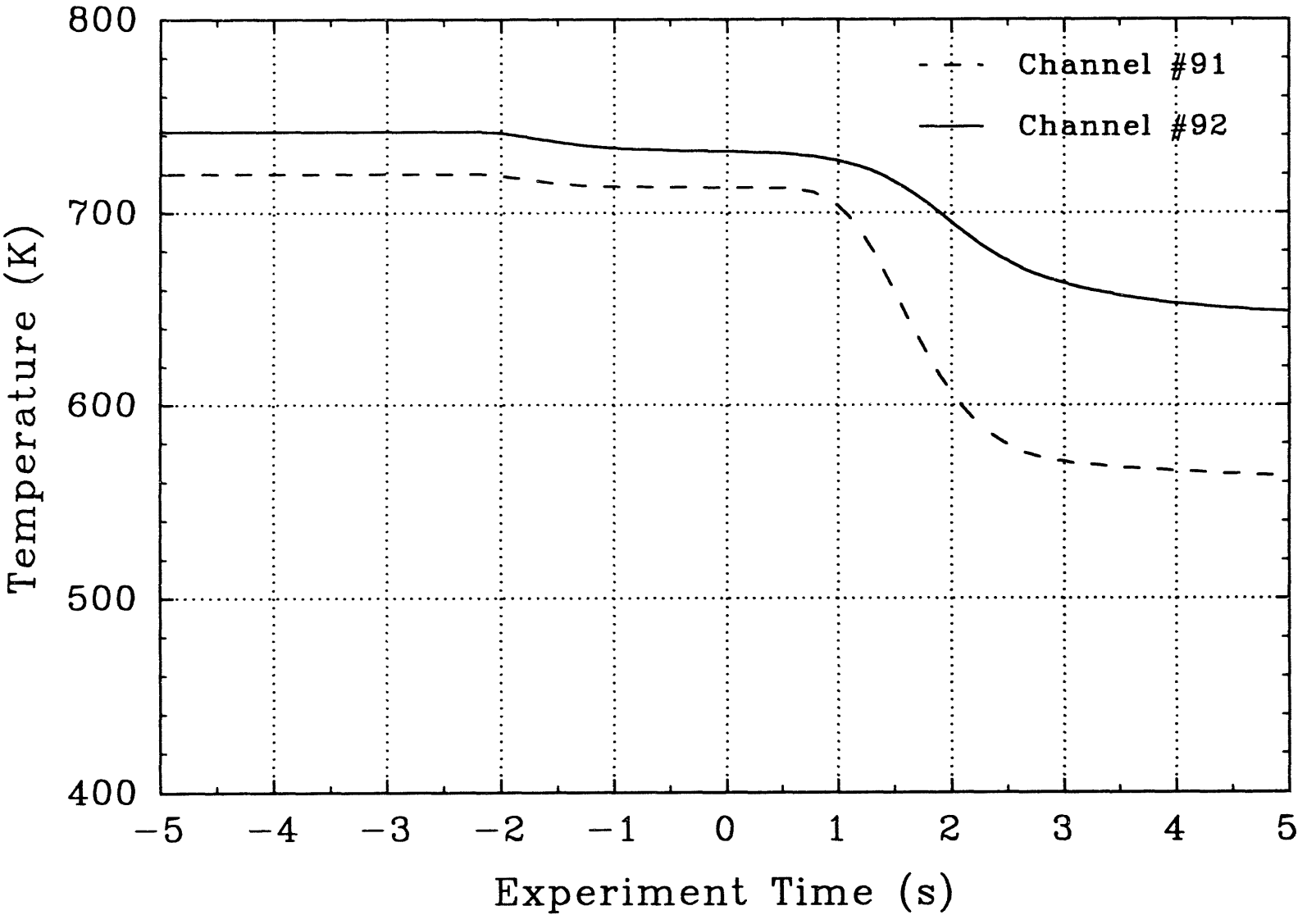

Figure 28. Steam temperatures measured in the steam accumulator tank with type-K thermocouples in the TDS-5 experiment.

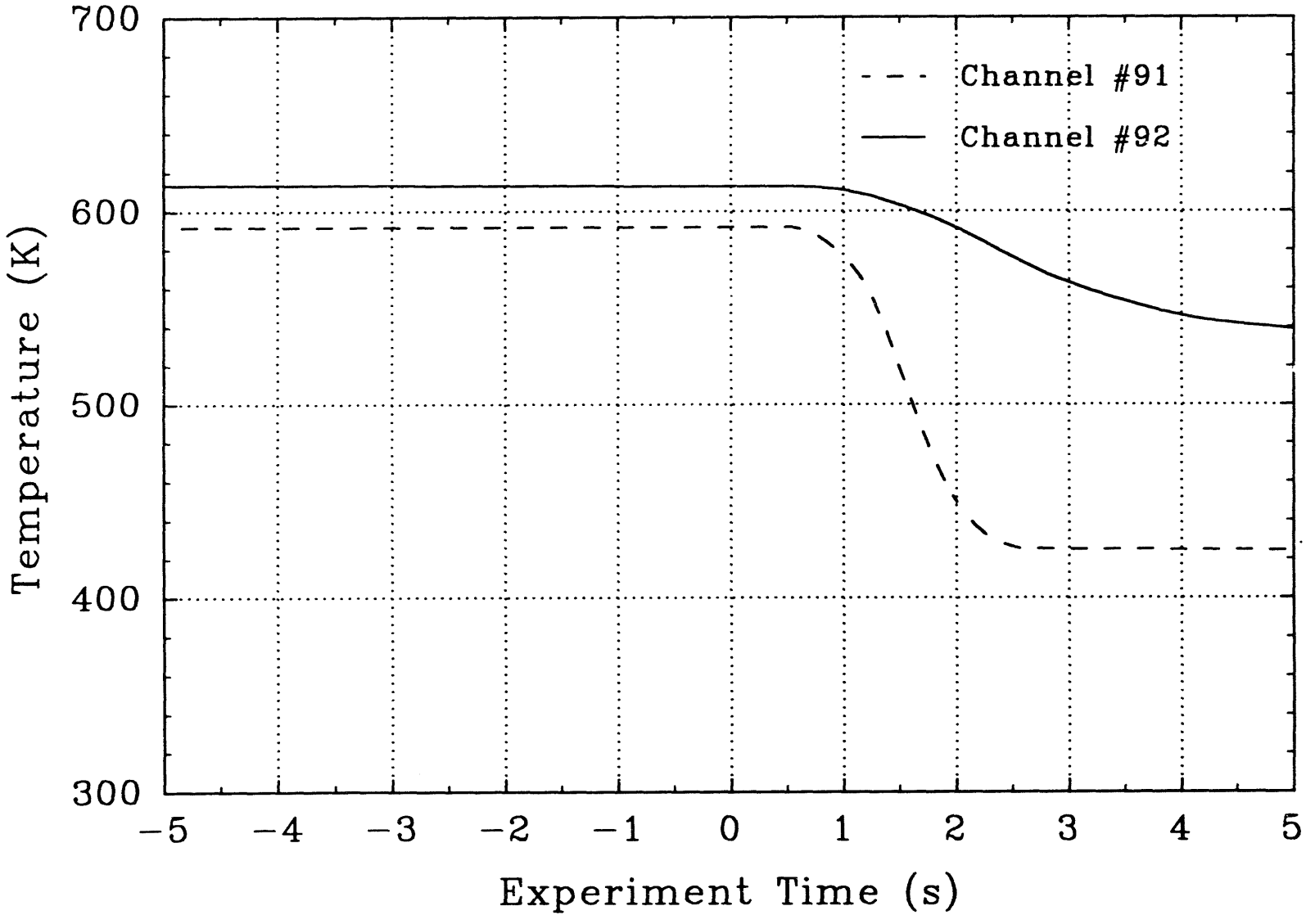

Figure 29. Steam temperatures measured in the steam accumulator tank with type−K thermocouples in the TDS−6 experiment.

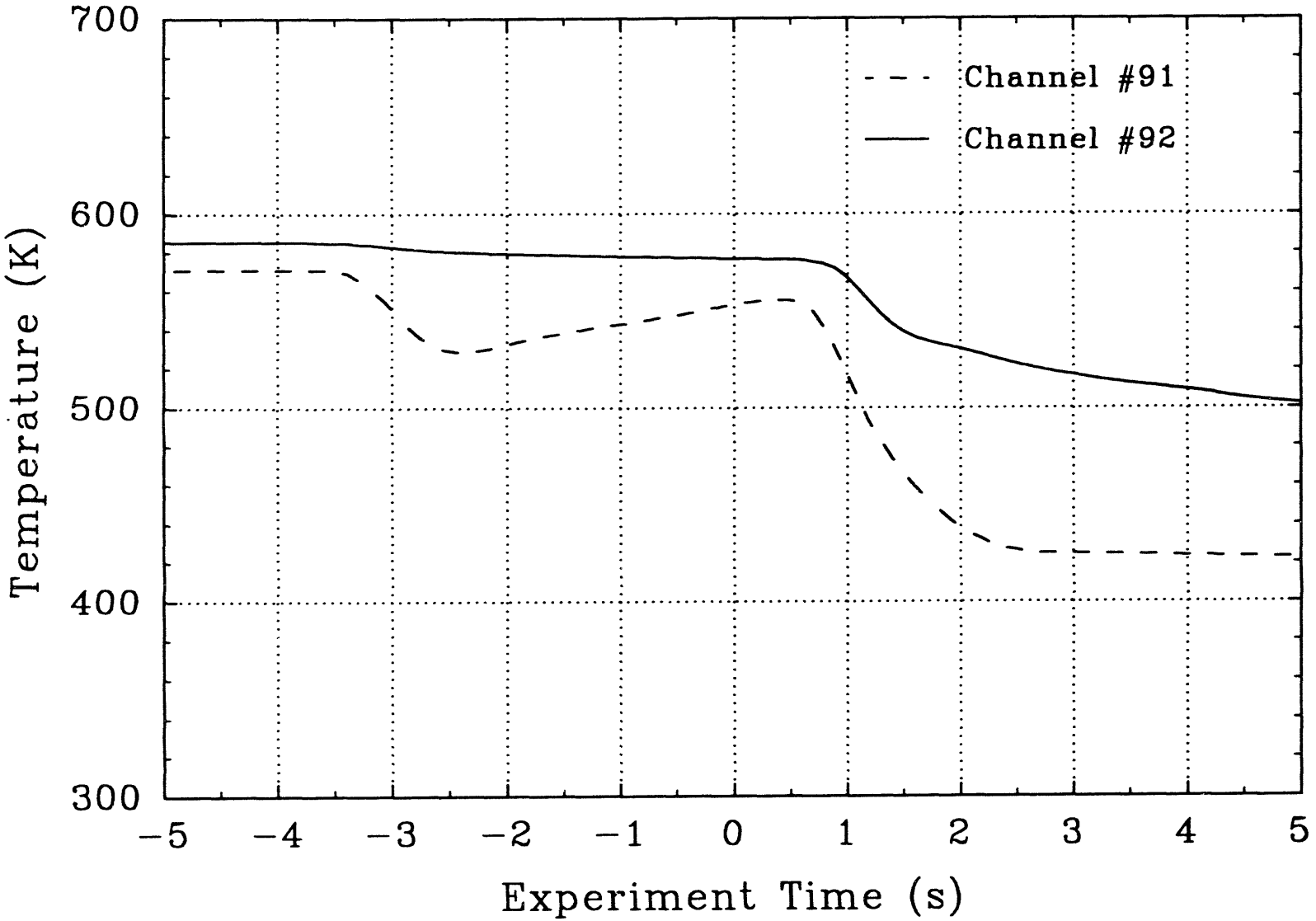

Figure 30. Steam temperatures measured in the steam accumulator tank with type-K thermocouples in the TDS-7 experiment.

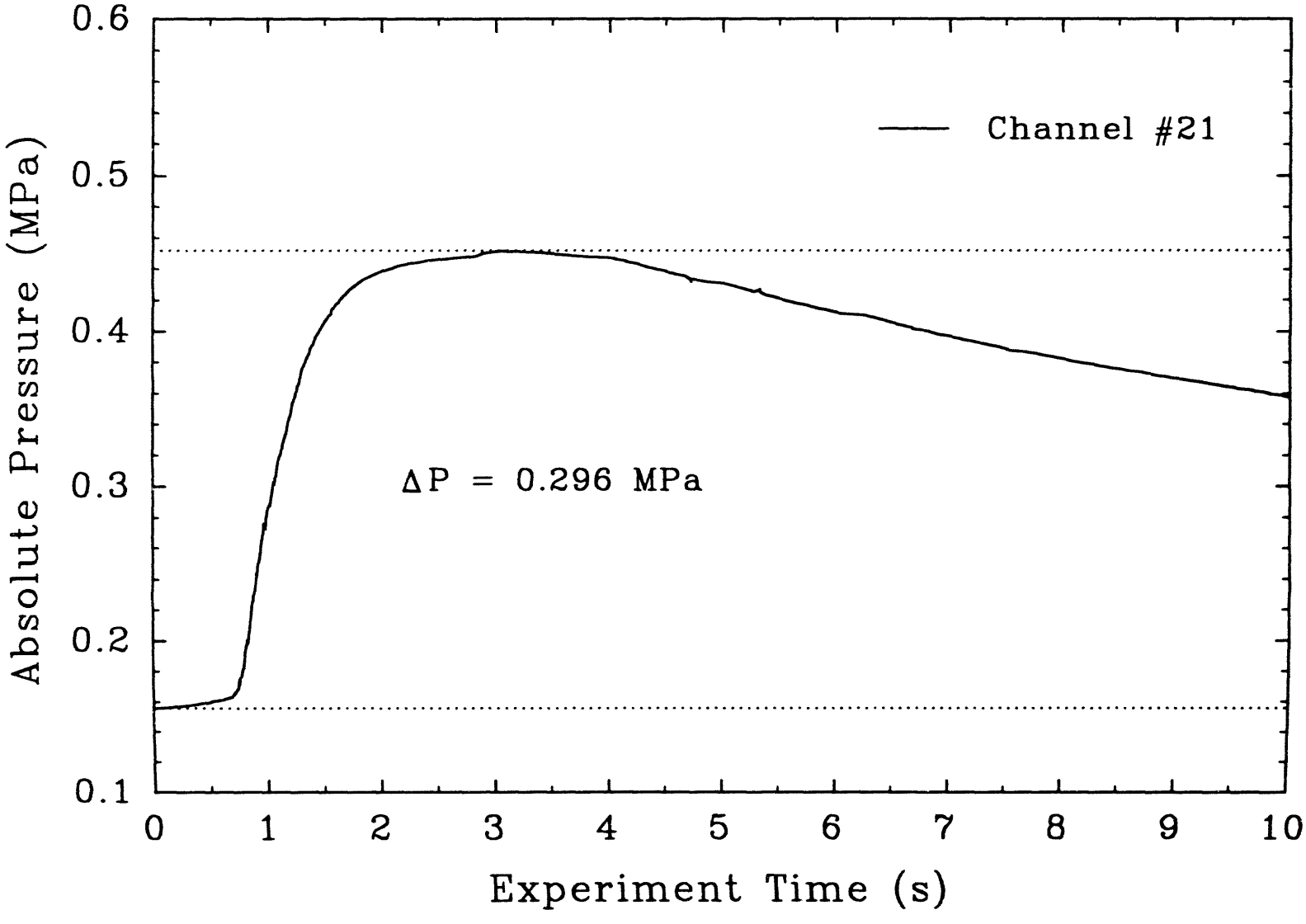

Figure 31. Surtsey vessel pressure versus time measured at level 1 in the TDS-1 experiment.

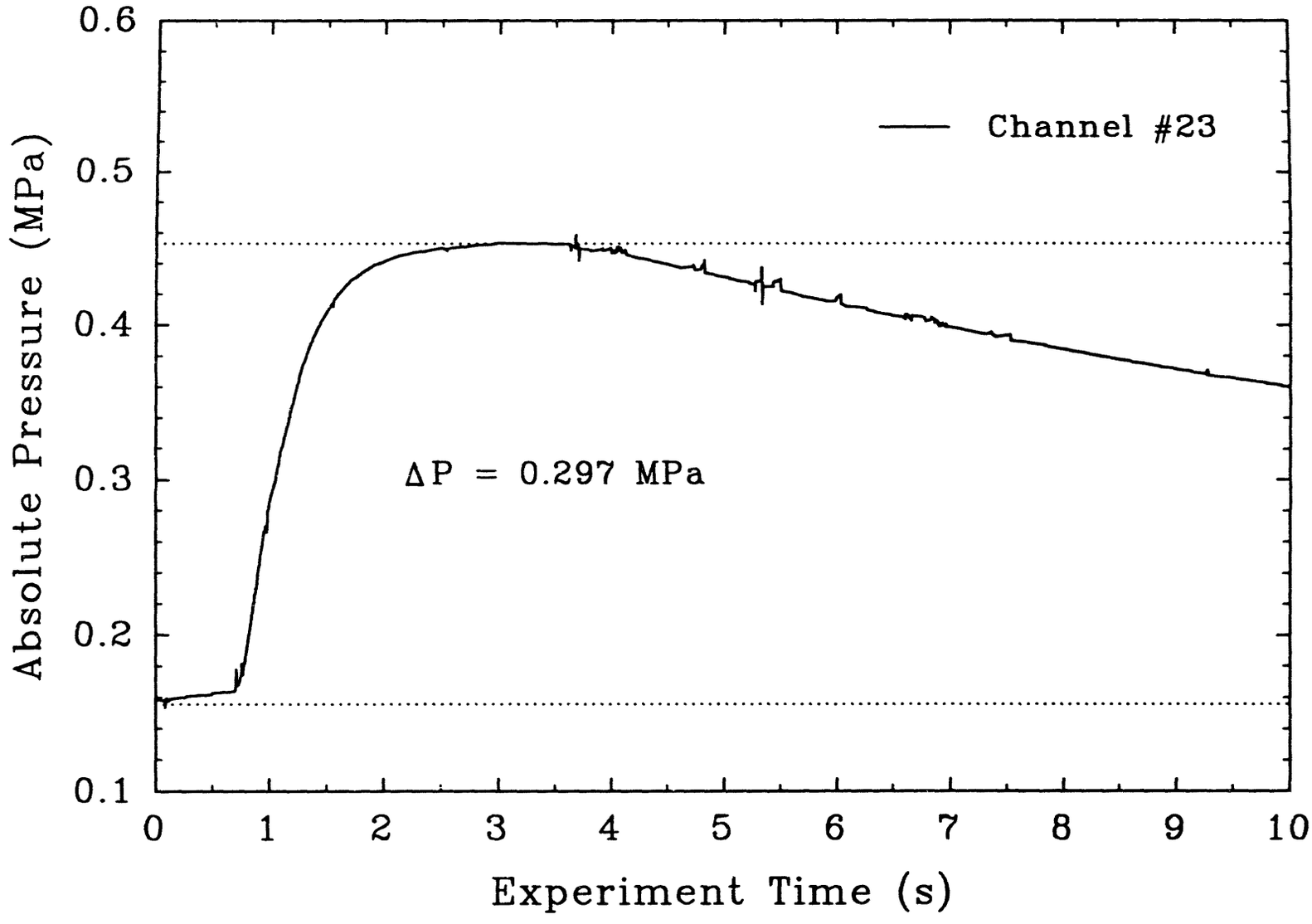

Figure 32. Surtsey vessel pressure versus time measured at level 3 in the TDS-1 experiment.

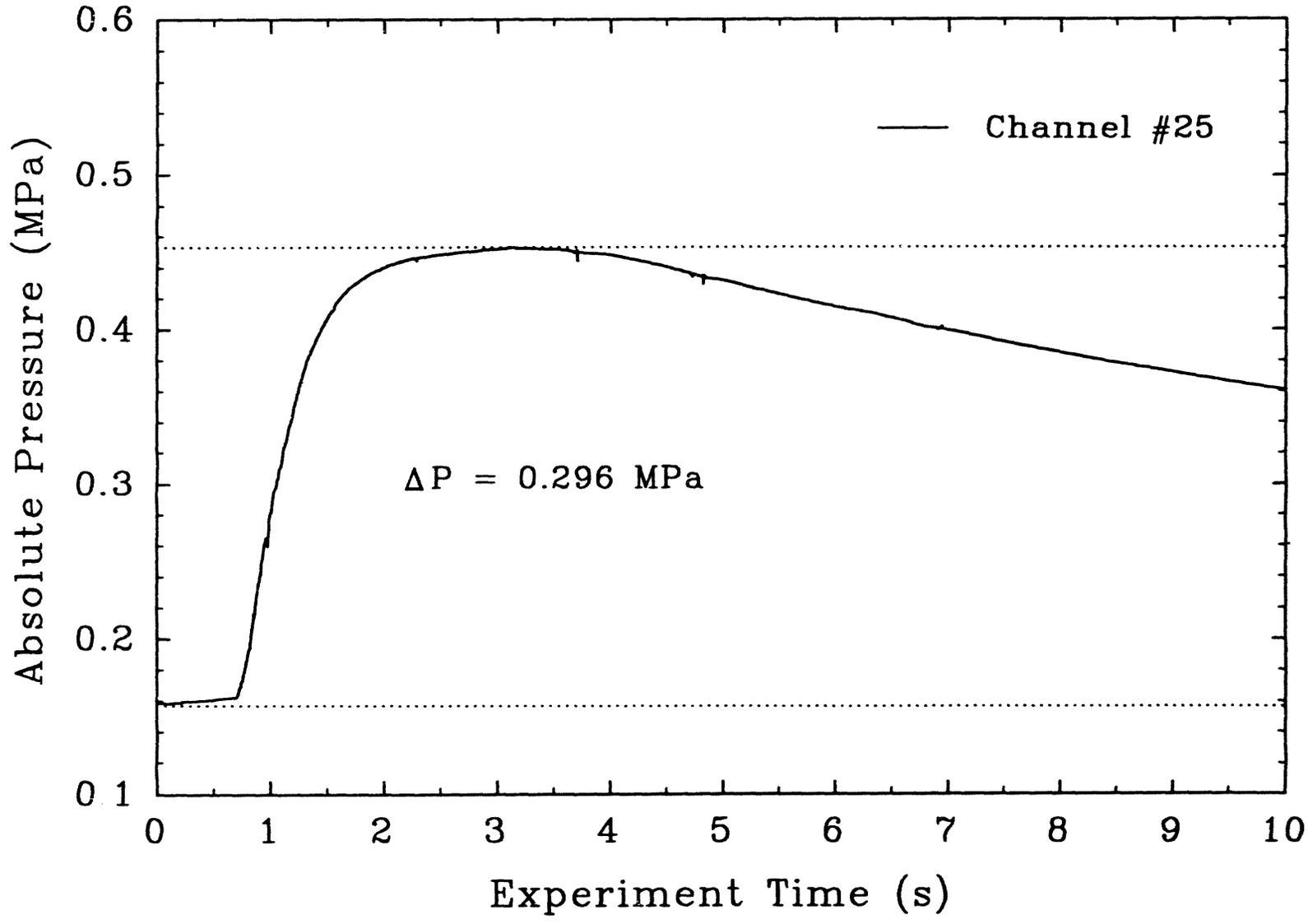

Figure 33. Surtsey vessel pressure versus time measured at level 5 in the TDS-1 experiment.

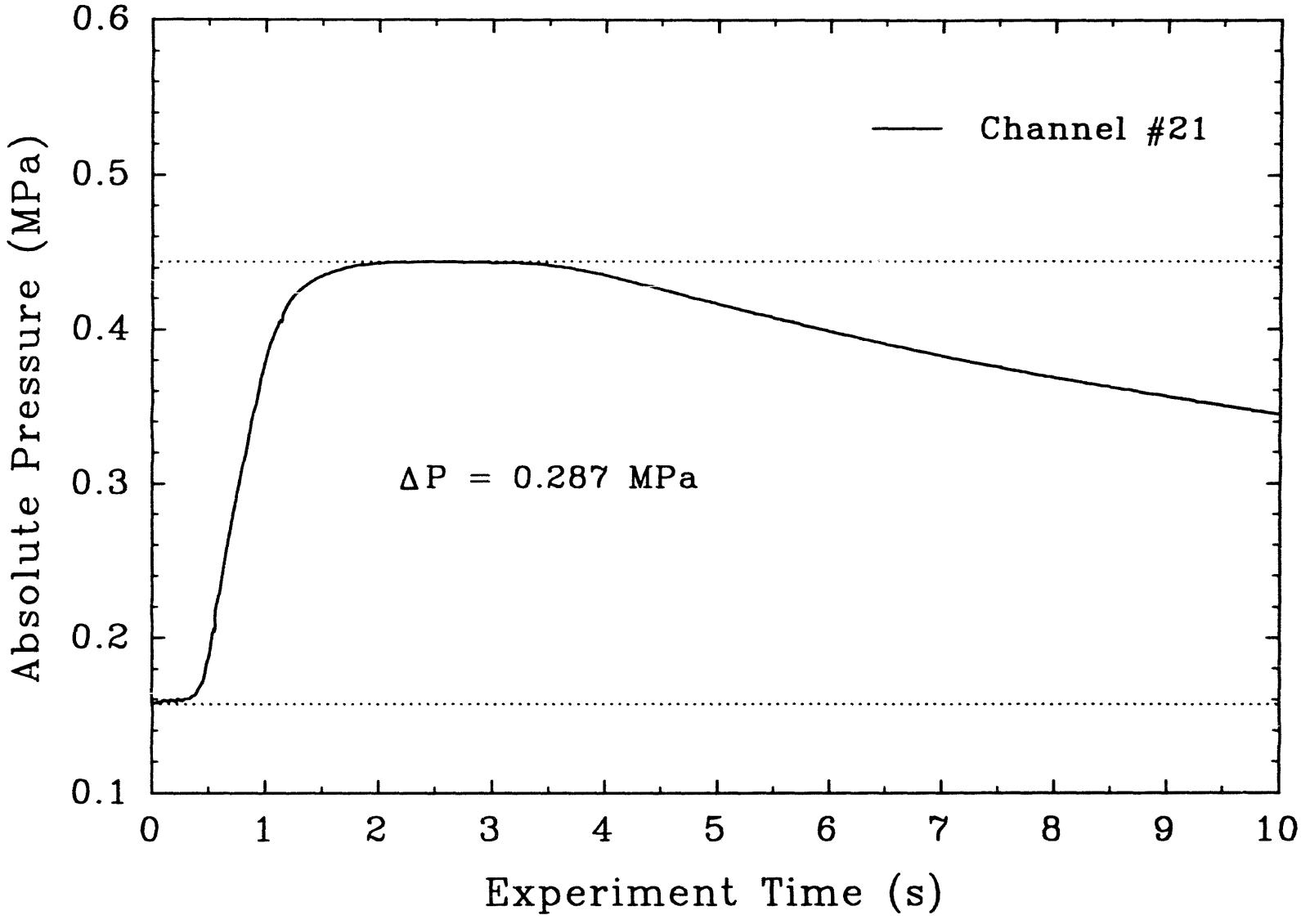

Figure 34. Surtsey vessel pressure versus time measured at level 1 in the TDS-2 experiment.

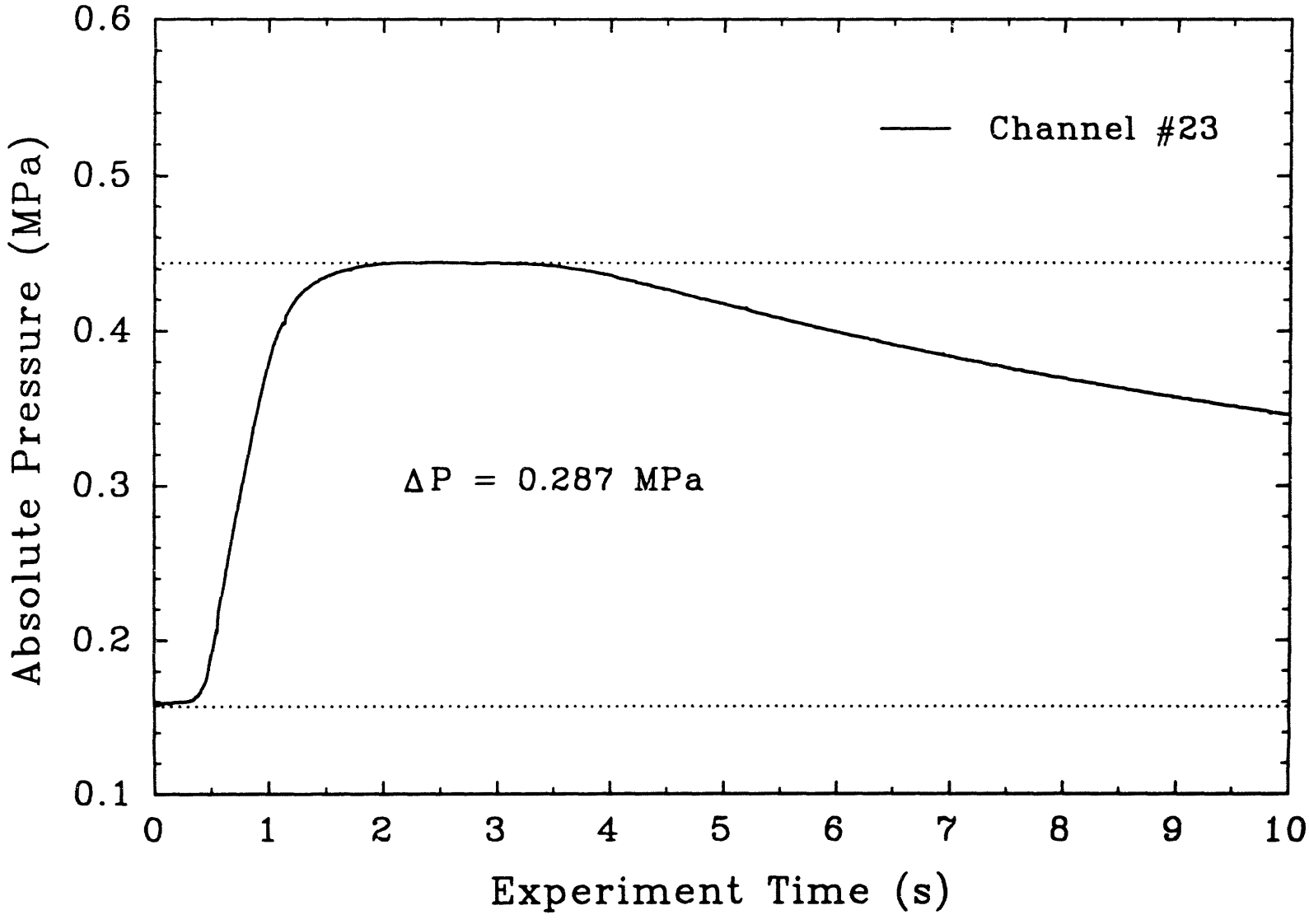

Figure 35. Surtsey vessel pressure versus time measured at level 3 in the TDS-2 experiment.

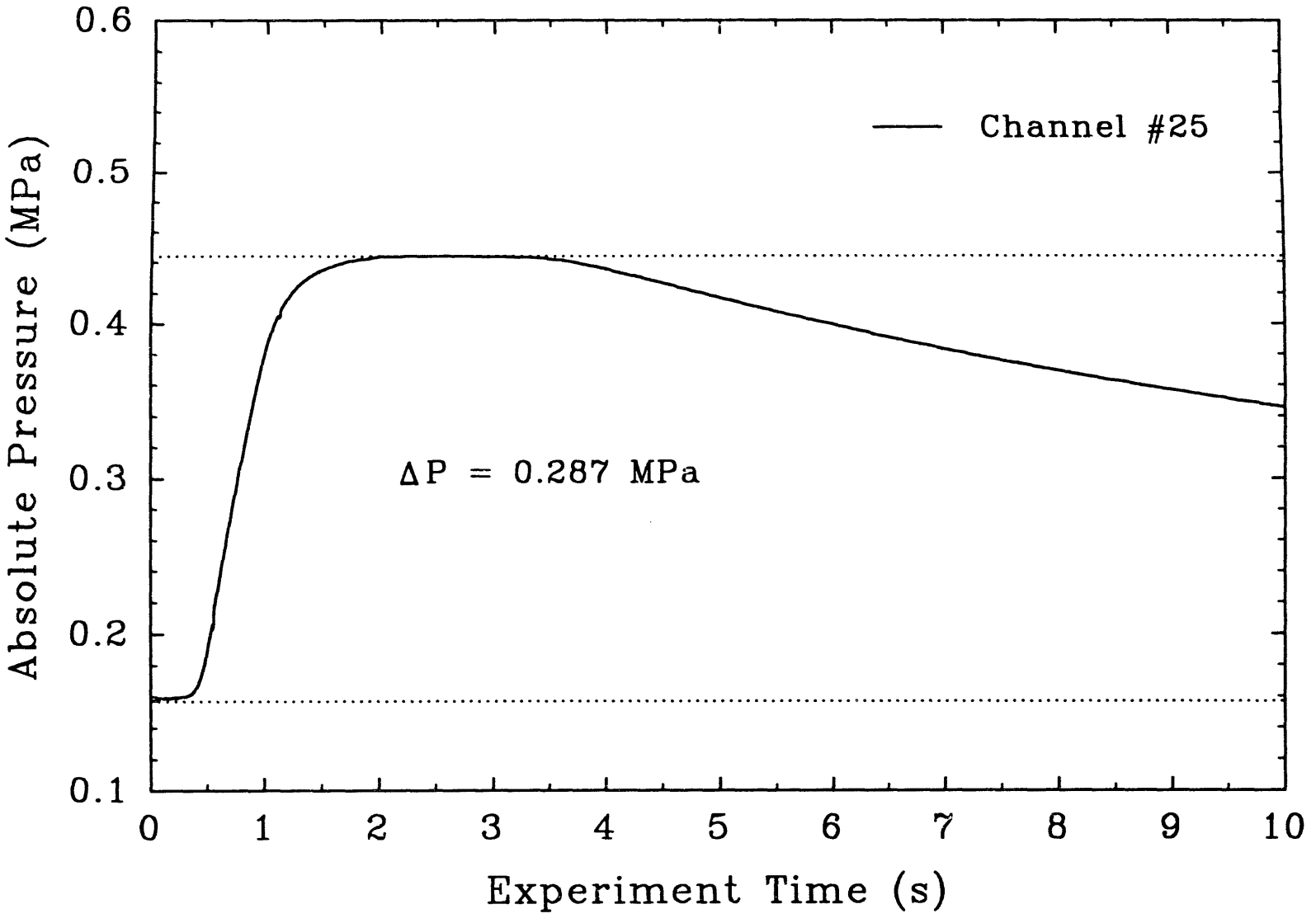

Figure 36. Surtsey vessel pressure versus time measured at level 5 in the TDS-2 experiment.

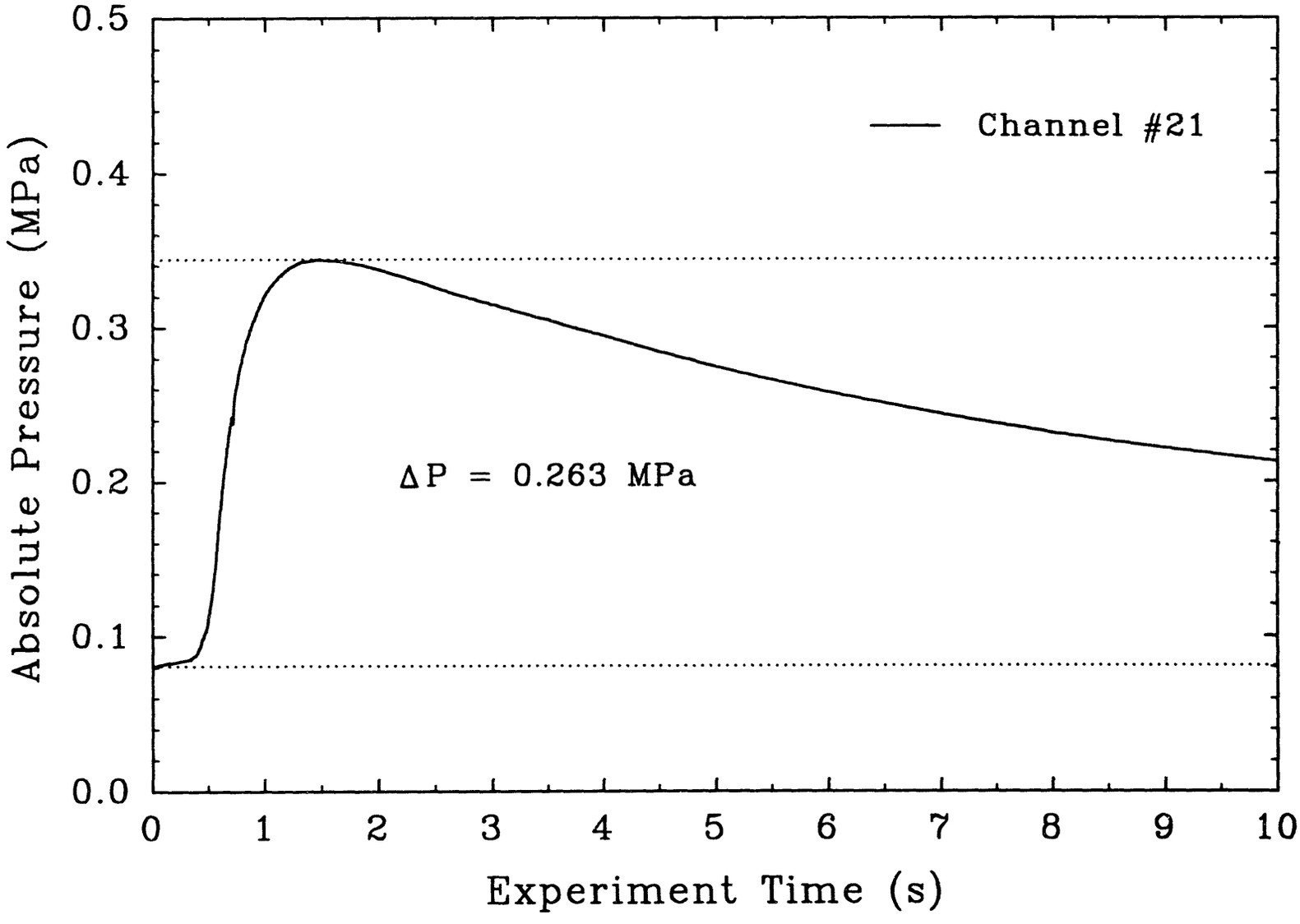

Figure 37. Surtsey vessel pressure versus time measured at level 1 in the TDS-3 experiment.

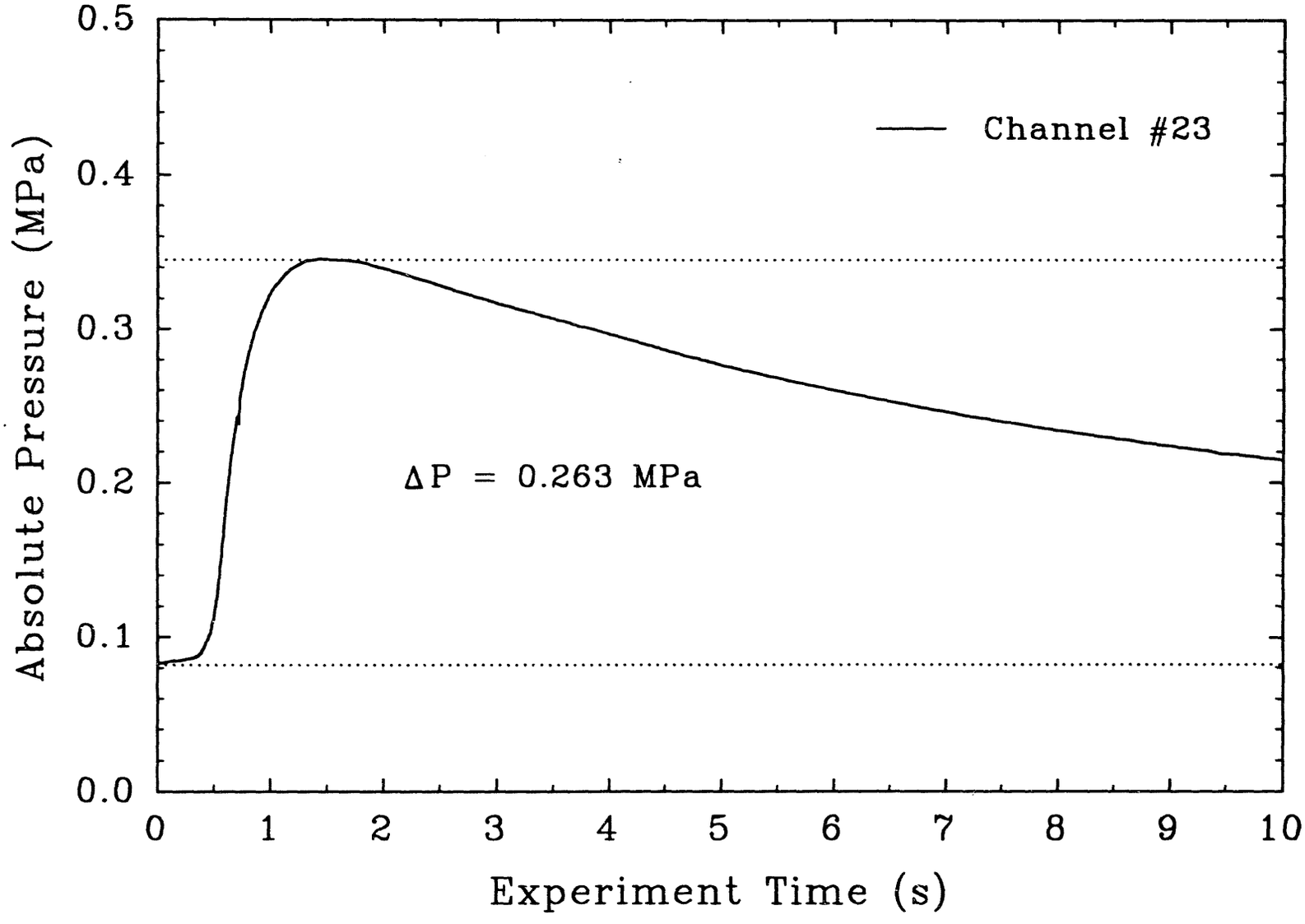

Figure 38. Surtsey vessel pressure versus time measured at level 3 in the TDS-3 experiment.

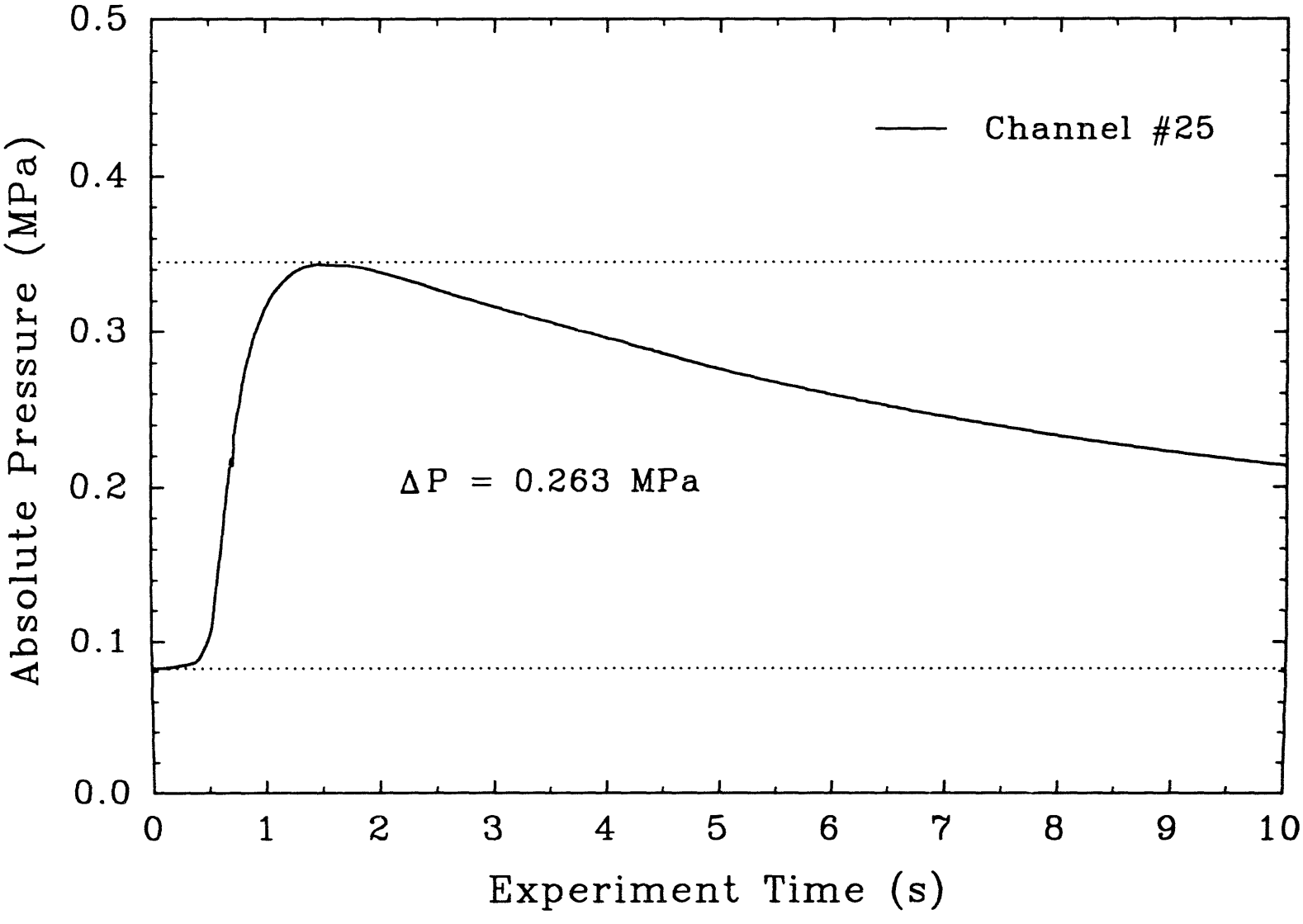

Figure 39. Surtsey vessel pressure versus time measured at level 5 in the TDS-3 experiment.

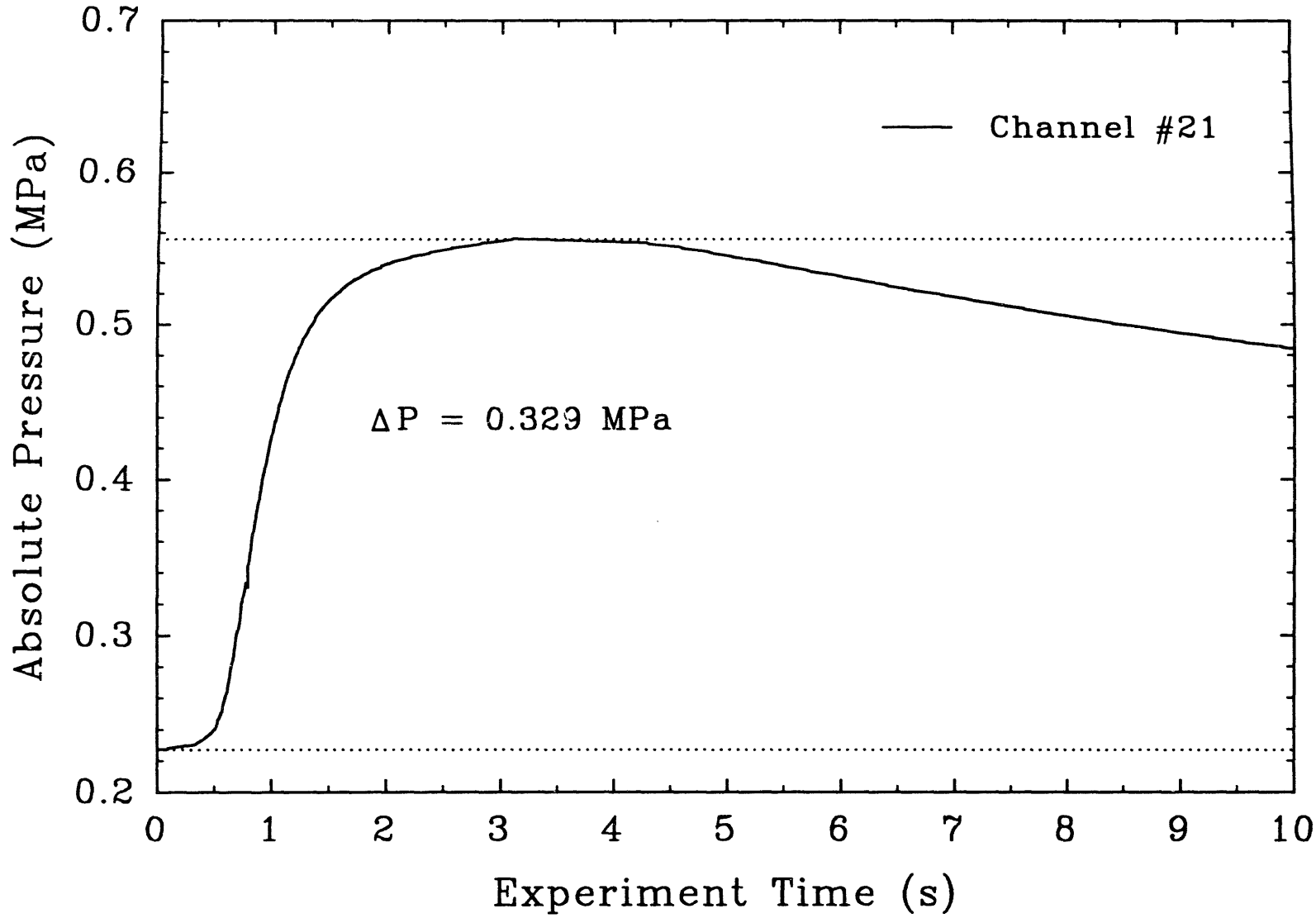

Figure 40. Surtsey vessel pressure versus time measured at level 1 in the TDS-4 experiment.

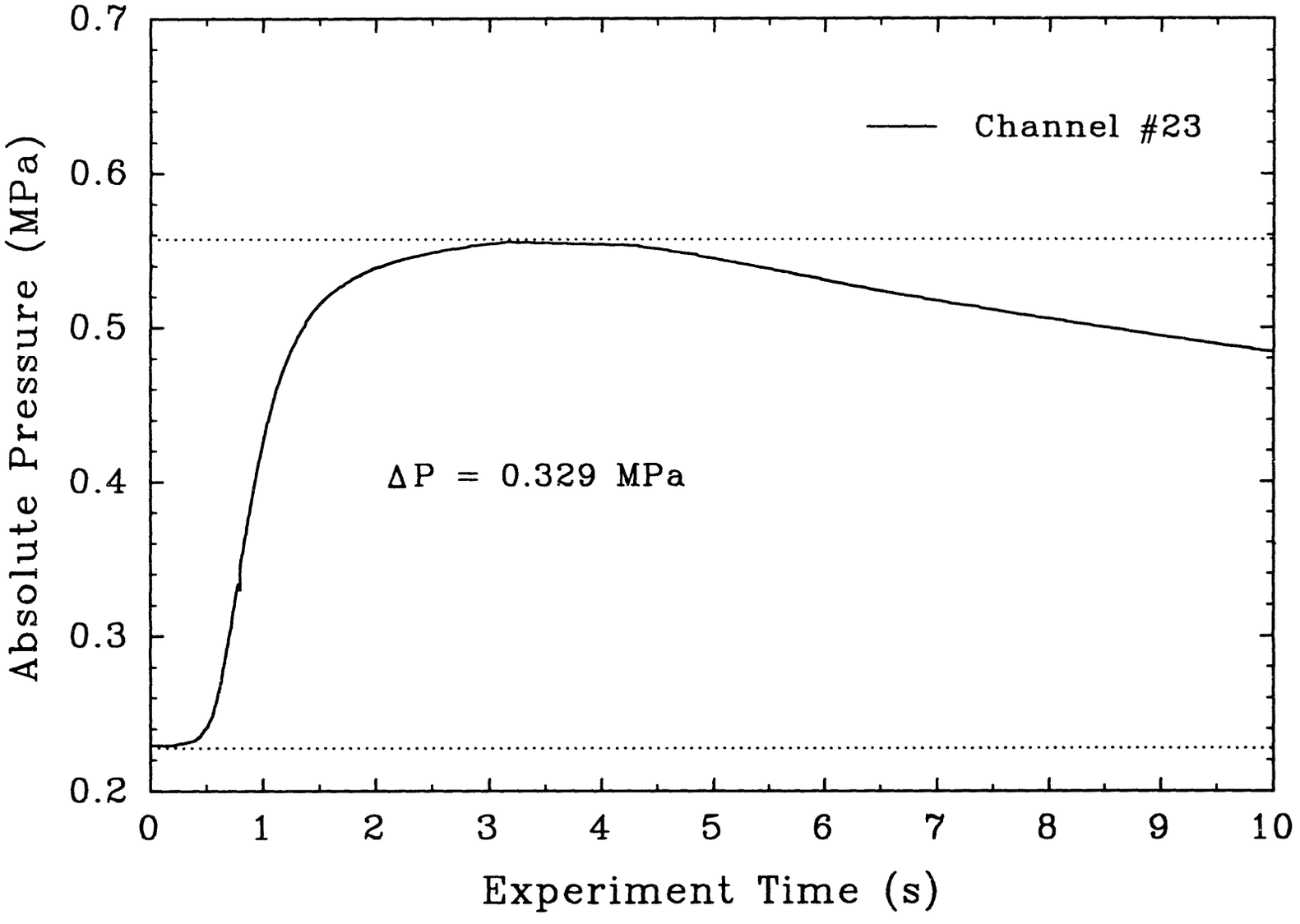

Figure 41. Surtsey vessel pressure versus time measured at level 3 in the TDS-4 experiment.

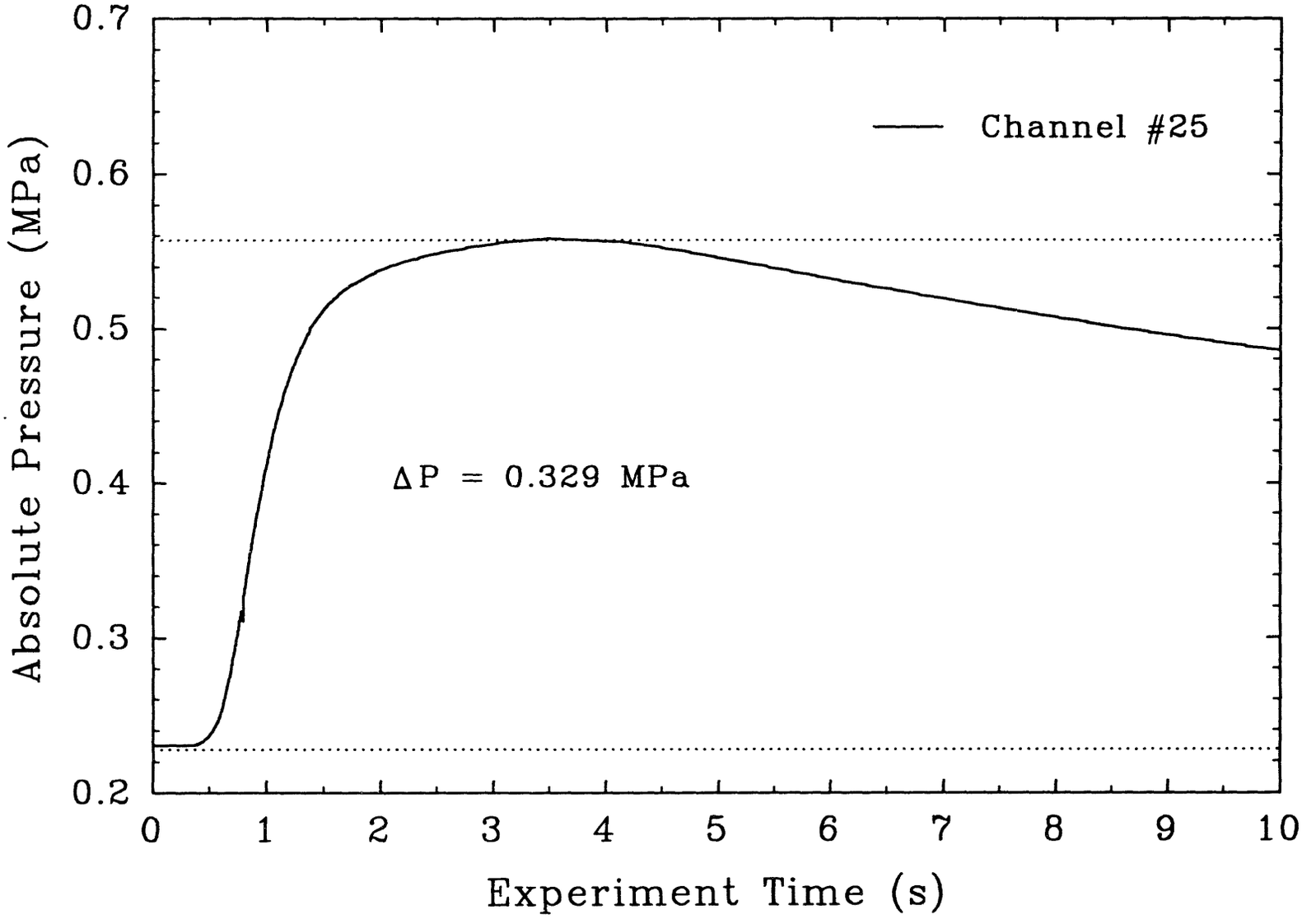

Figure 42. Surtsey vessel pressure versus time measured at level 5 in the TDS-4 experiment.

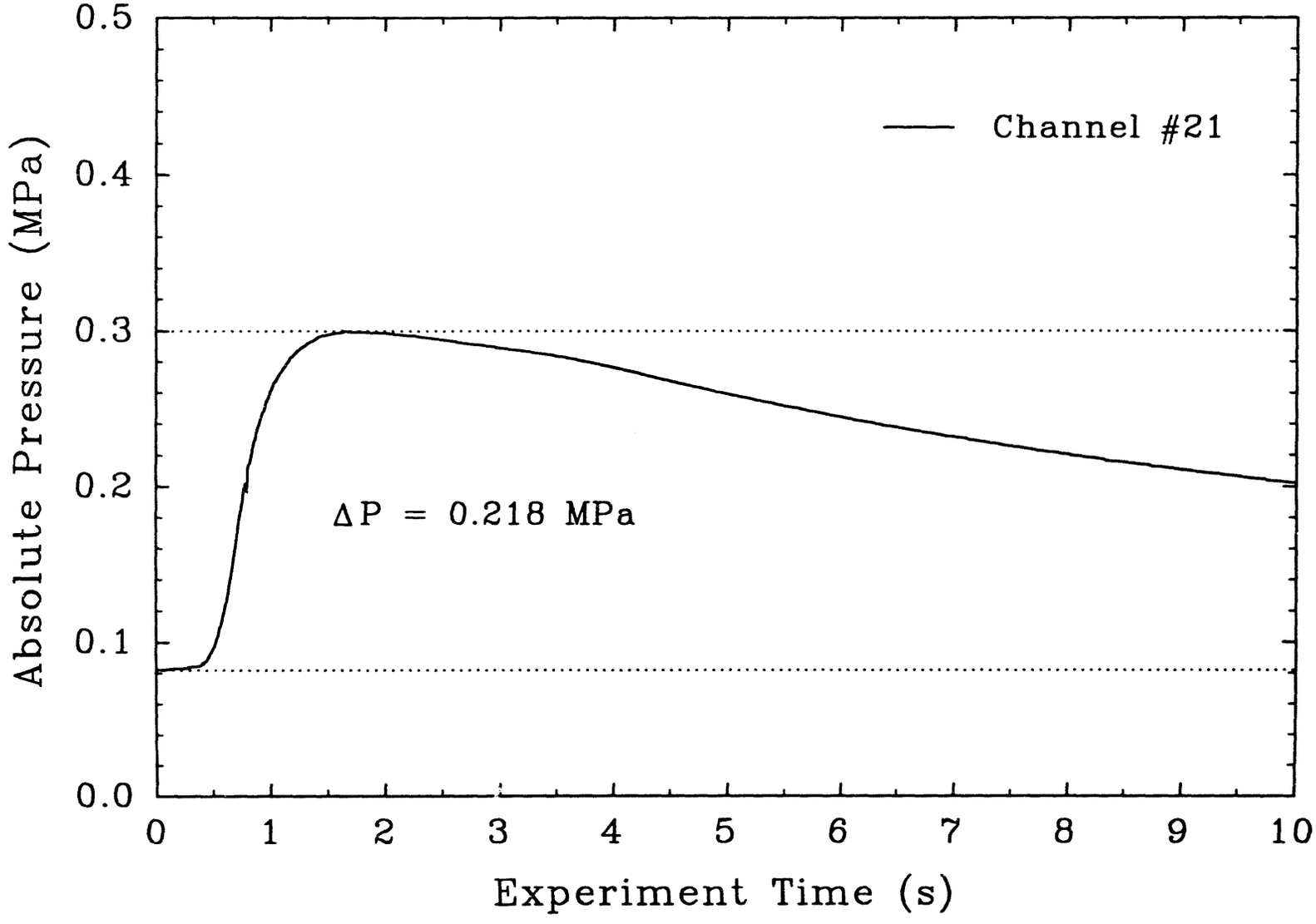

Figure 43. Surtsey vessel pressure versus time measured at level 1 in the TDS-5 experiment.

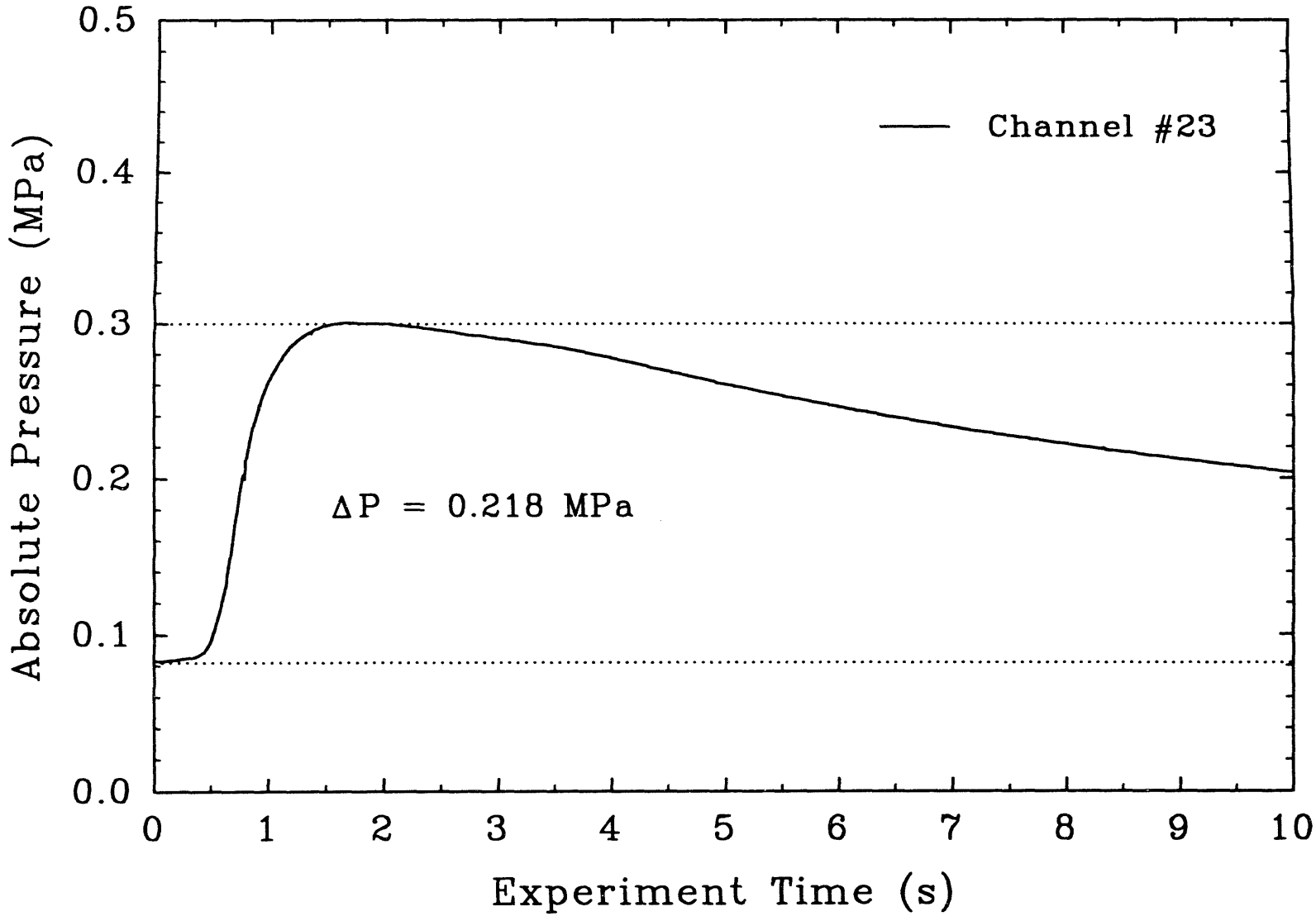

Figure 44. Surtsey vessel pressure versus time measured at level 3 in the TDS–5 experiment.

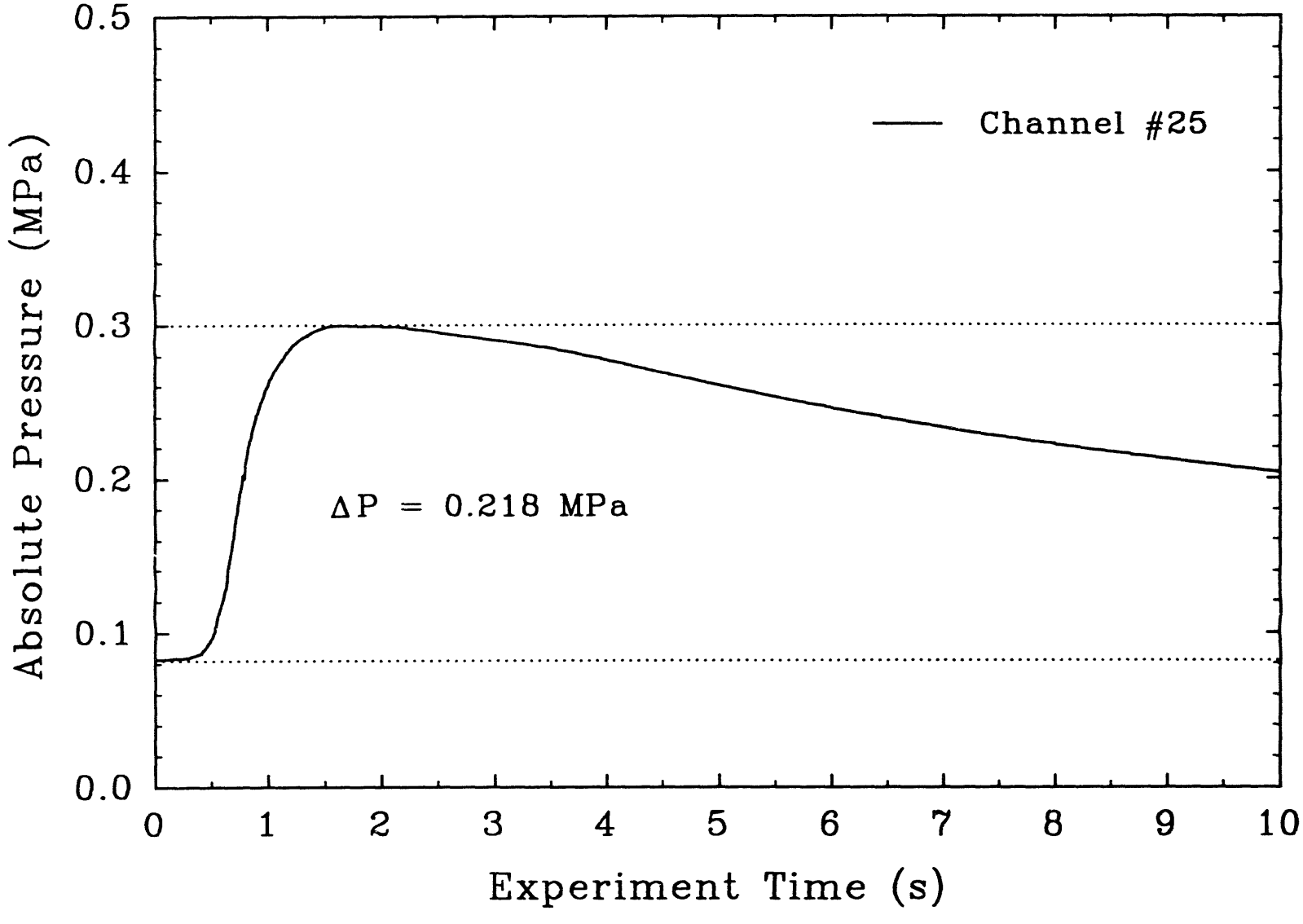

Figure 45. Surtsey vessel pressure versus time measured at level 5 in the TDS-5 experiment.

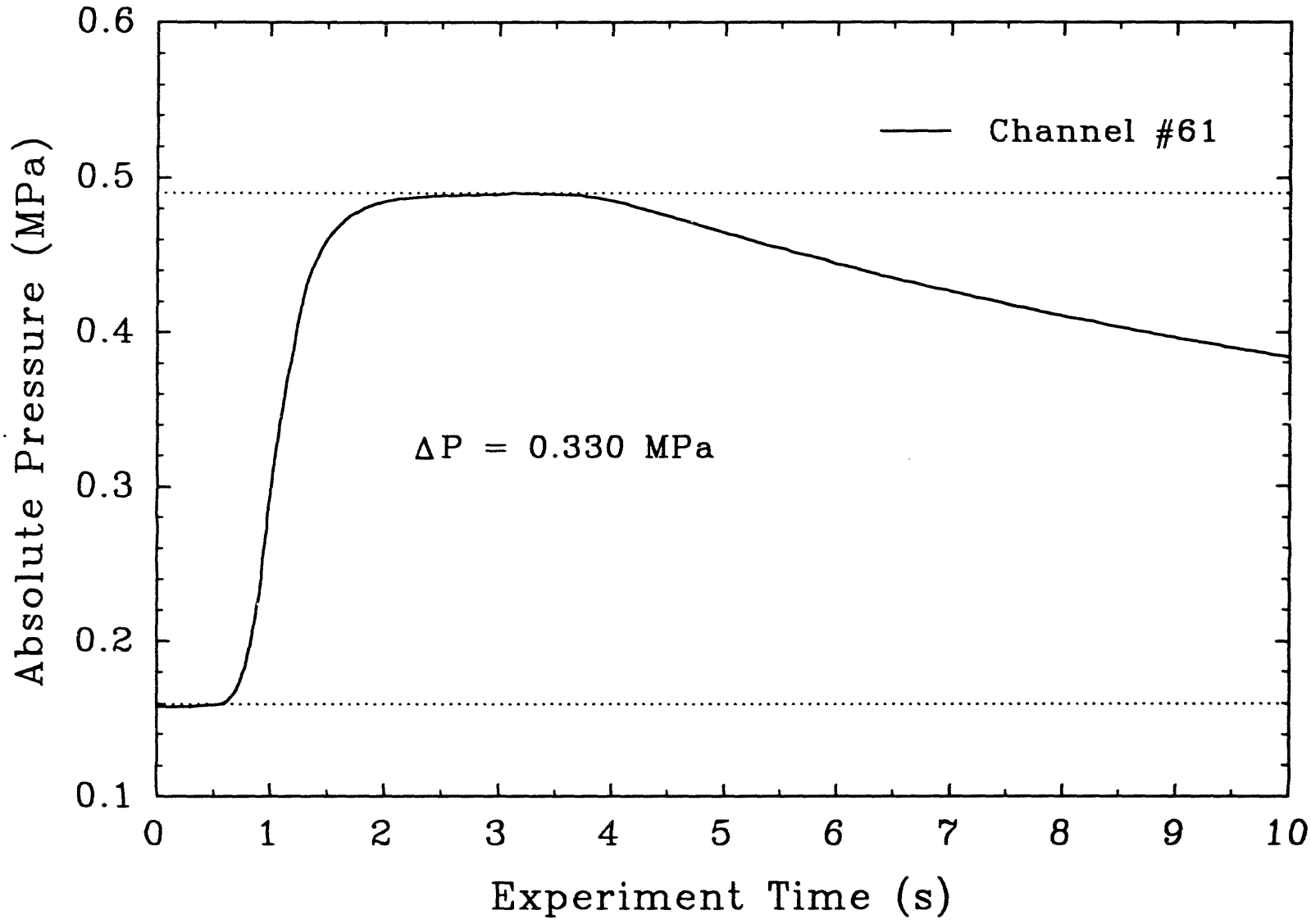

Figure 46. Surtsey vessel pressure versus time measured at level 1 in the TDS-6 experiment.

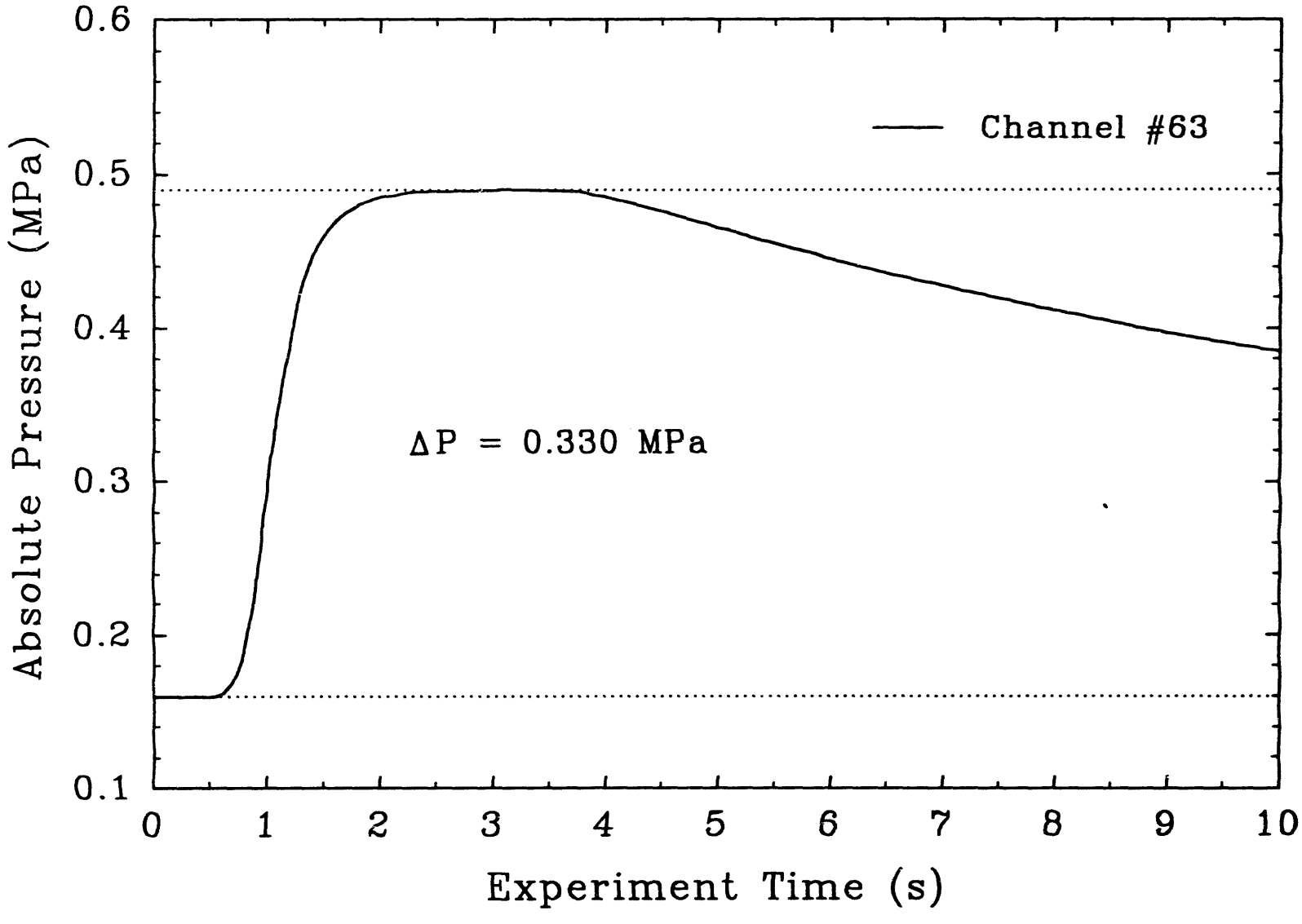

Figure 47. Surtsey vessel pressure versus time measured at level 3 in the TDS-6 experiment.

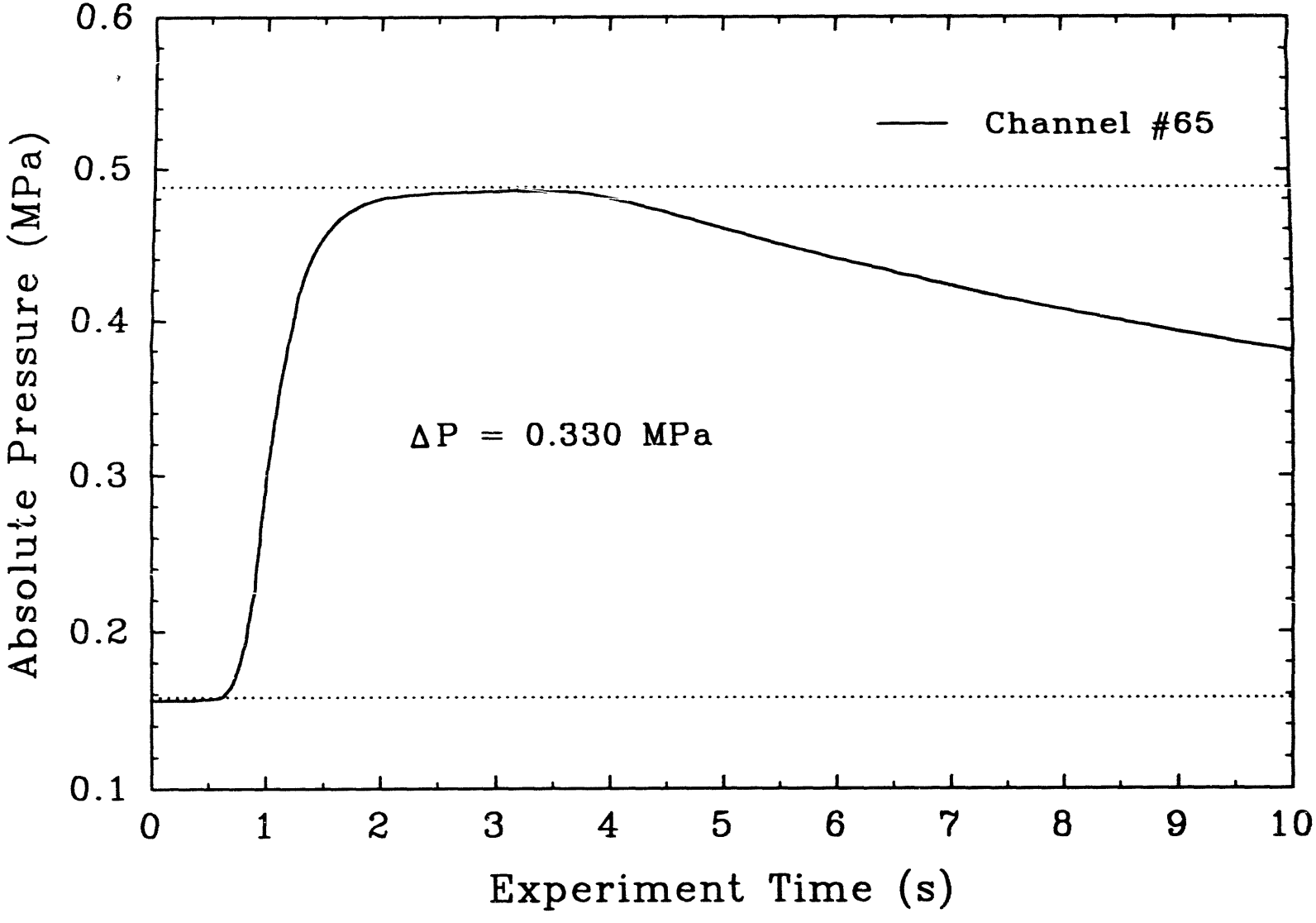

Figure 48. Surtsey vessel pressure versus time measured at level 5 in the TDS-6 experiment.

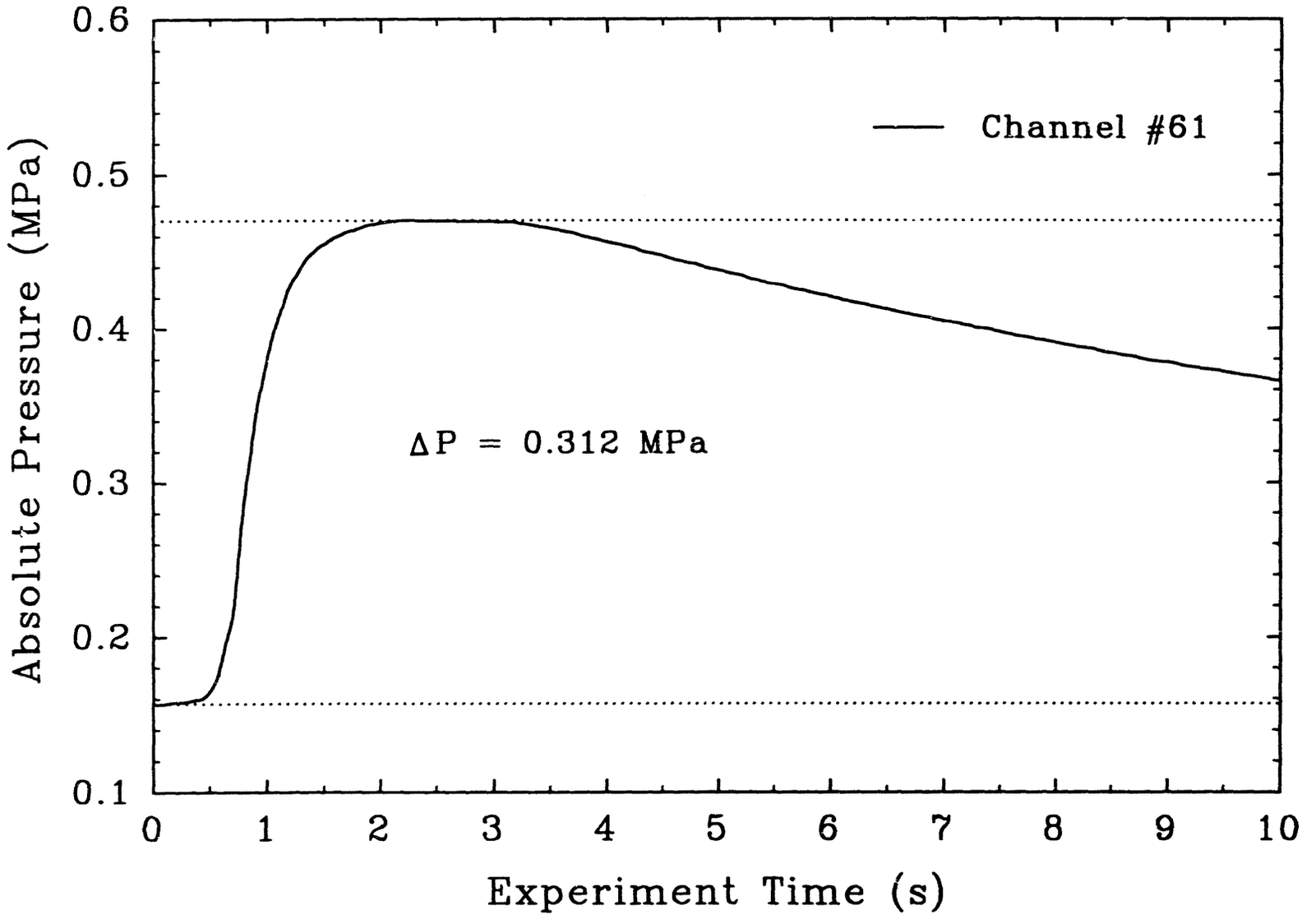

Figure 49. Surtsey vessel pressure versus time measured at level 1 in the TDS-7 experiment.

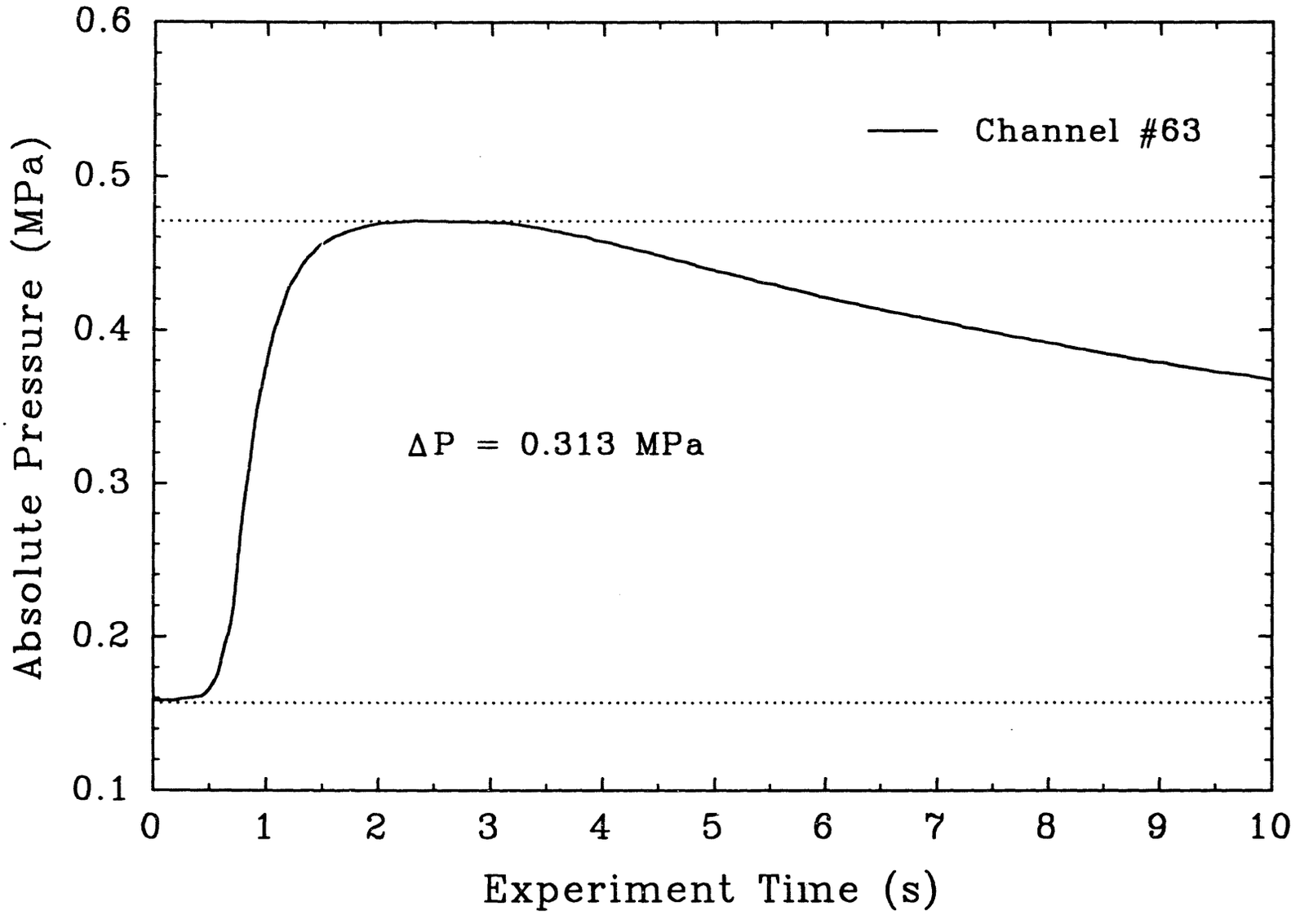

Figure 50. Surtsey vessel pressure versus time measured at level 3 in the TDS-7 experiment.

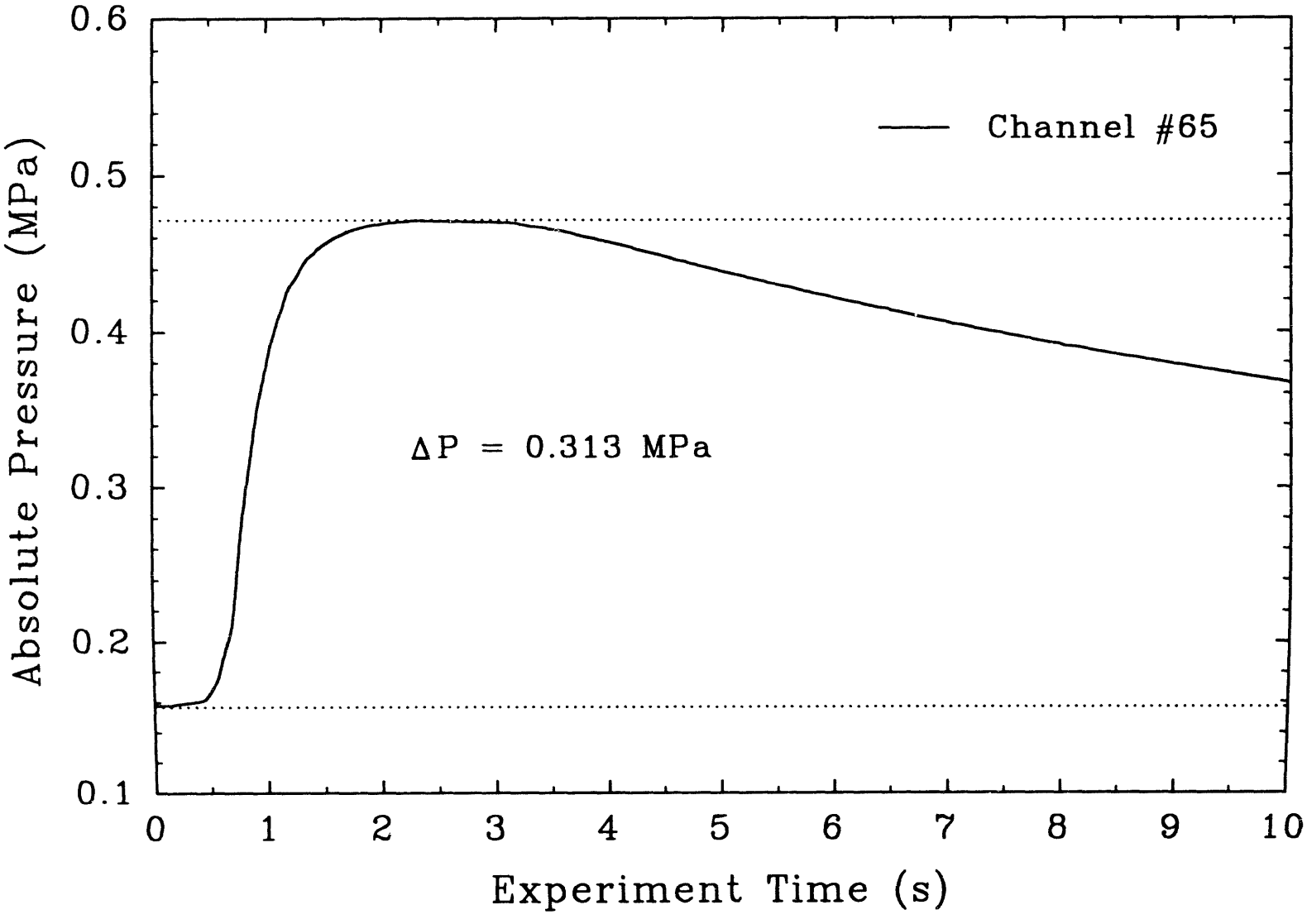

Figure 51. Surtsey vessel pressure versus time measured at level 5 in the TDS-7 experiment.

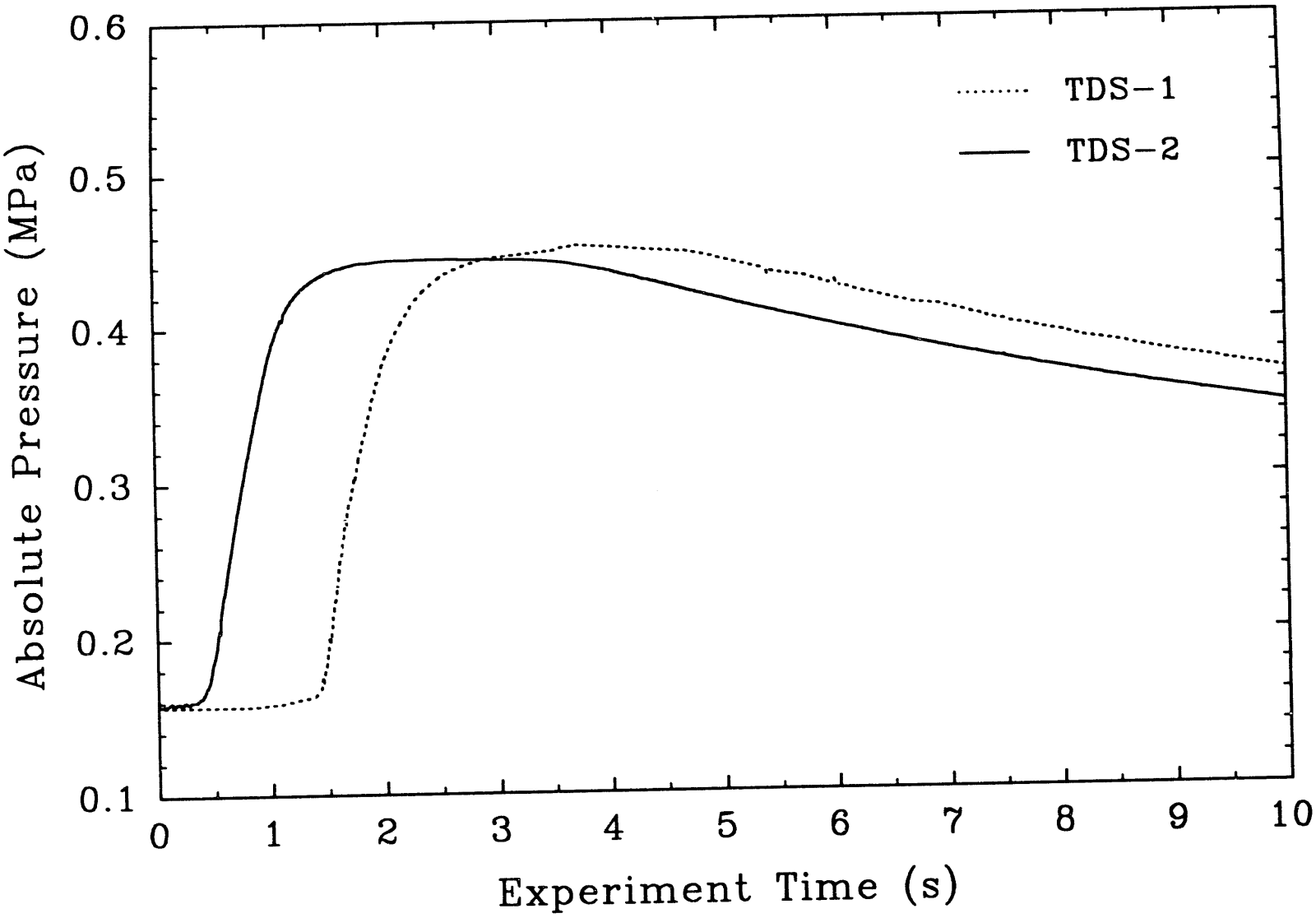

Figure 52. Comparison of the Surtsey vessel pressures measured in TDS-1 and TDS-2.

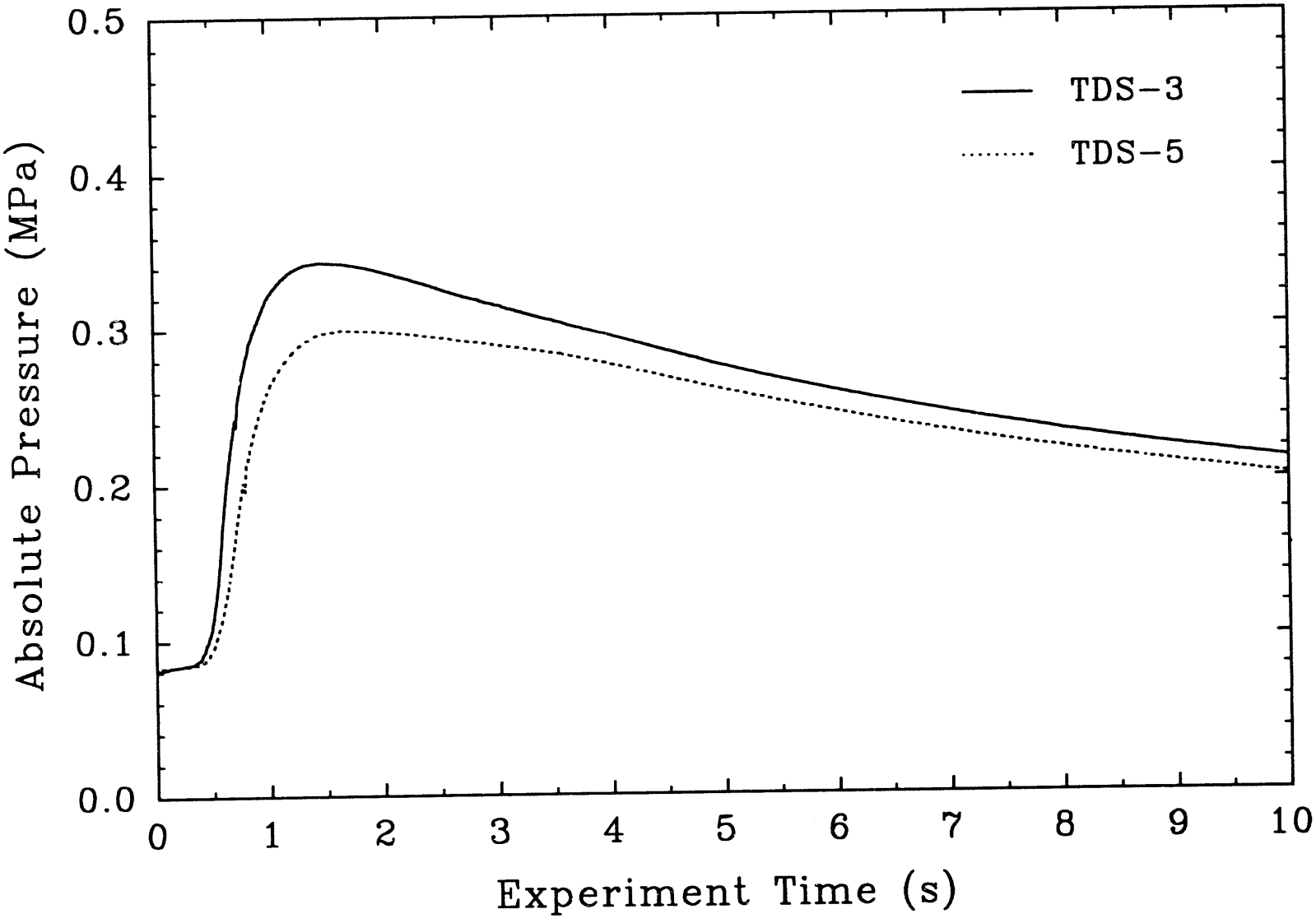

Figure 53. Comparison of the Surtsey vessel pressures measured in TDS-3 and TDS-5.

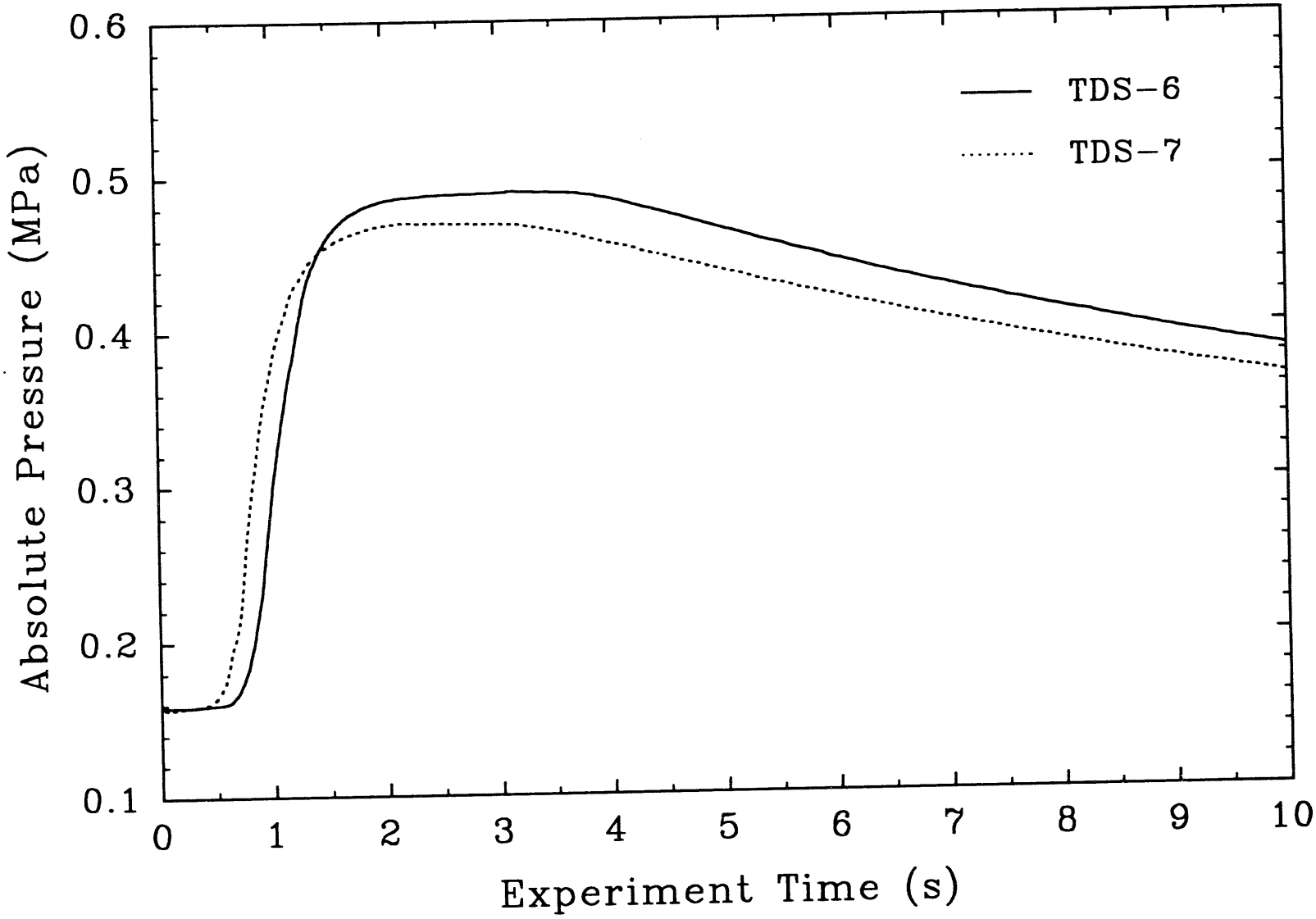

Figure 54. Comparison of the Surtsey vessel pressures measured in TDS-6 and TDS-7.

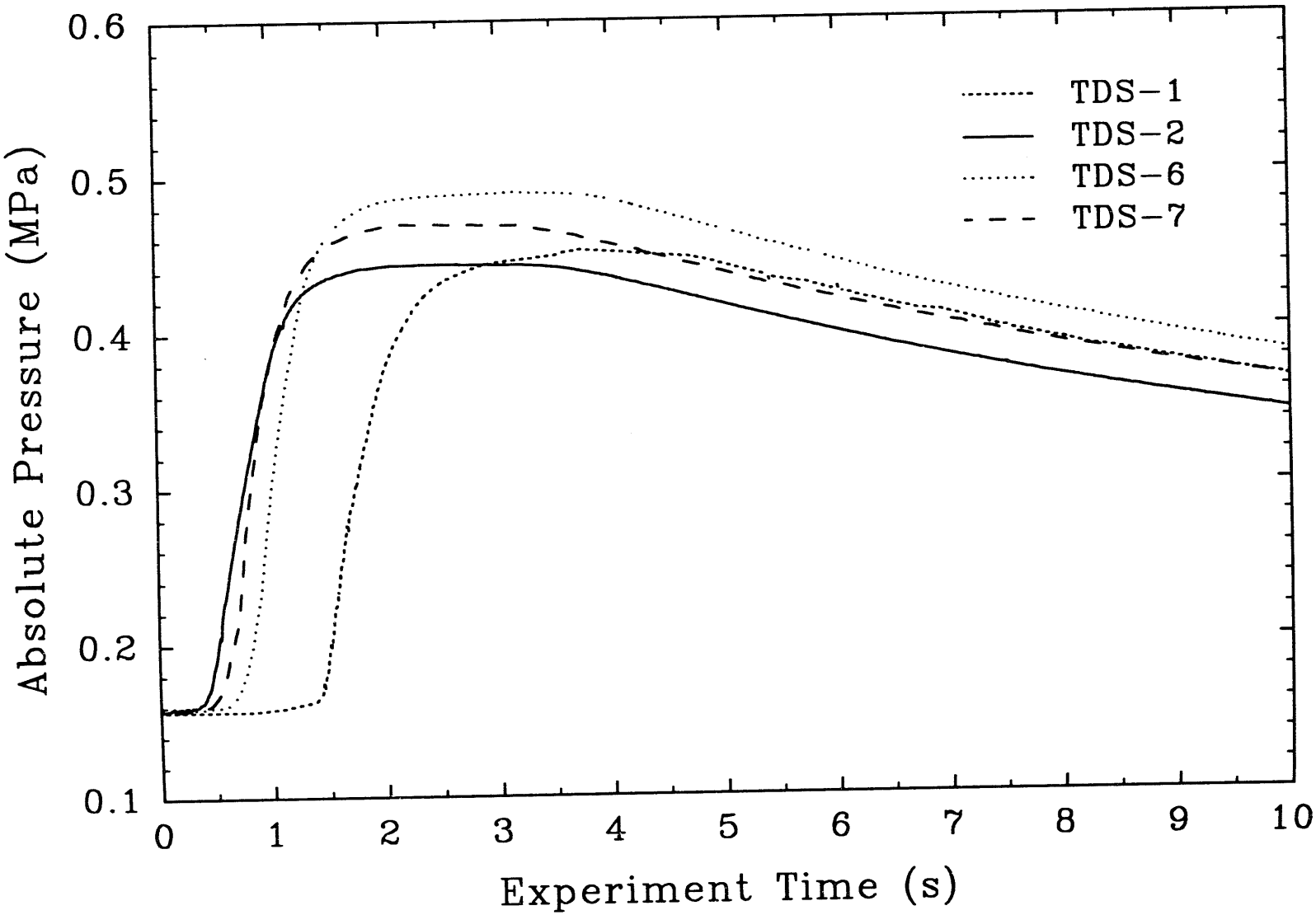

Figure 55. Comparison of the Surtsey vessel pressures measured in the TDS tests having an initial vessel pressure of 0.156 MPa.

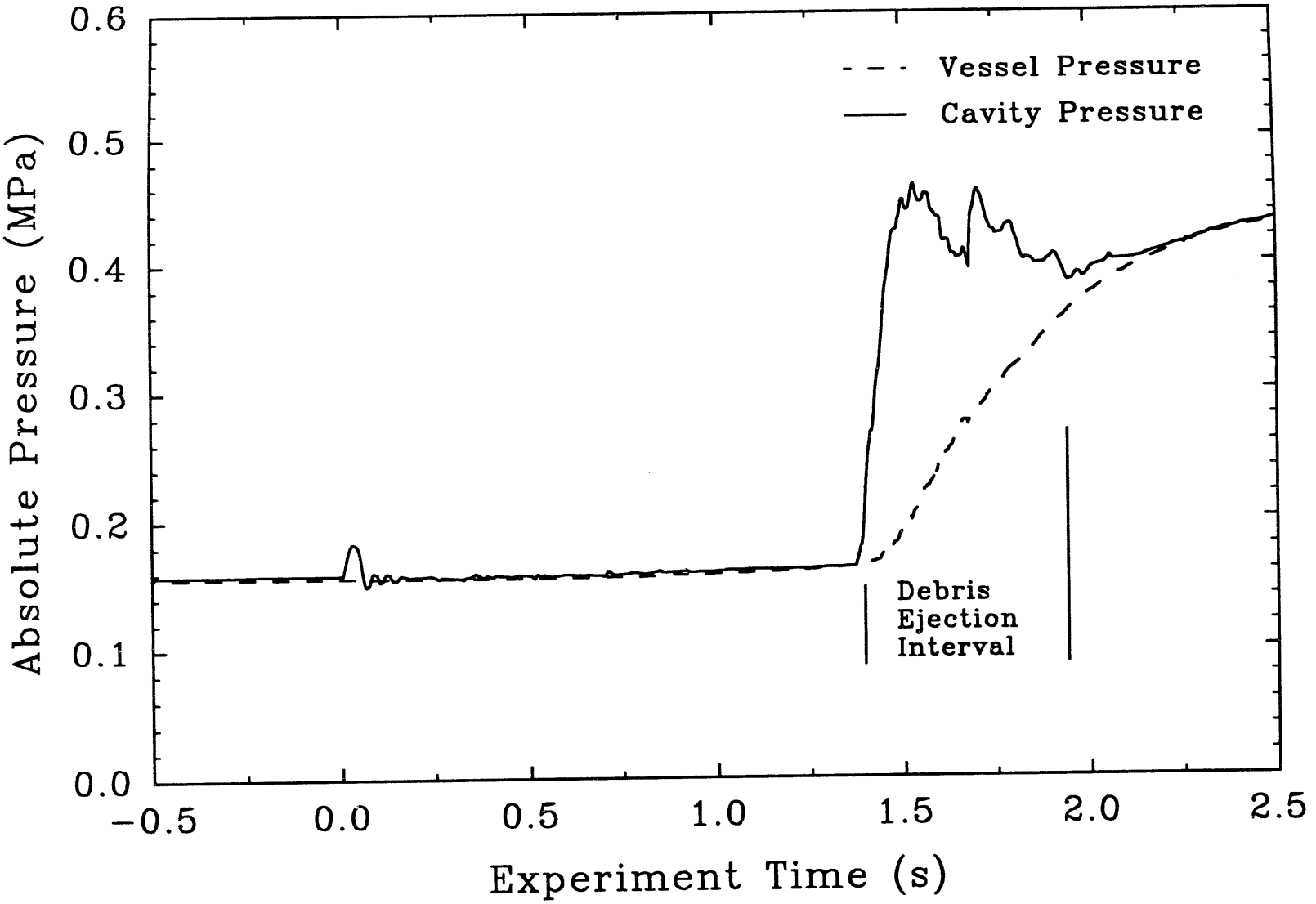

Figure 56. Cavity pressure and Surtsey vessel pressure versus time for the TDS−1 experiment.

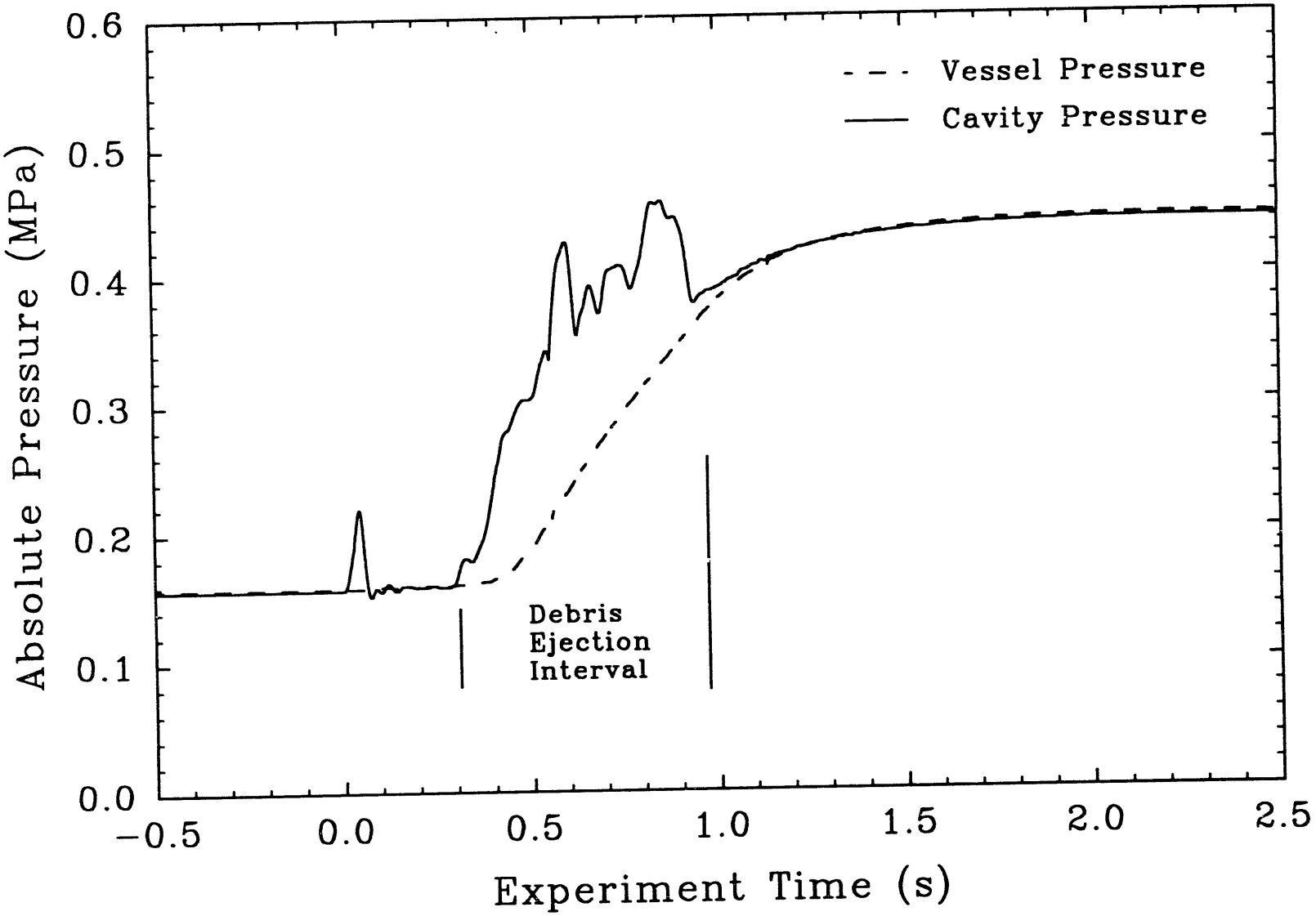

Figure 57. Cavity pressure and Surtsey vessel pressure versus time for the TDS−2 experiment.

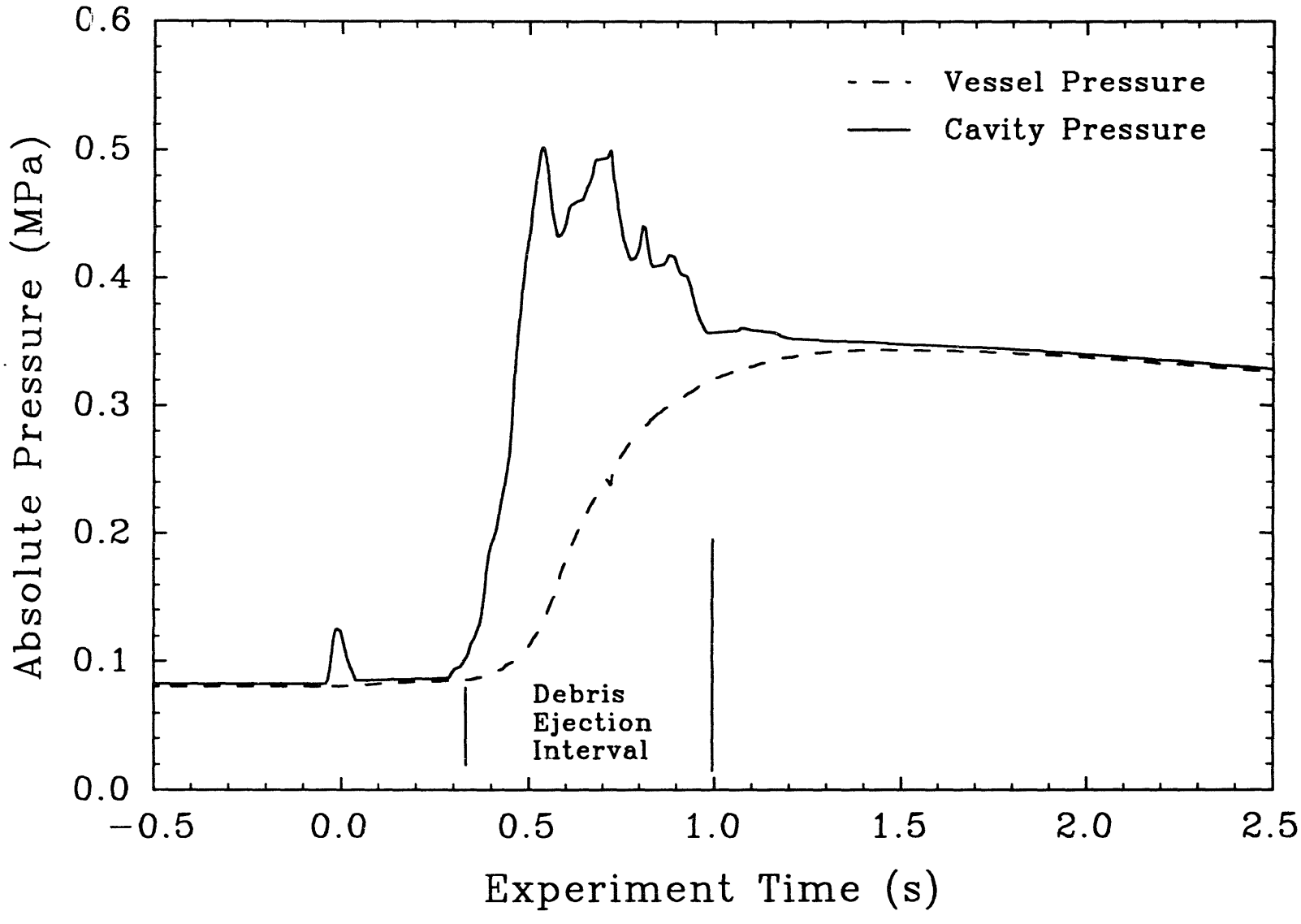

Figure 58. Cavity pressure and Surtsey vessel pressure versus time for the TDS−3 experiment.

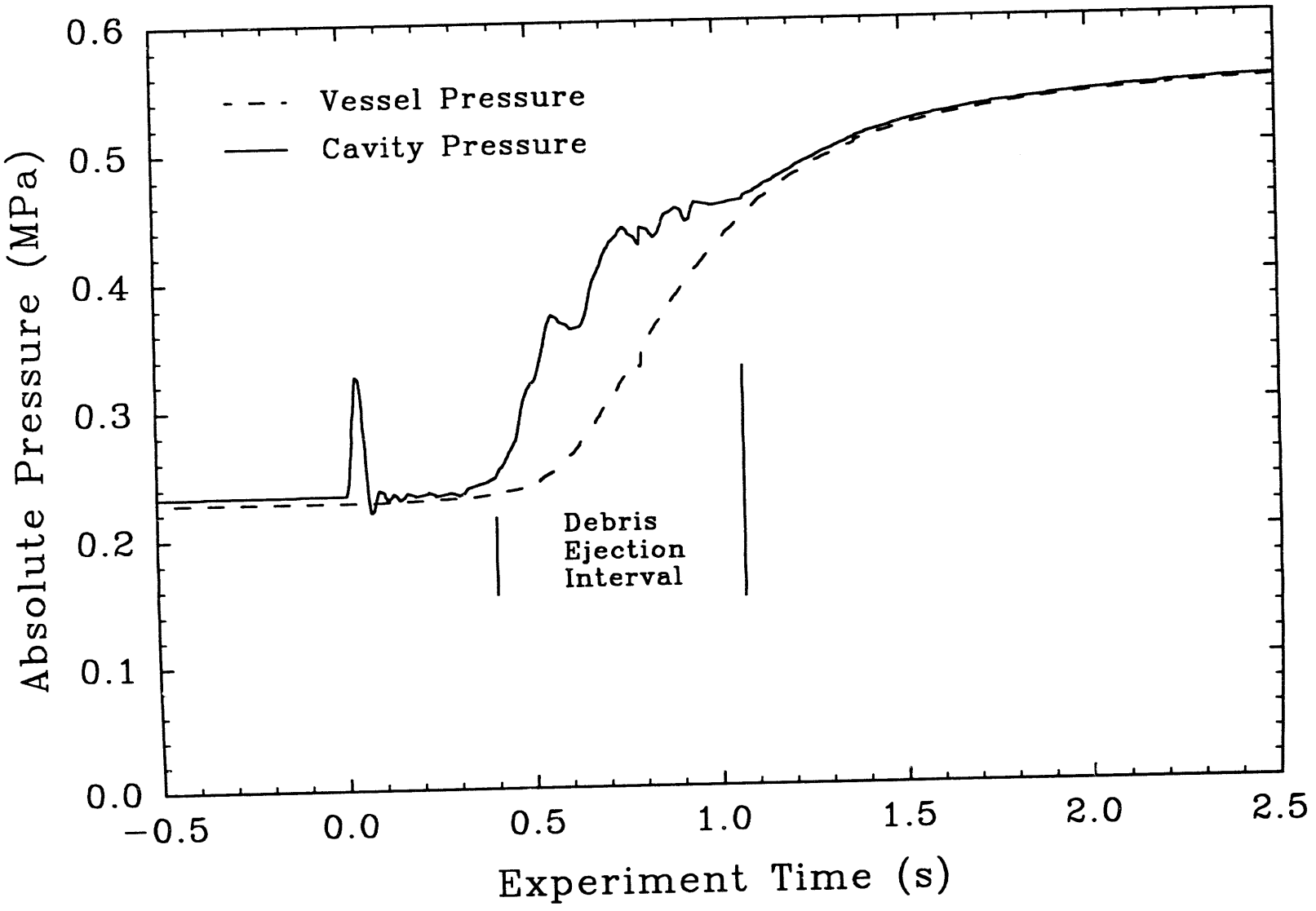

Figure 59. Cavity pressure and Surtsey vessel pressure versus time for the TDS−4 experiment.

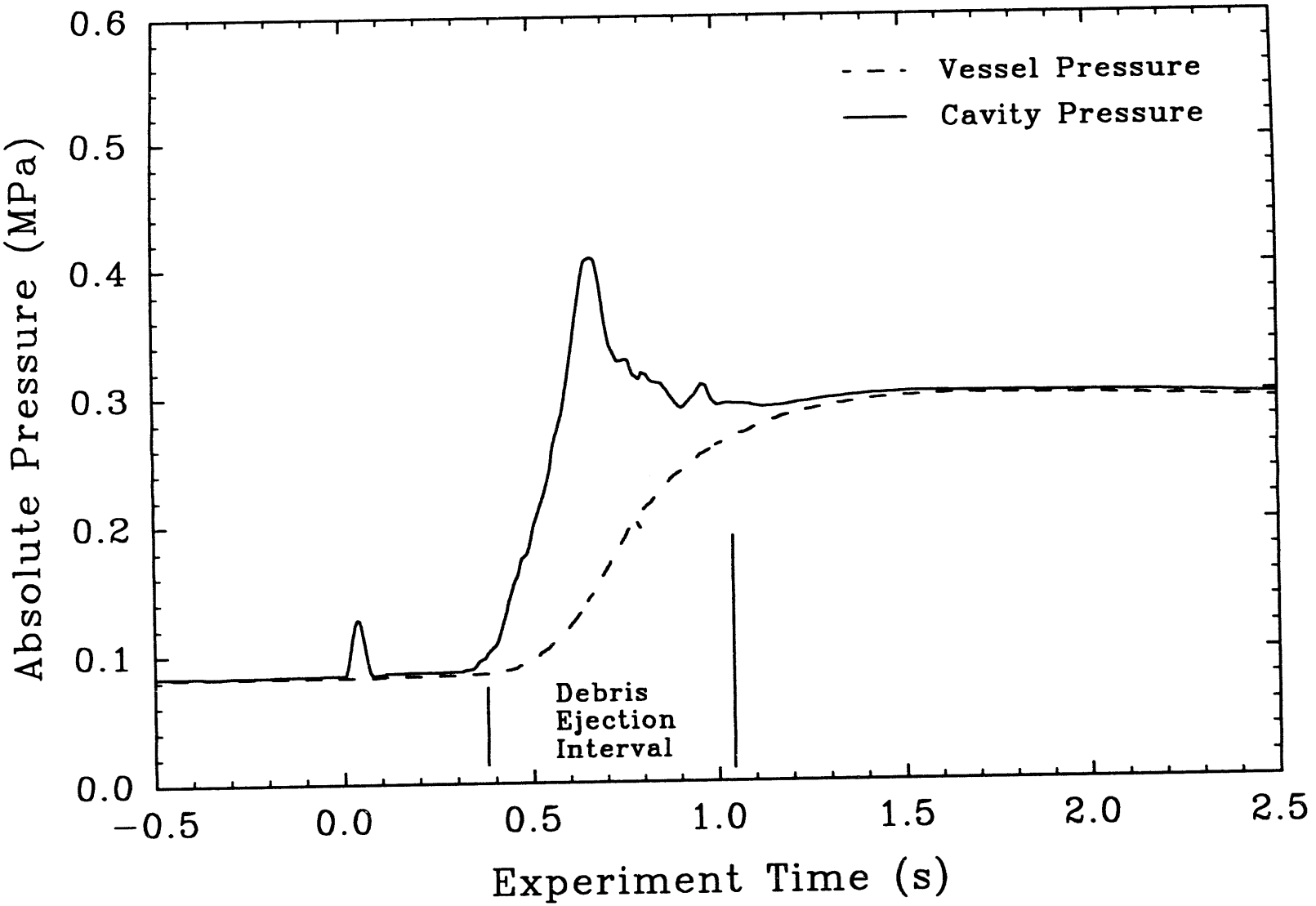

Figure 60. Cavity pressure and Surtsey vessel pressure versus time for the TDS−5 experiment.

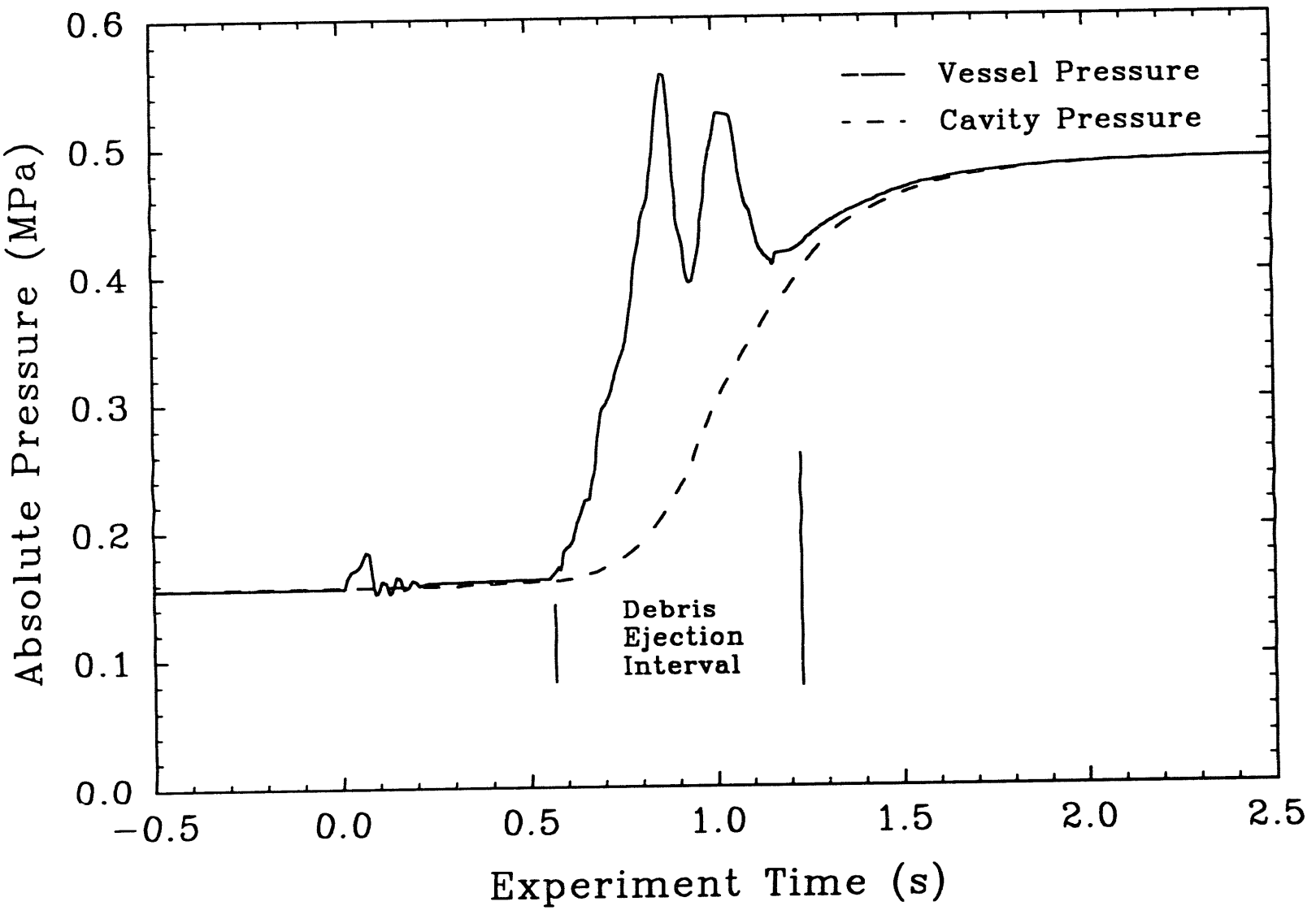

Figure 61. Cavity pressure and Surtsey vessel pressure versus time for the TDS−6 experiment.

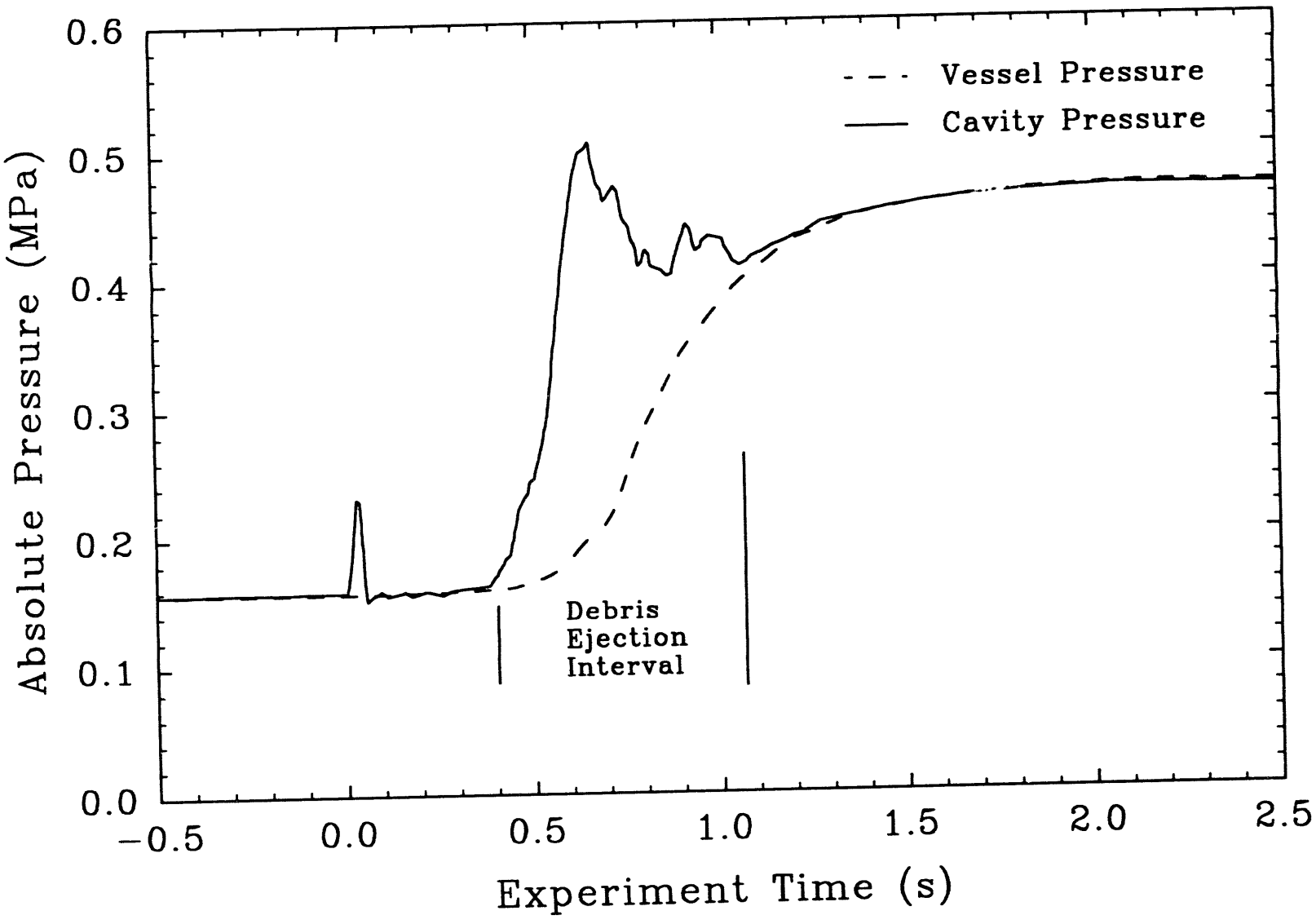

Figure 62. Cavity pressure and Surtsey vessel pressure versus time for the TDS−7 experiment.

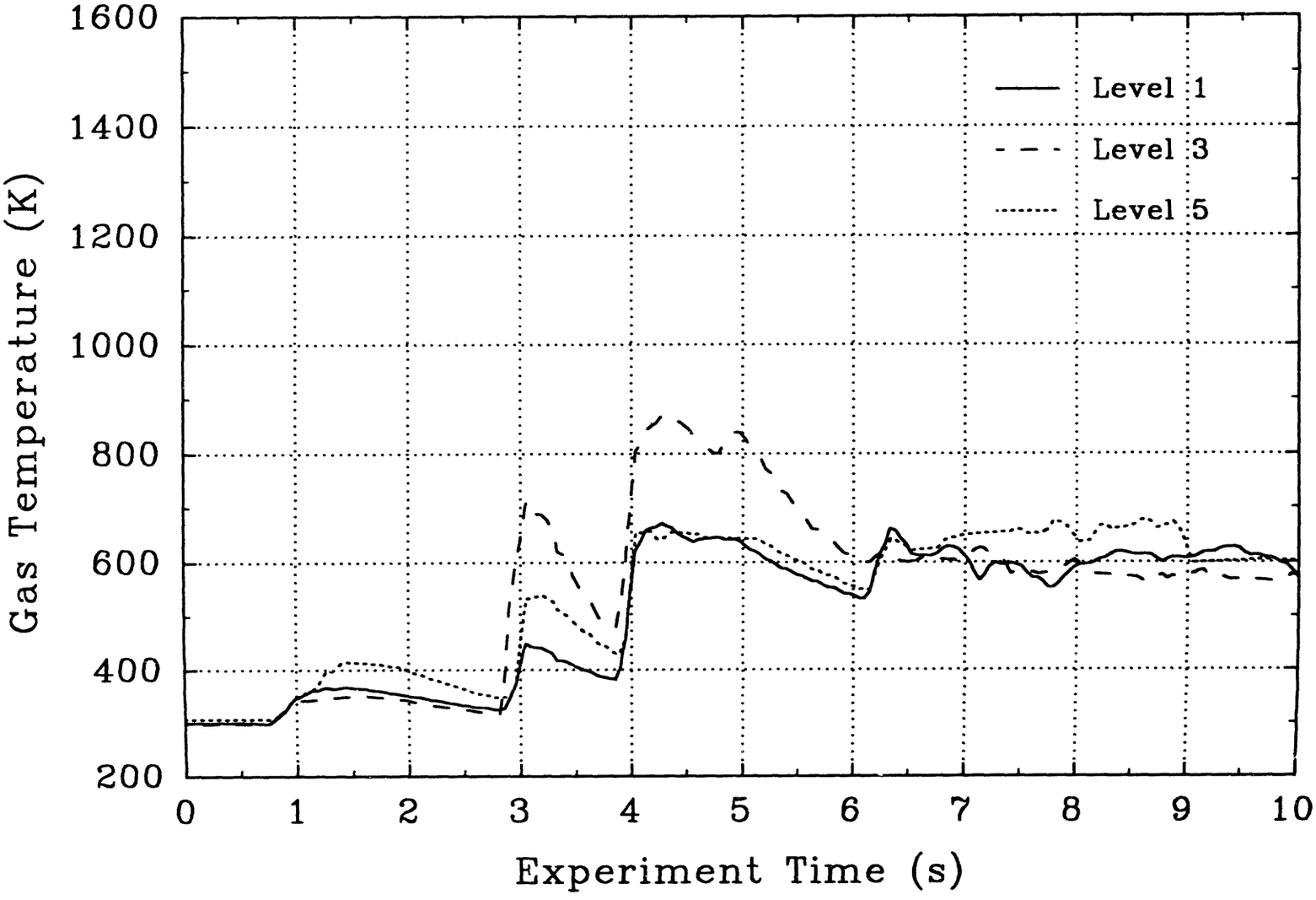

Figure 63. Gas temperatures measured in Surtsey with aspirated thermocouples in the TDS-1 experiment.

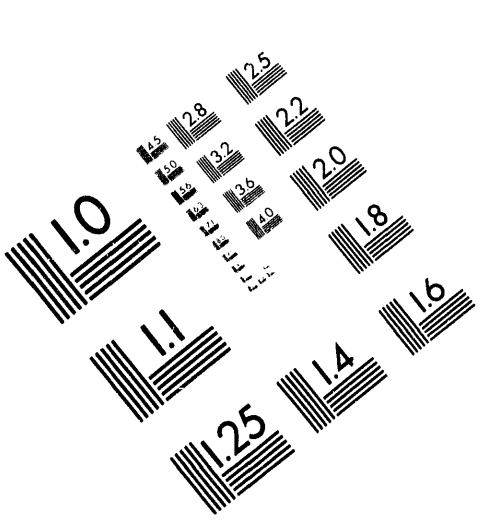

Association for Information and Image Management
1100 Wayne Avenue, Suite 1100
Silver Spring, Maryland 20910
301/587-8202

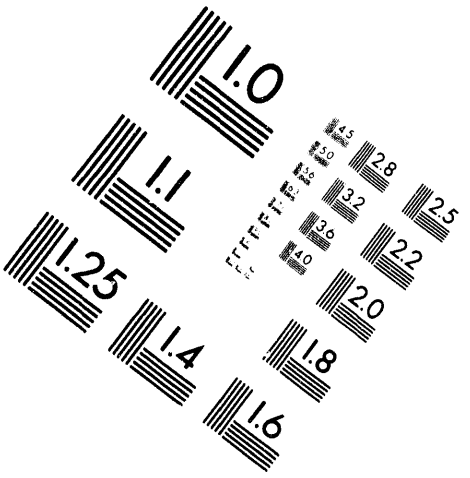

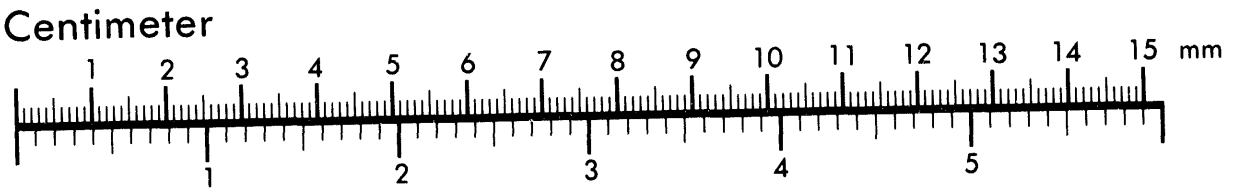

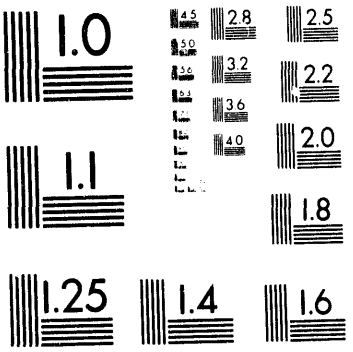

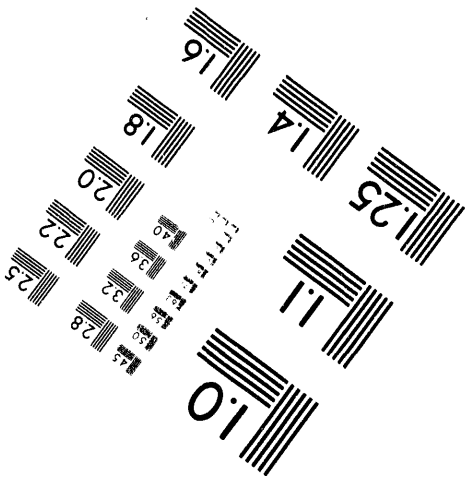

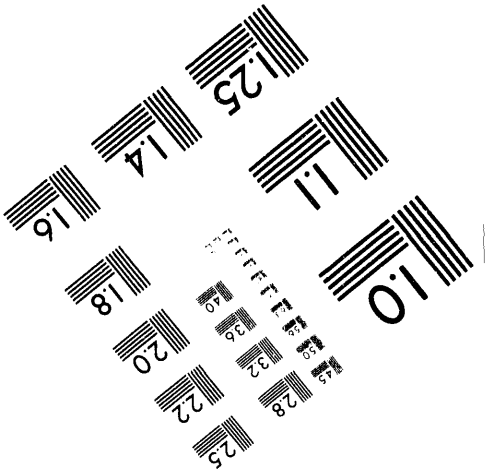

2 of 2

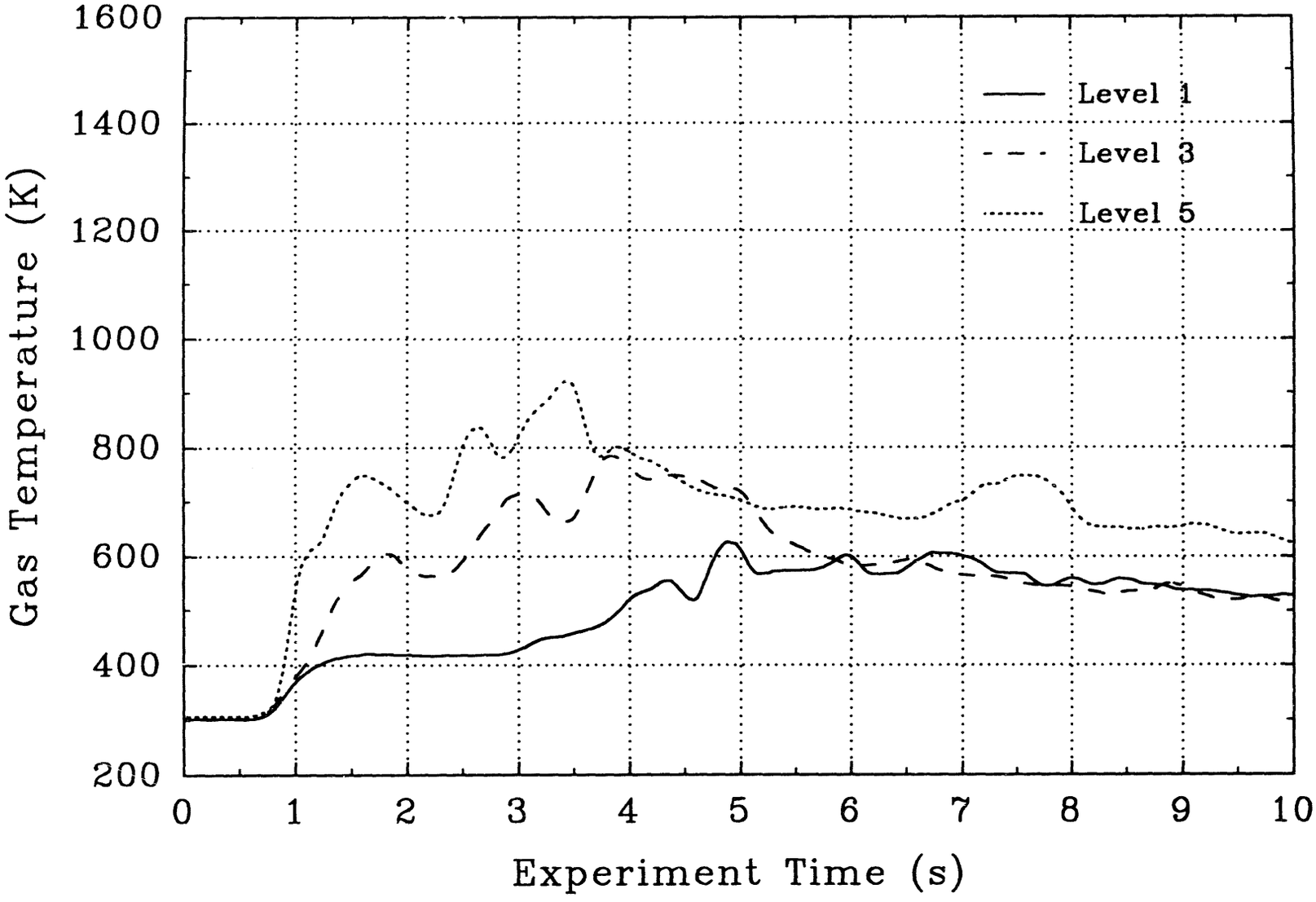

Figure 64. Gas temperatures measured in Surtsey with aspirated thermocouples in the TDS-2 experiment.

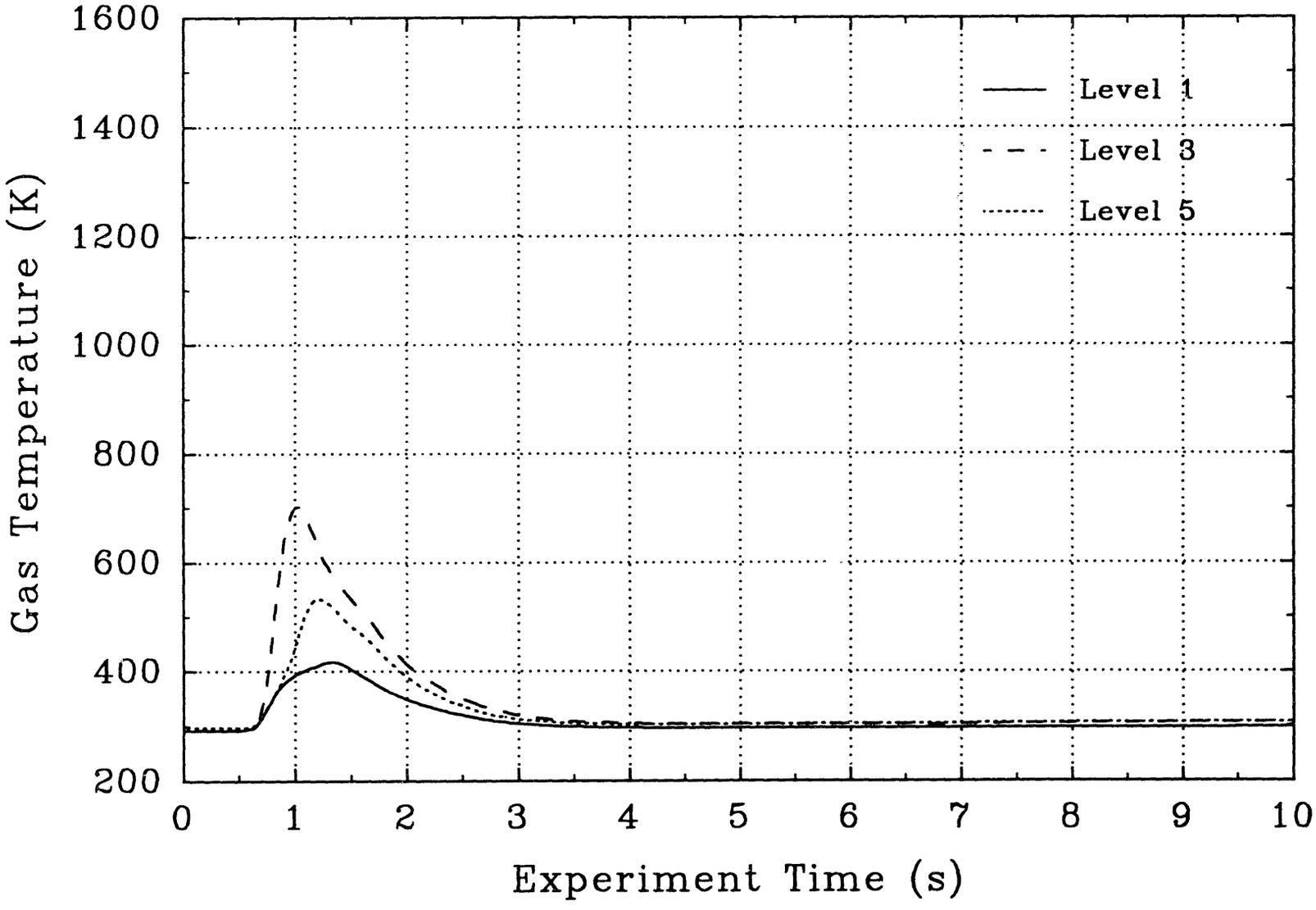

Figure 65. Gas temperatures measured in Surtsey with aspirated thermocouples in the TDS-3 experiment.

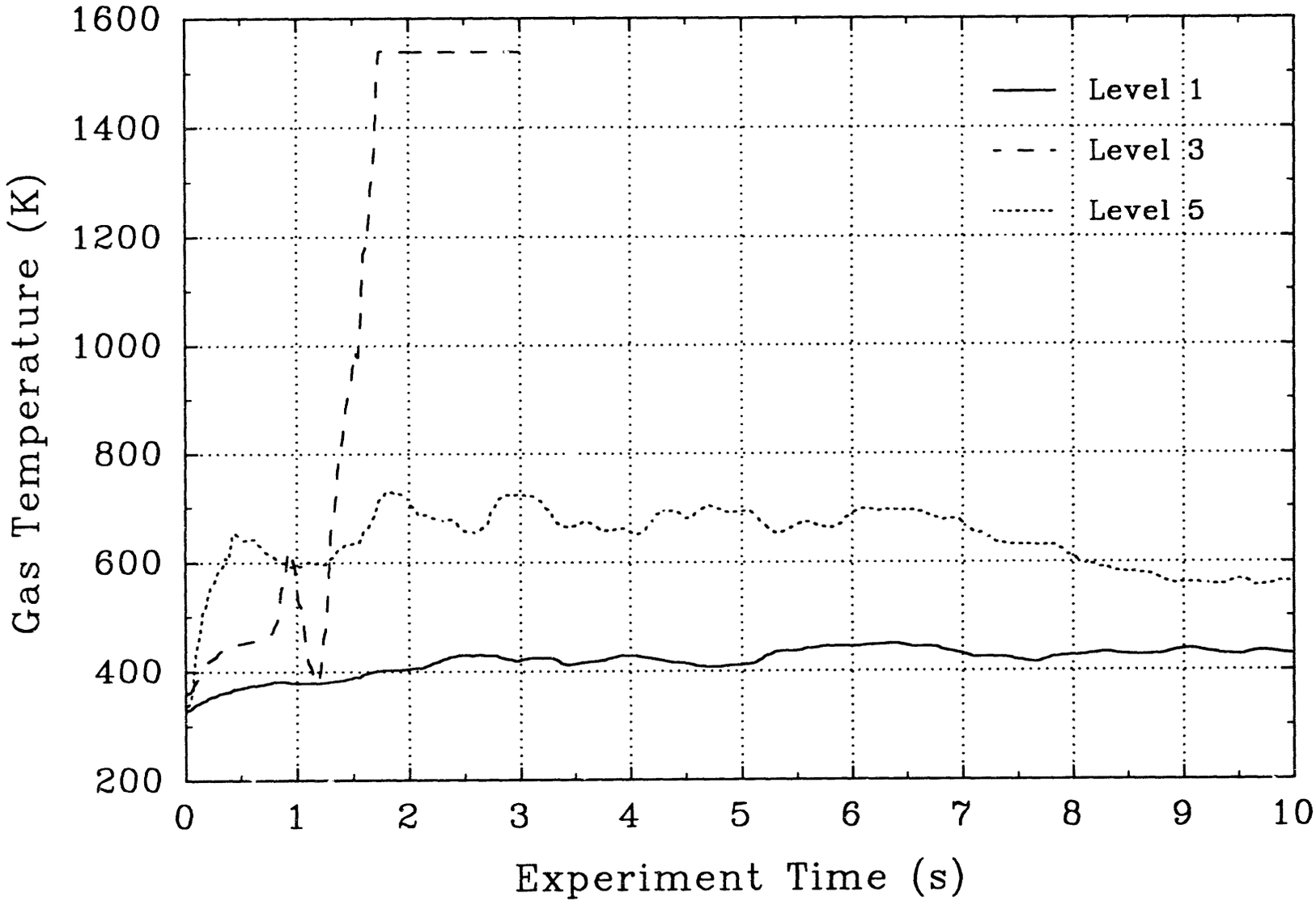

Figure 66. Gas temperatures measured in Surtsey with aspirated thermocouples in the TDS-4 experiment.

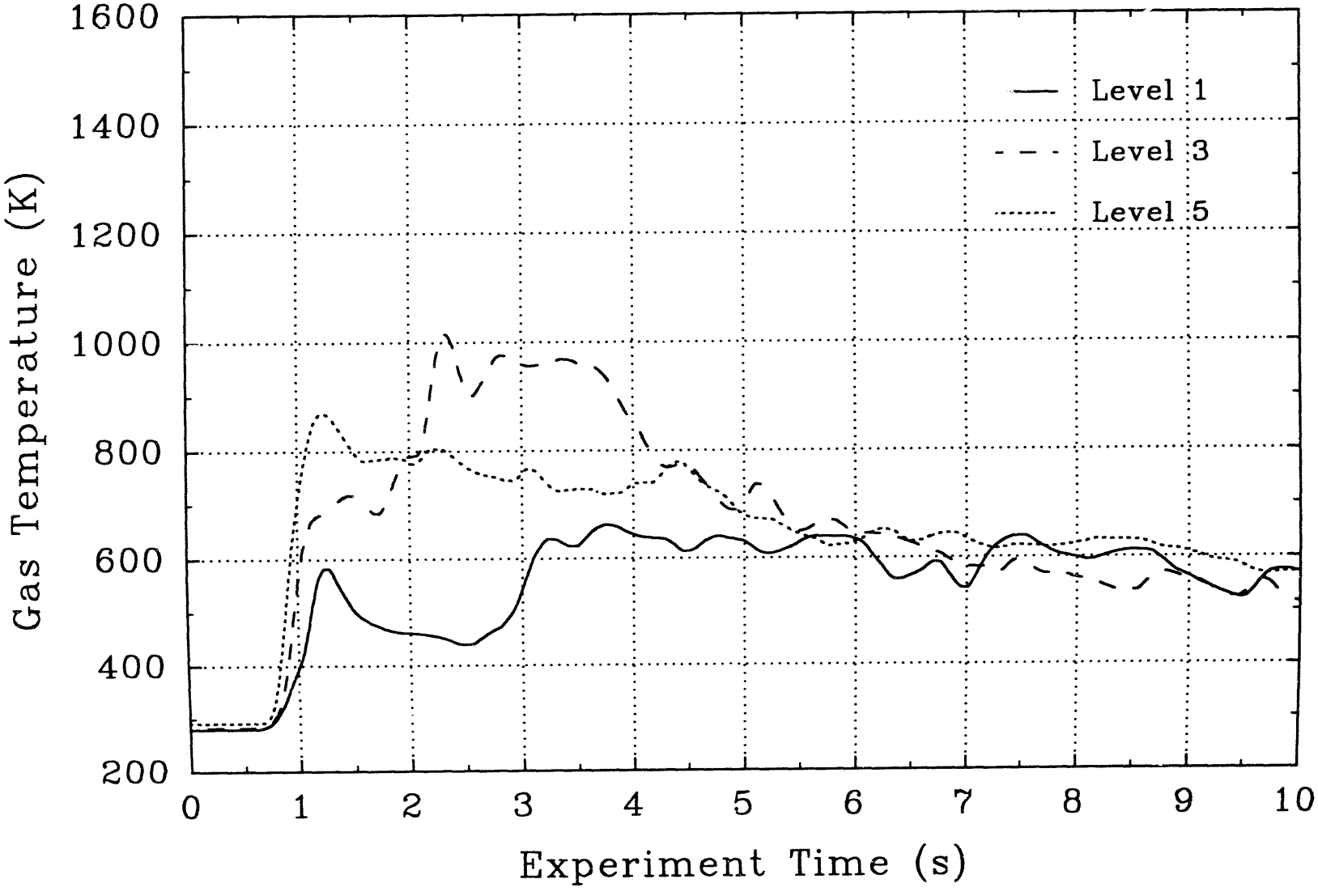

Figure 67. Gas temperatures measured in Surtsey with aspirated thermocouples in the TDS-5 experiment.

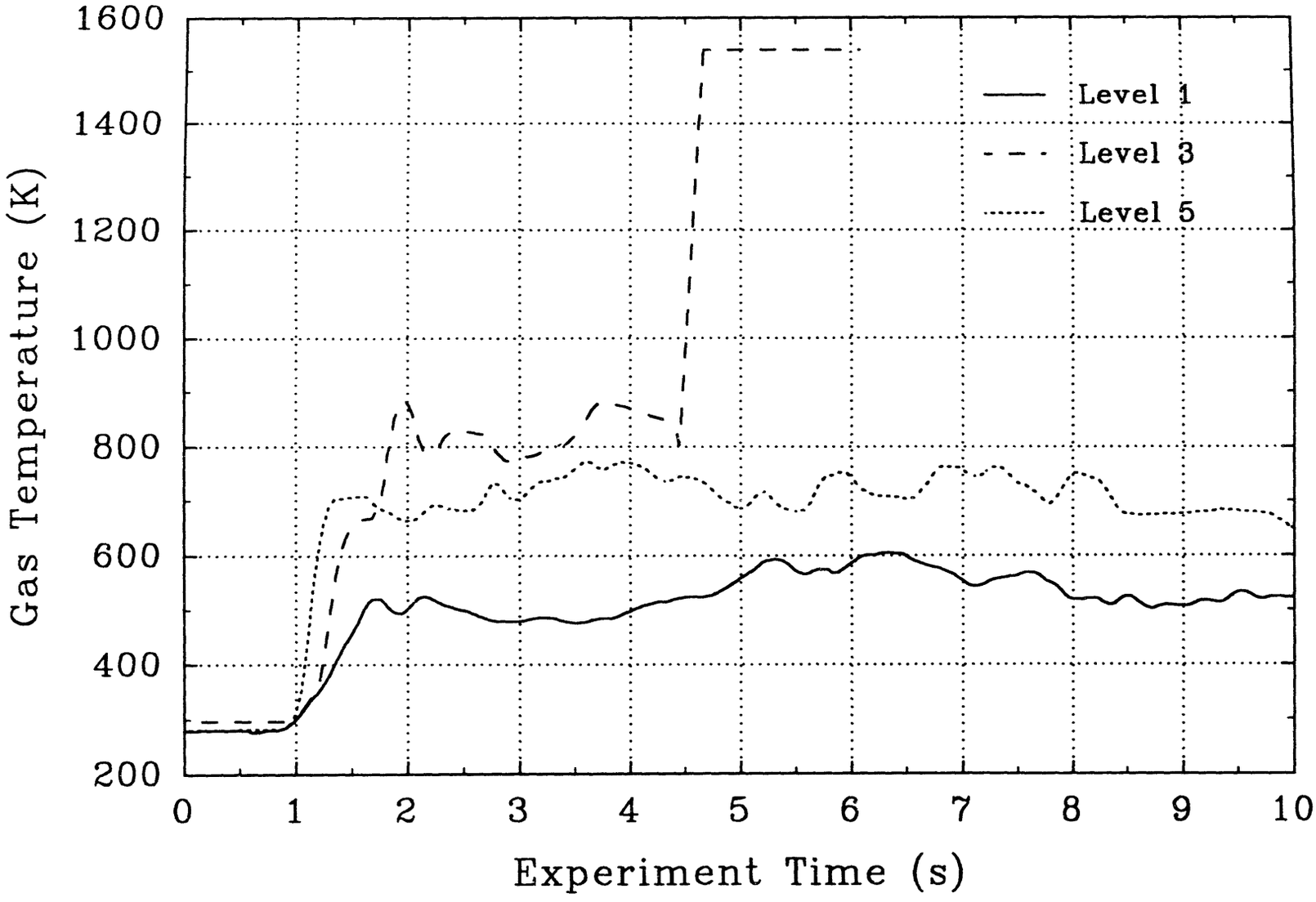

Figure 68. Gas temperatures measured in Surtsey with aspirated thermocouples in the TDS-6 experiment.

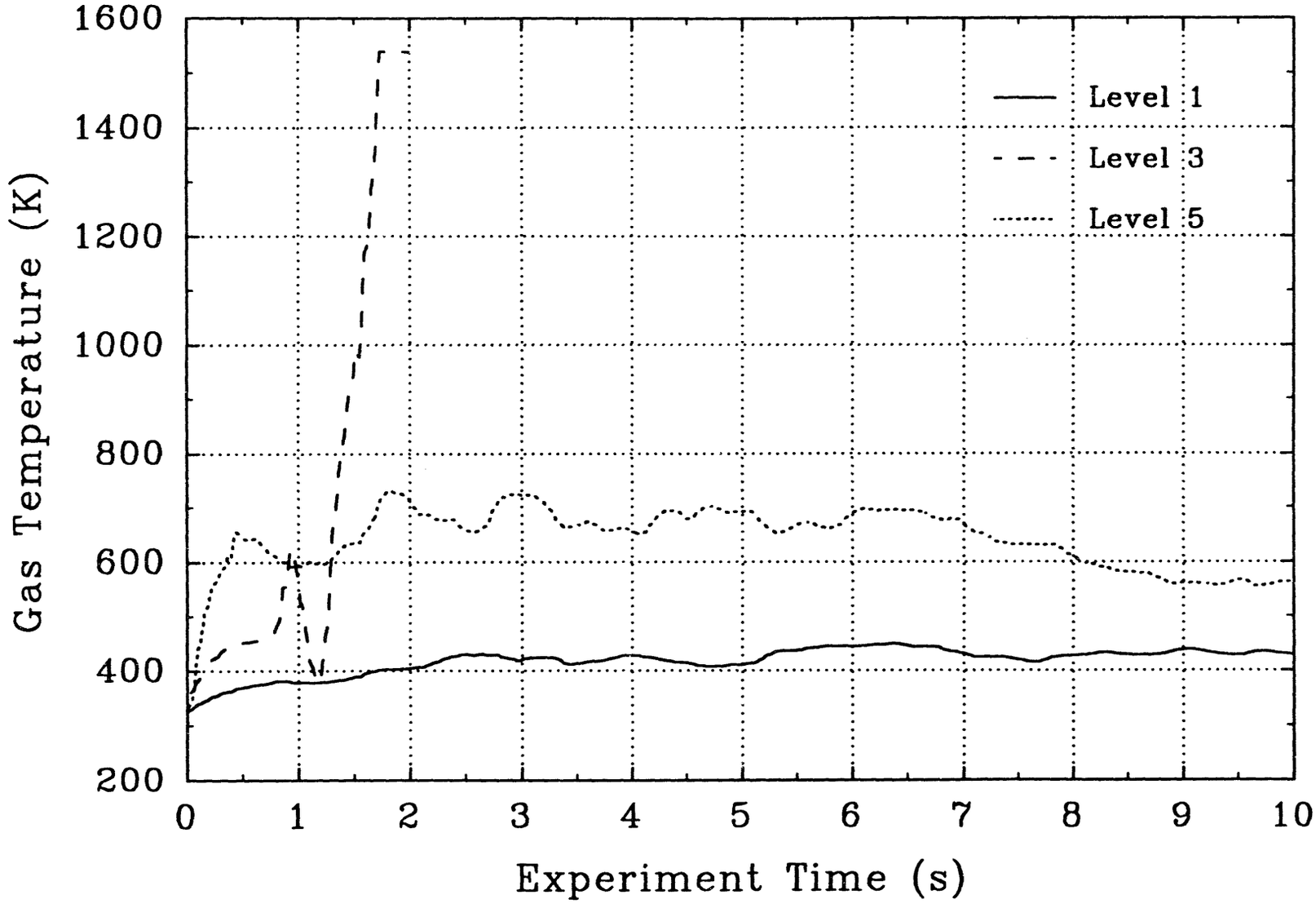

Figure 69. Gas temperatures measured in Surtsey with aspirated thermocouples in the TDS-7 experiment.

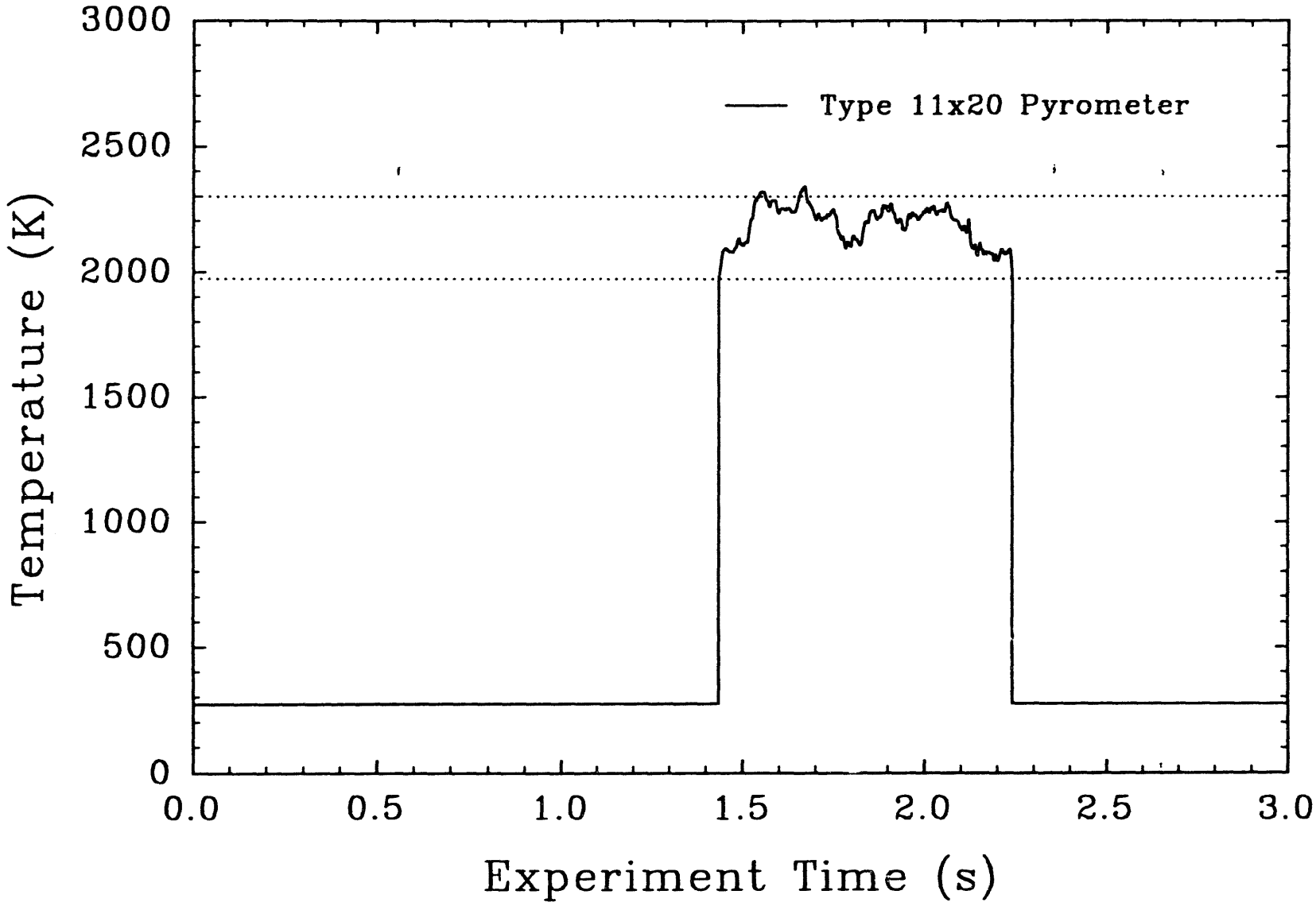

Figure 70. Debris temperature at the chute exit measured with a type 11x20 optical pyrometer in the TDS-1 experiment.

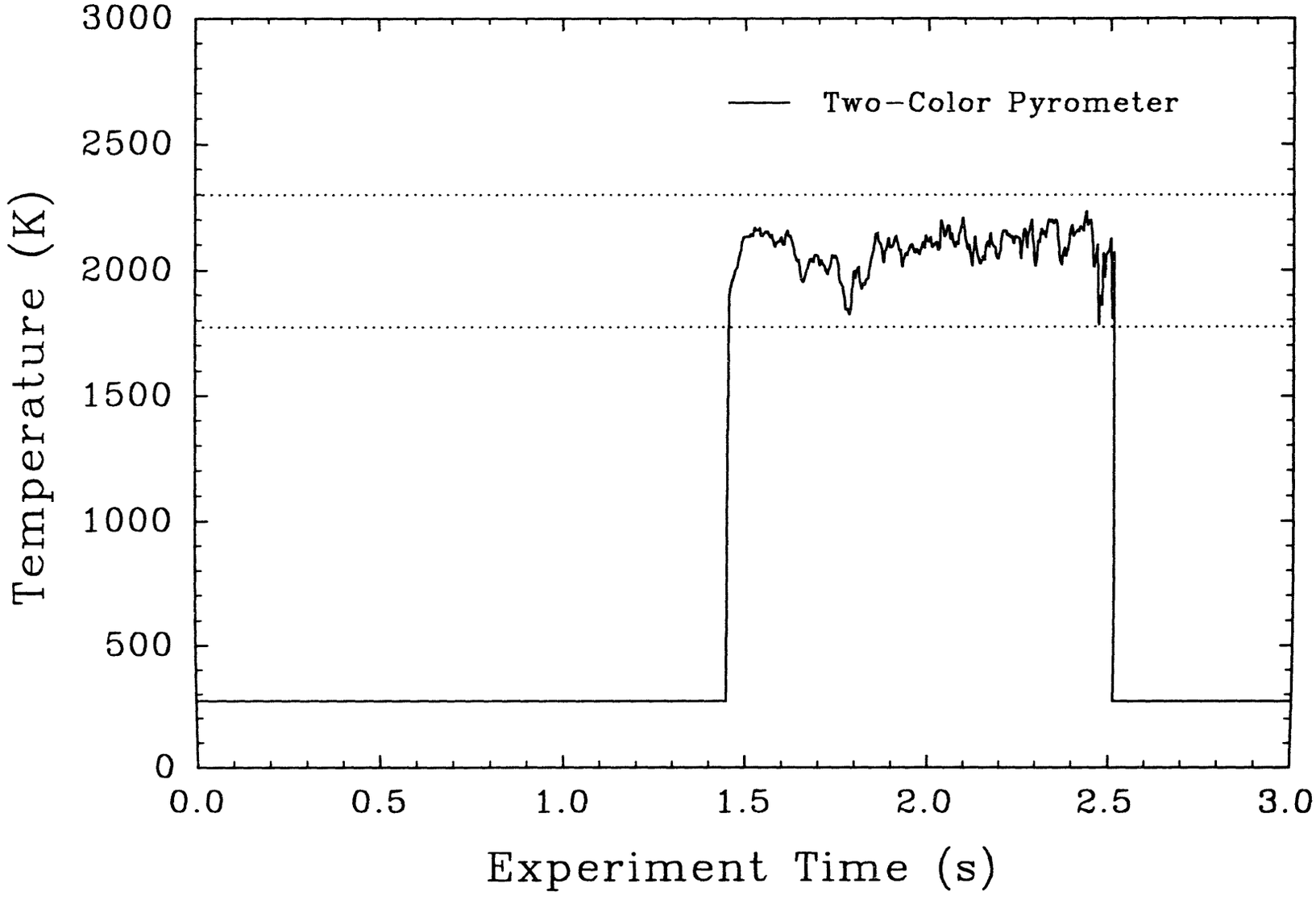

Figure 71. Debris temperature at the chute exit measured with a two-color pyrometer in the TDS-1 experiment.

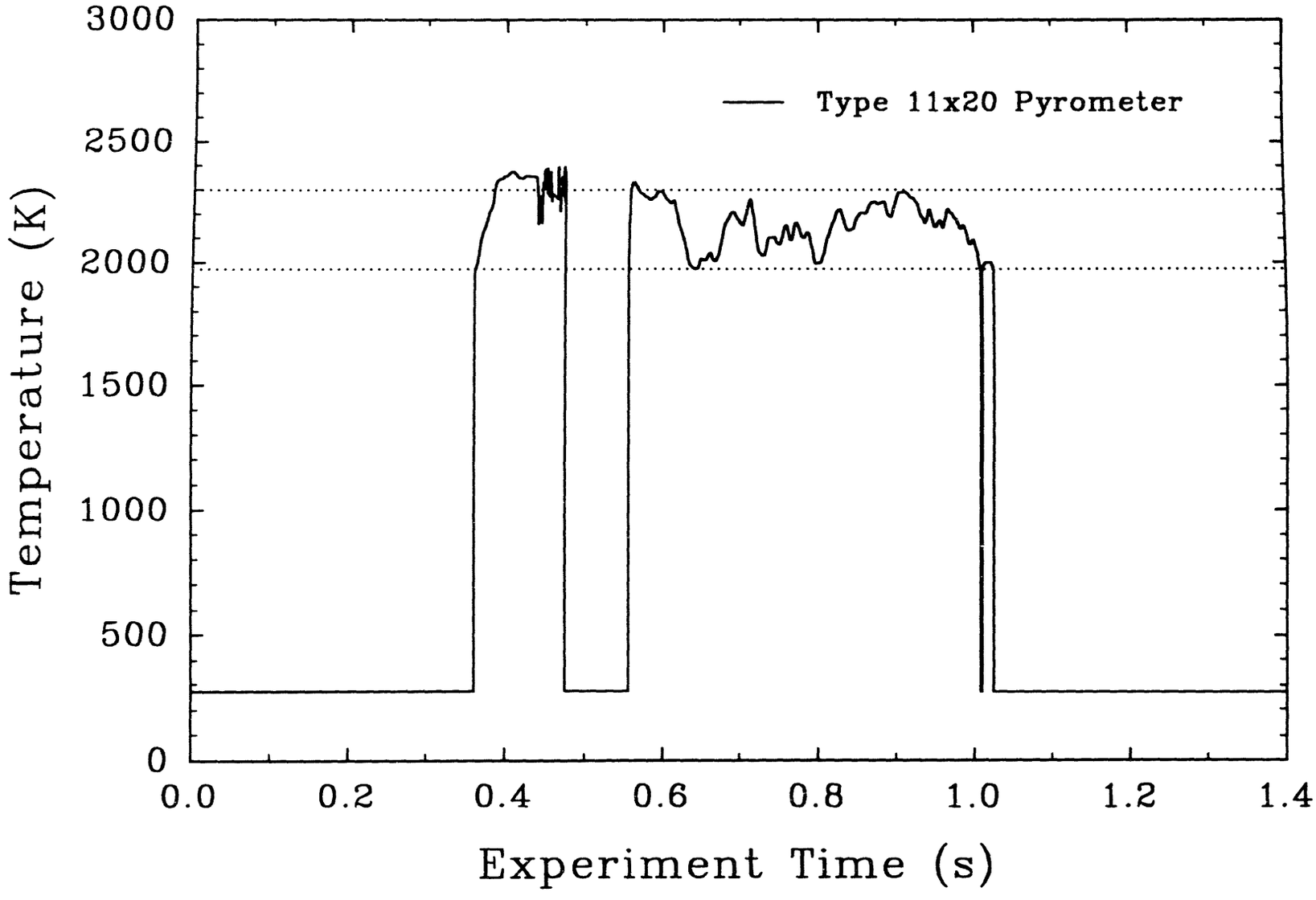

Figure 72. Debris temperature at the chute exit measured with a type 11x20 optical pyrometer in the TDS-2 experiment.

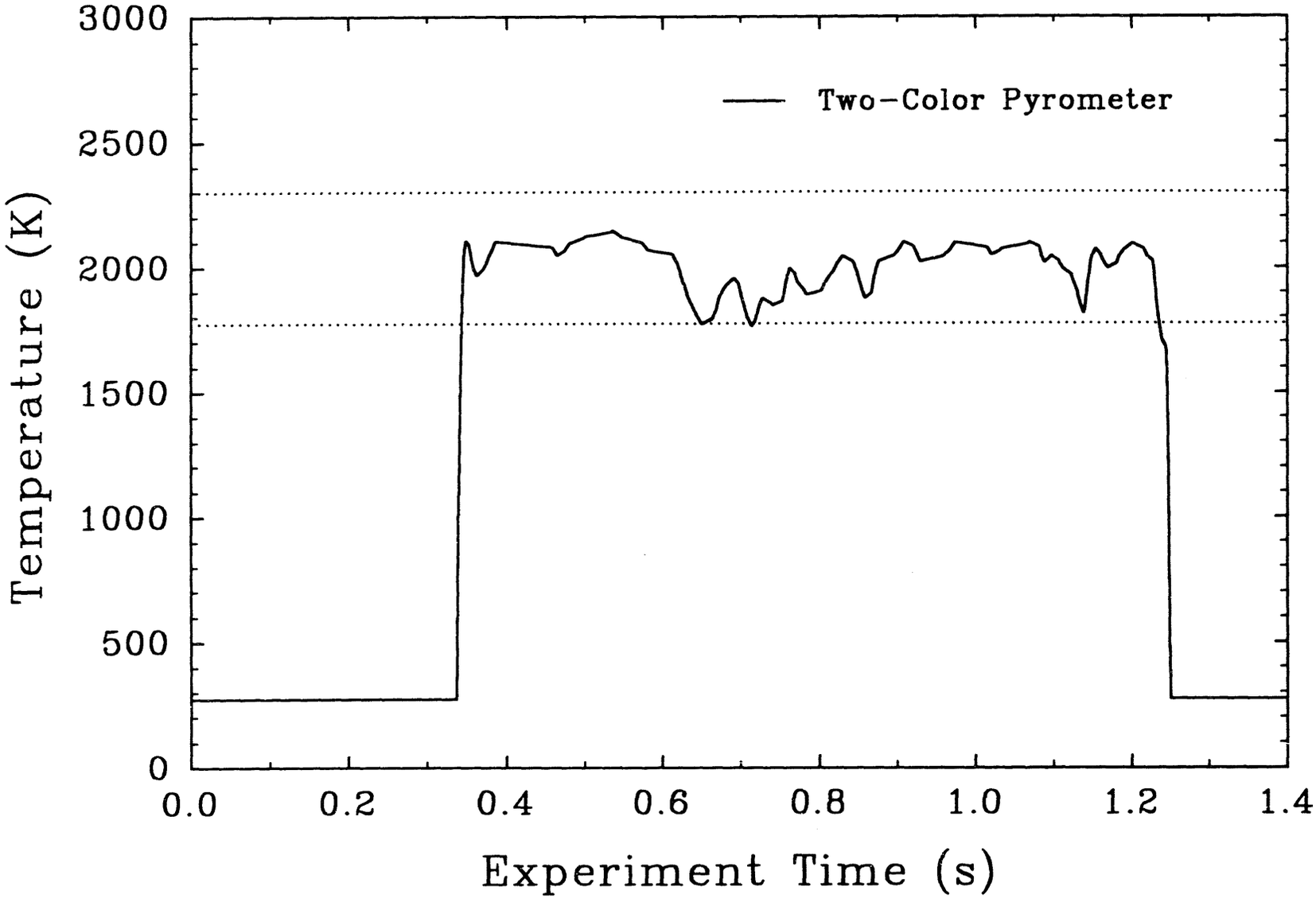

Figure 73. Debris temperature at the chute exit measured with a two-color pyrometer in the TDS-2 experiment.

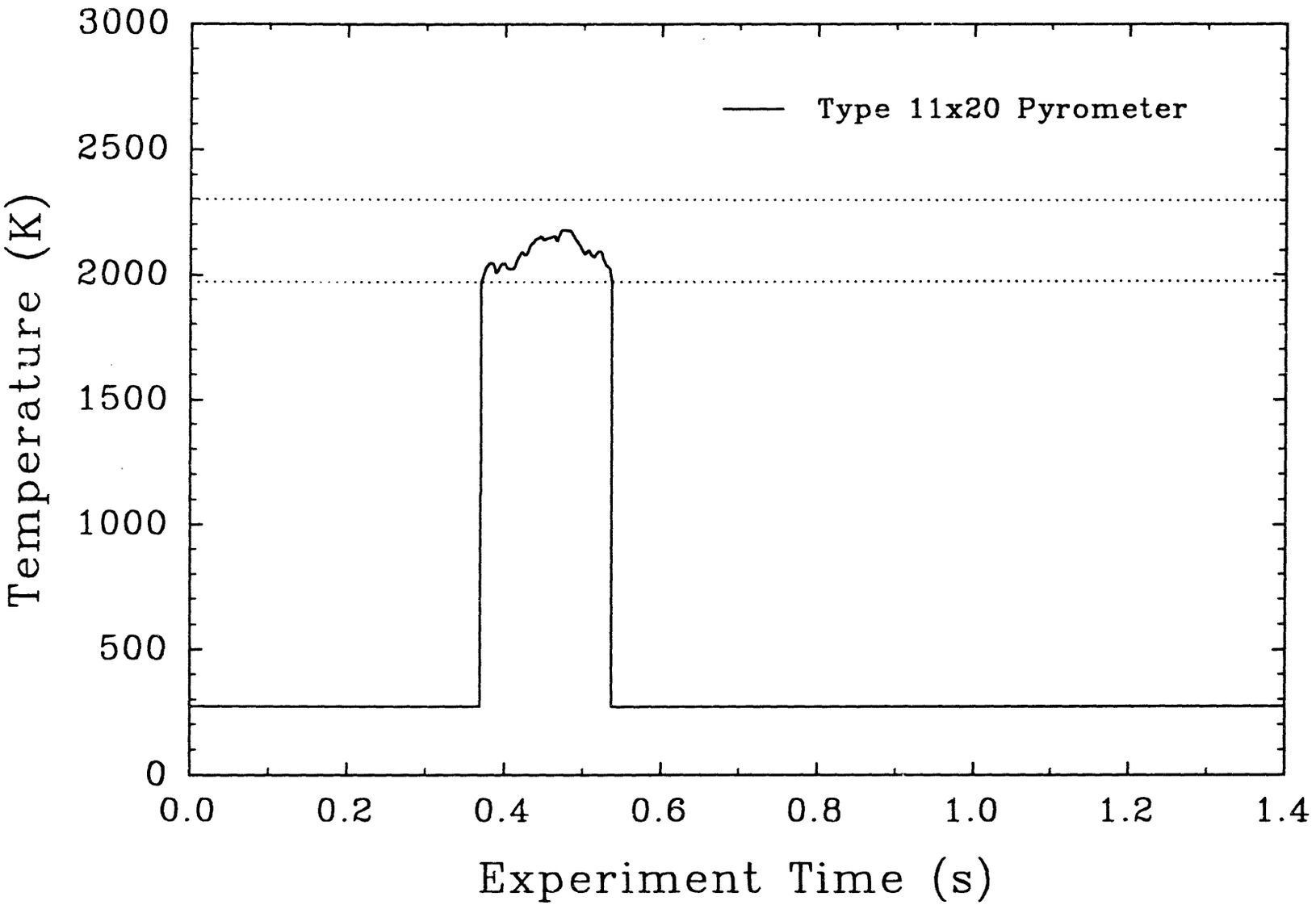

Figure 74. Debris temperature at the chute exit measured with a type 11x20 optical pyrometer in the TDS-3 experiment.

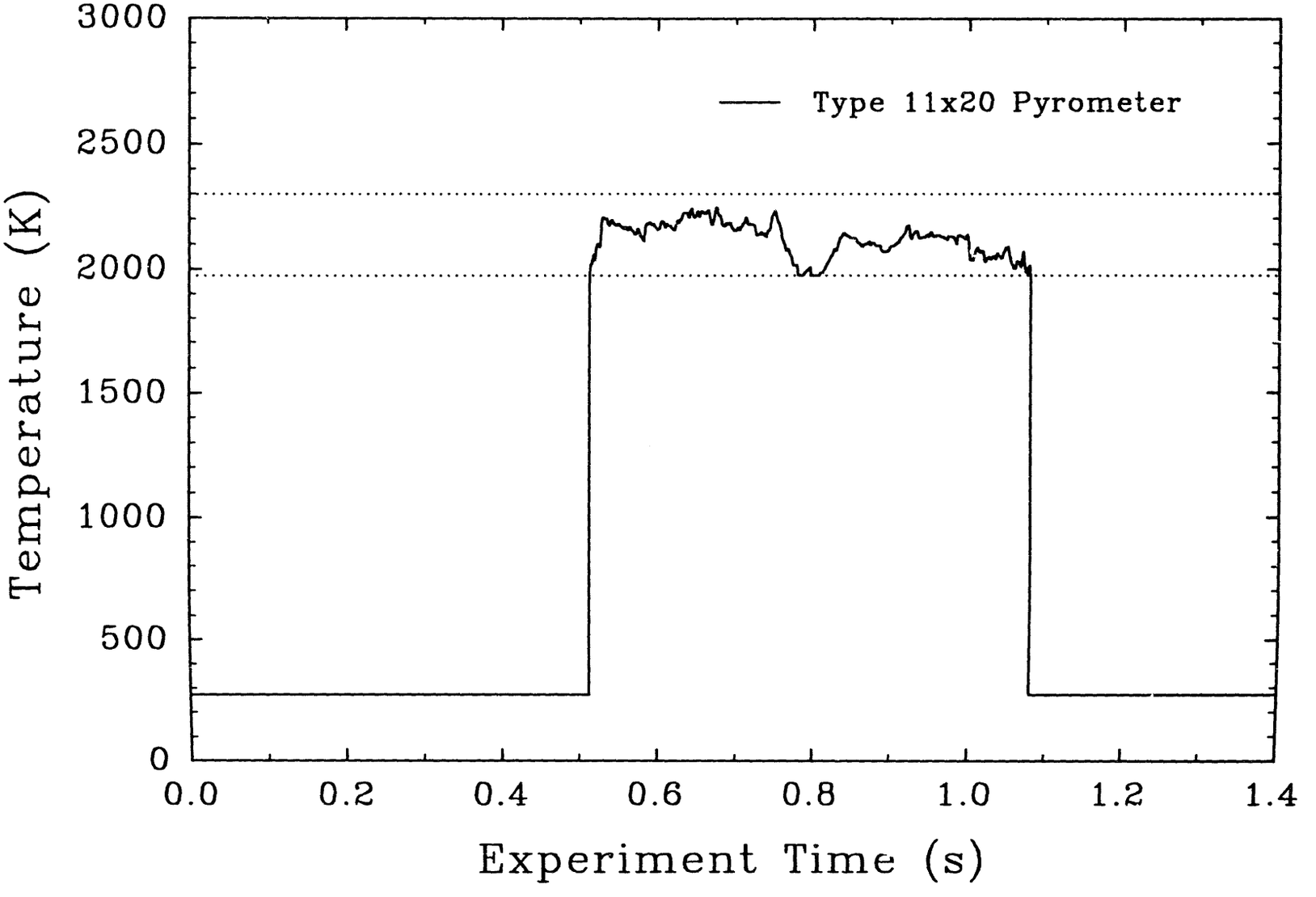

Figure 75. Debris temperature at the chute exit measured with a type 11x20 optical pyrometer in the TDS-4 experiment.

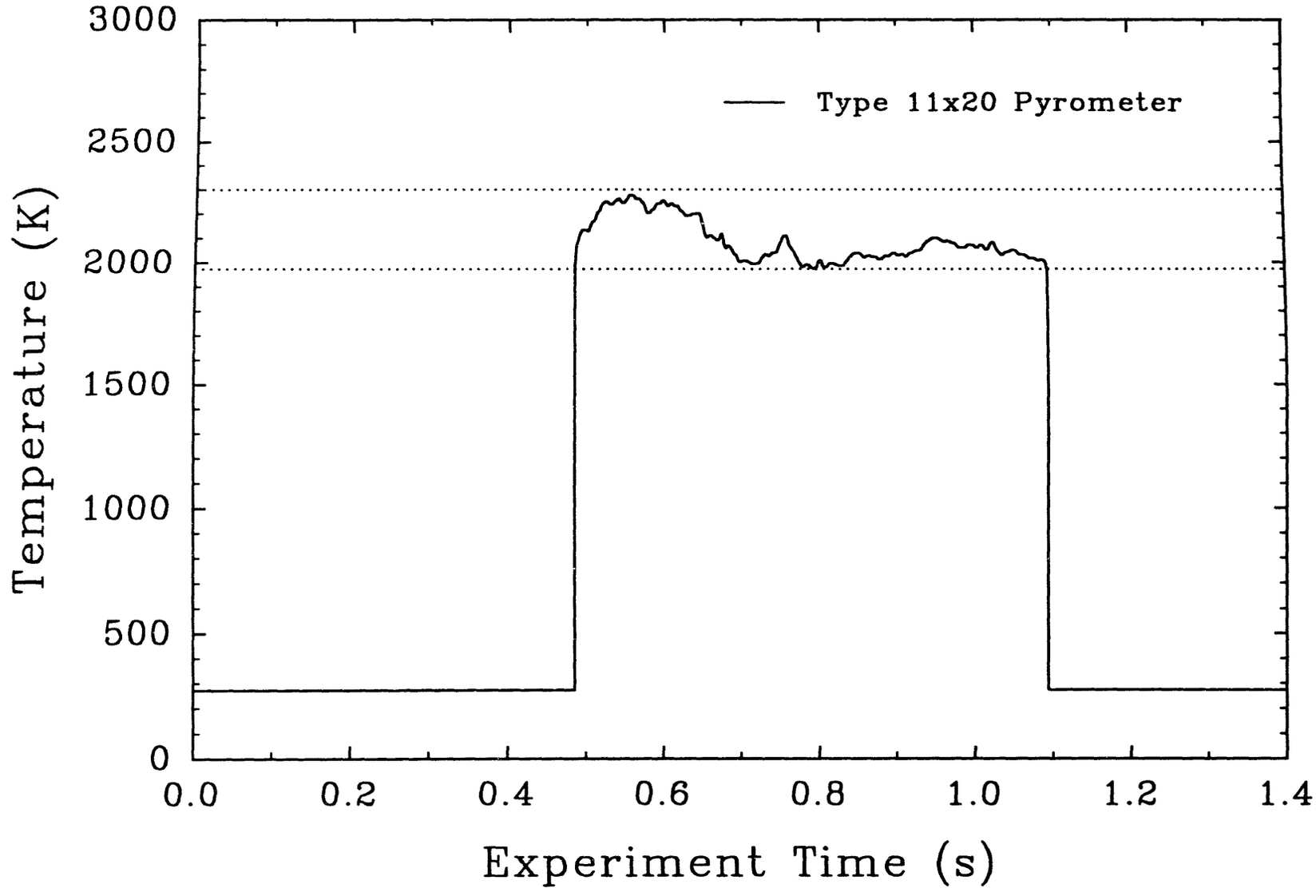

Figure 76. Debris temperature at the chute exit measured with a type 11x20 optical pyrometer in the TDS-5 experiment.

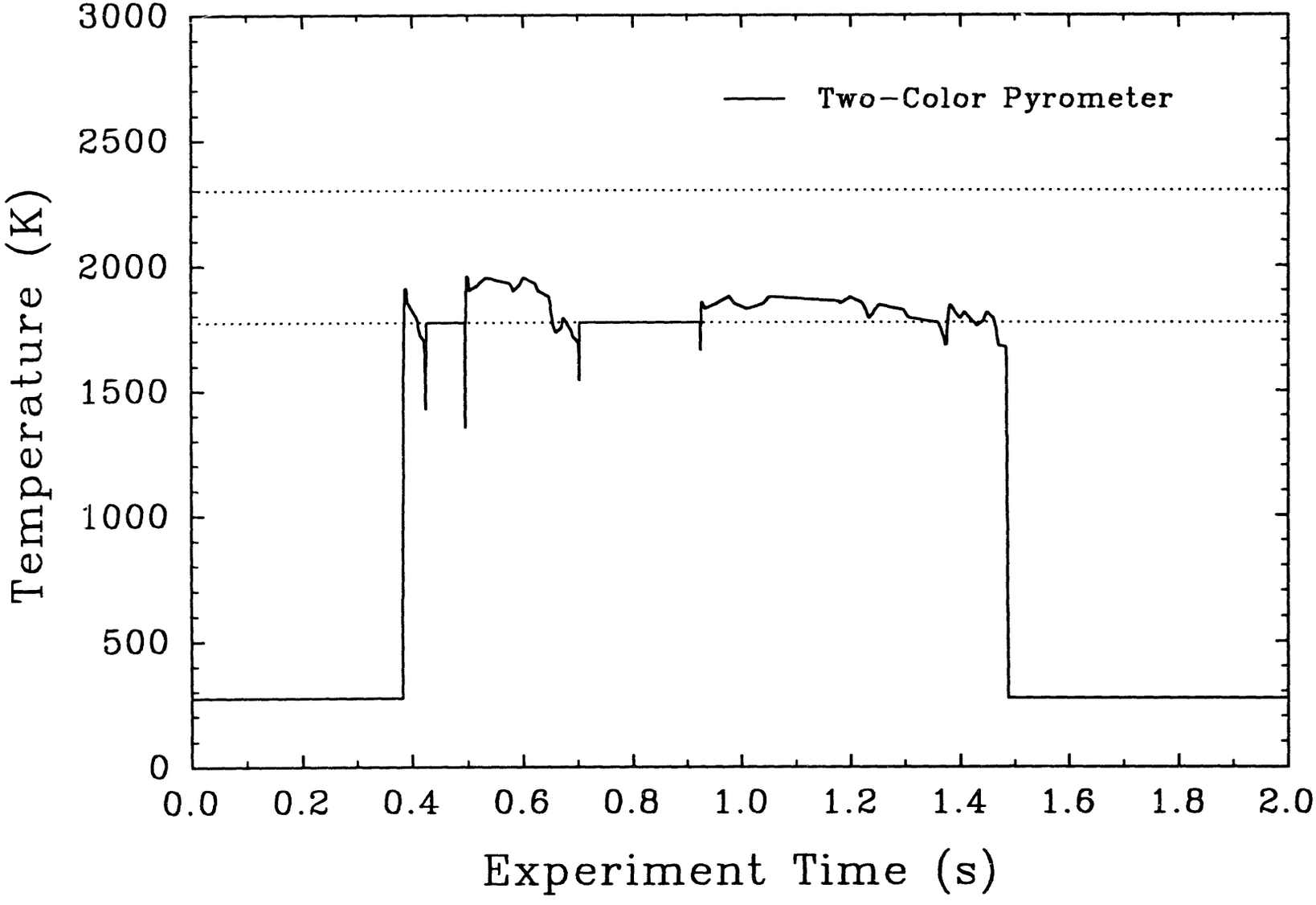

Figure 77. Debris temperature at the chute exit measured with a two-color pyrometer in the TDS-5 experiment.

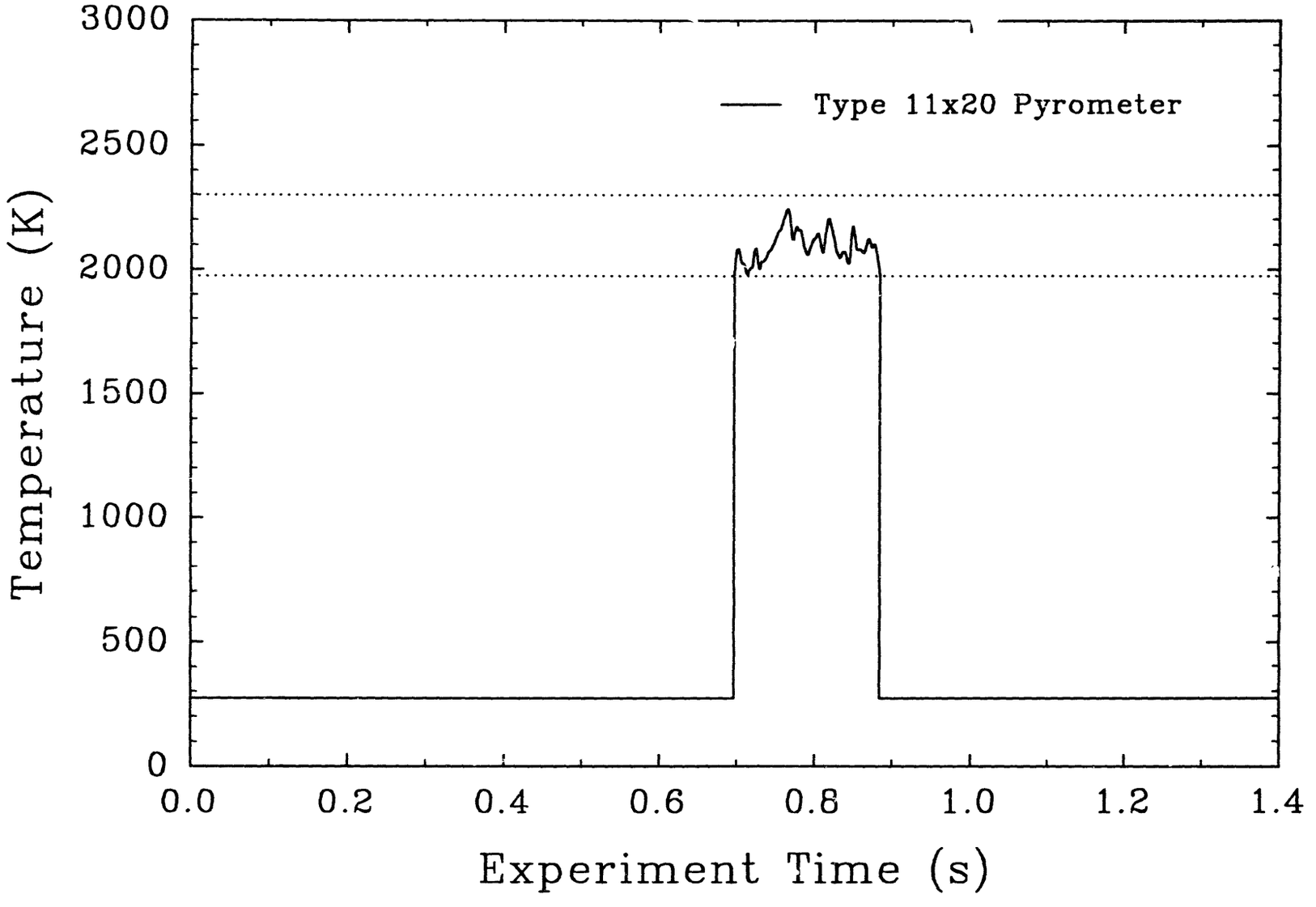

Figure 78. Debris temperature at the chute exit measured with a type 11x20 optical pyrometer in the TDS-6 experiment.

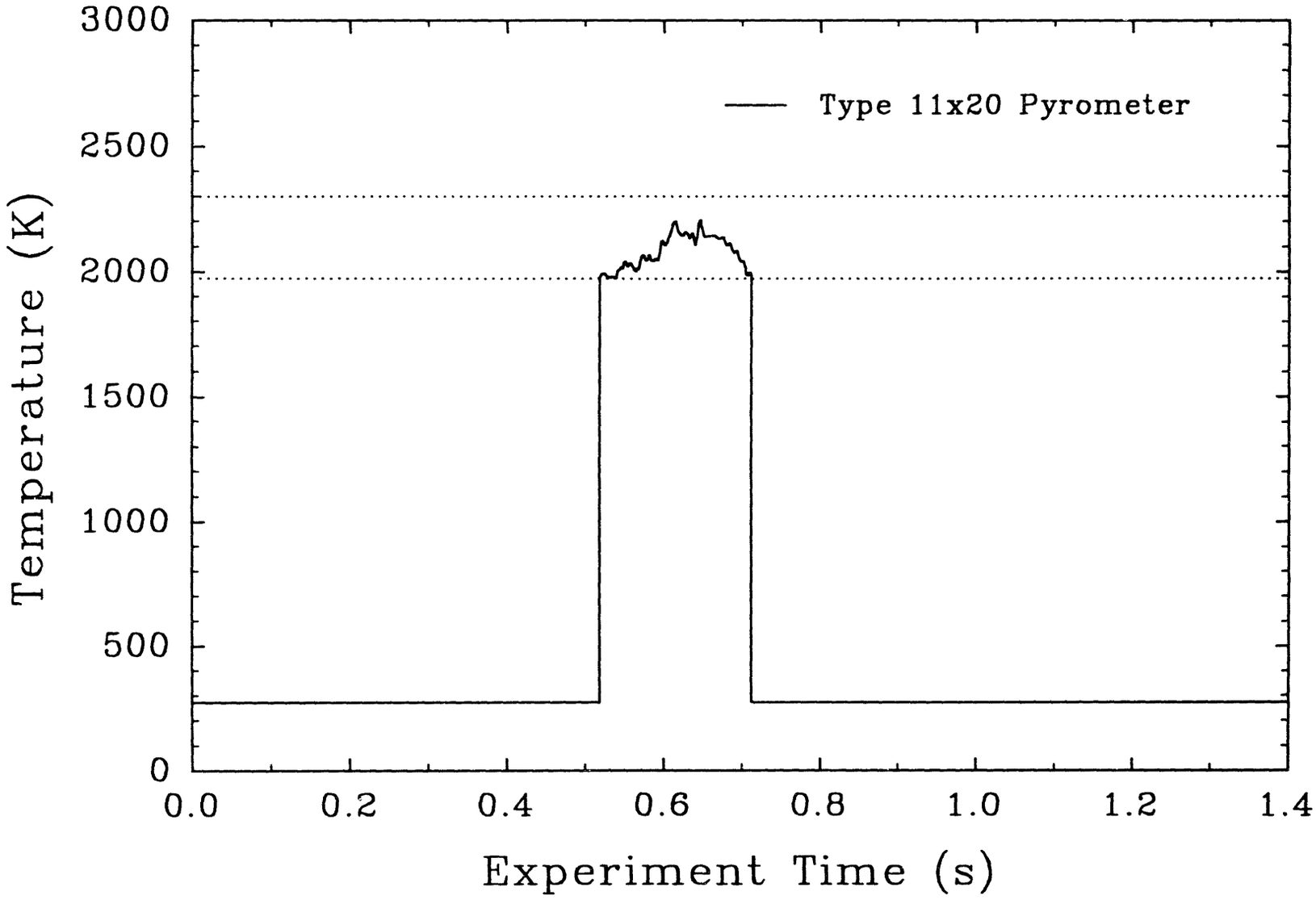

Figure 79. Debris temperature at the chute exit measured with a type 11x20 optical pyrometer in the TDS-7 experiment.

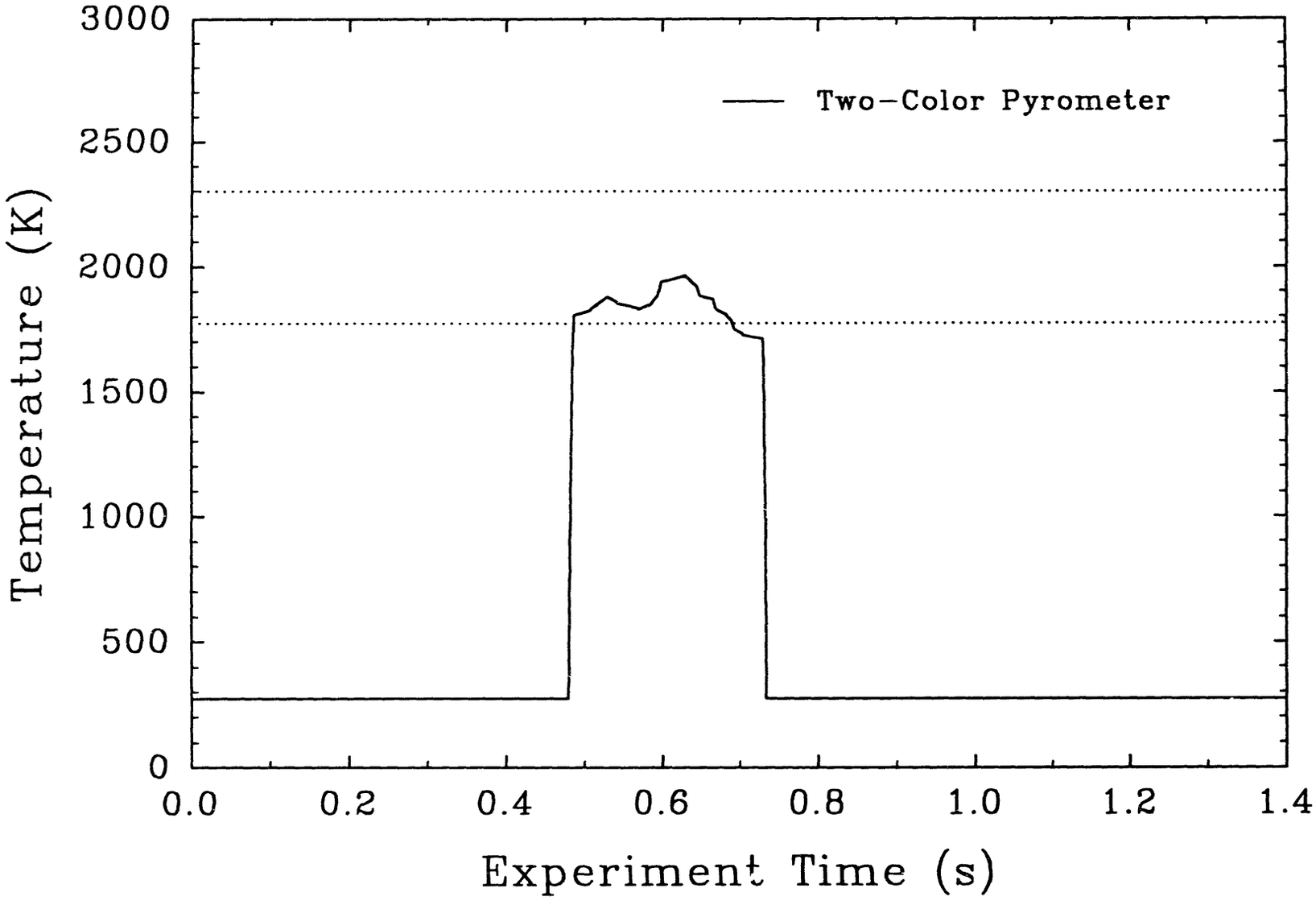

Figure 80. Debris temperature at the chute exit measured with a two-color pyrometer in the TDS-7 experiment.

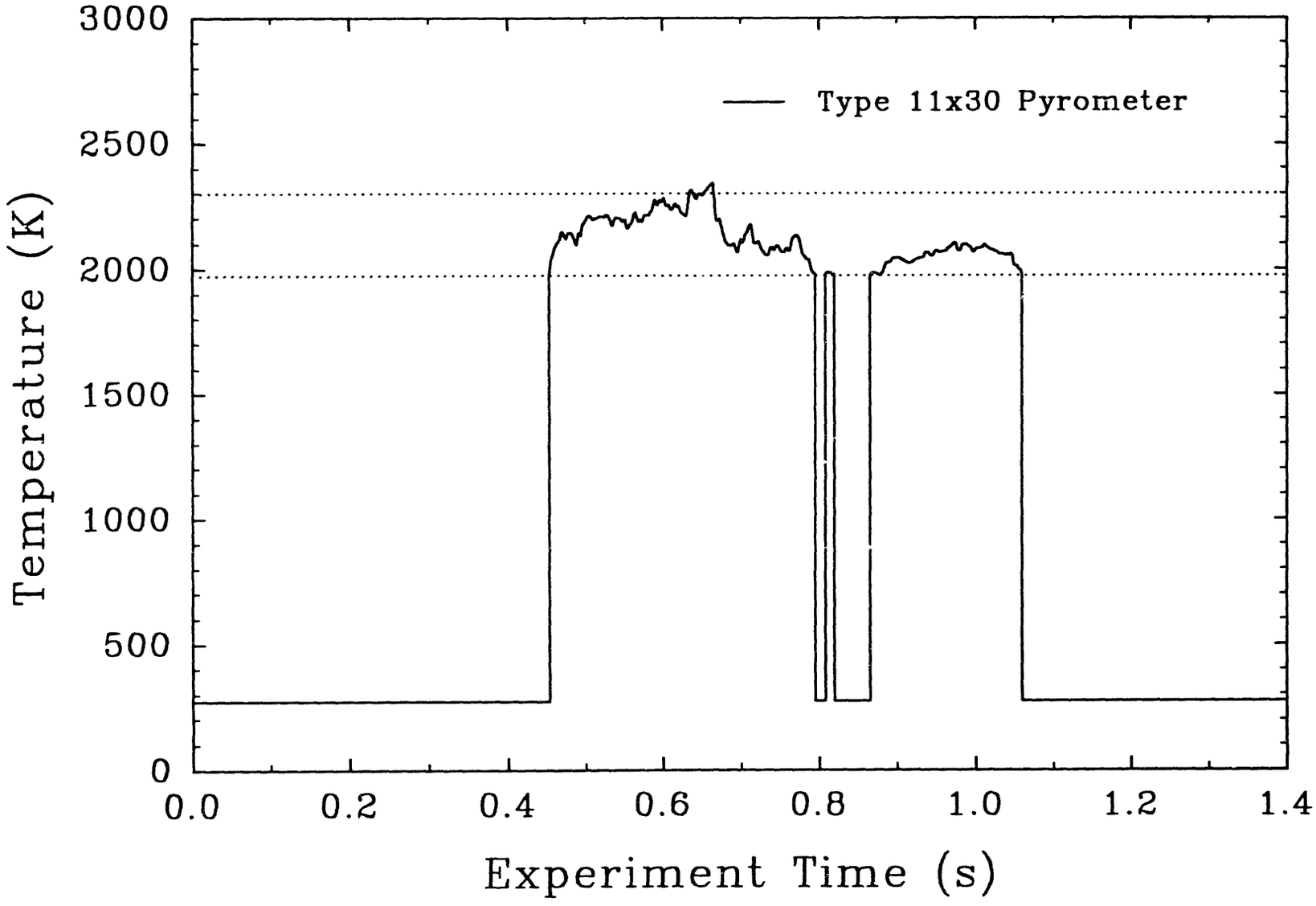

Figure 81. Debris temperature at the chute exit measured with a type 11x30 optical pyrometer in the TDS-7 experiment.

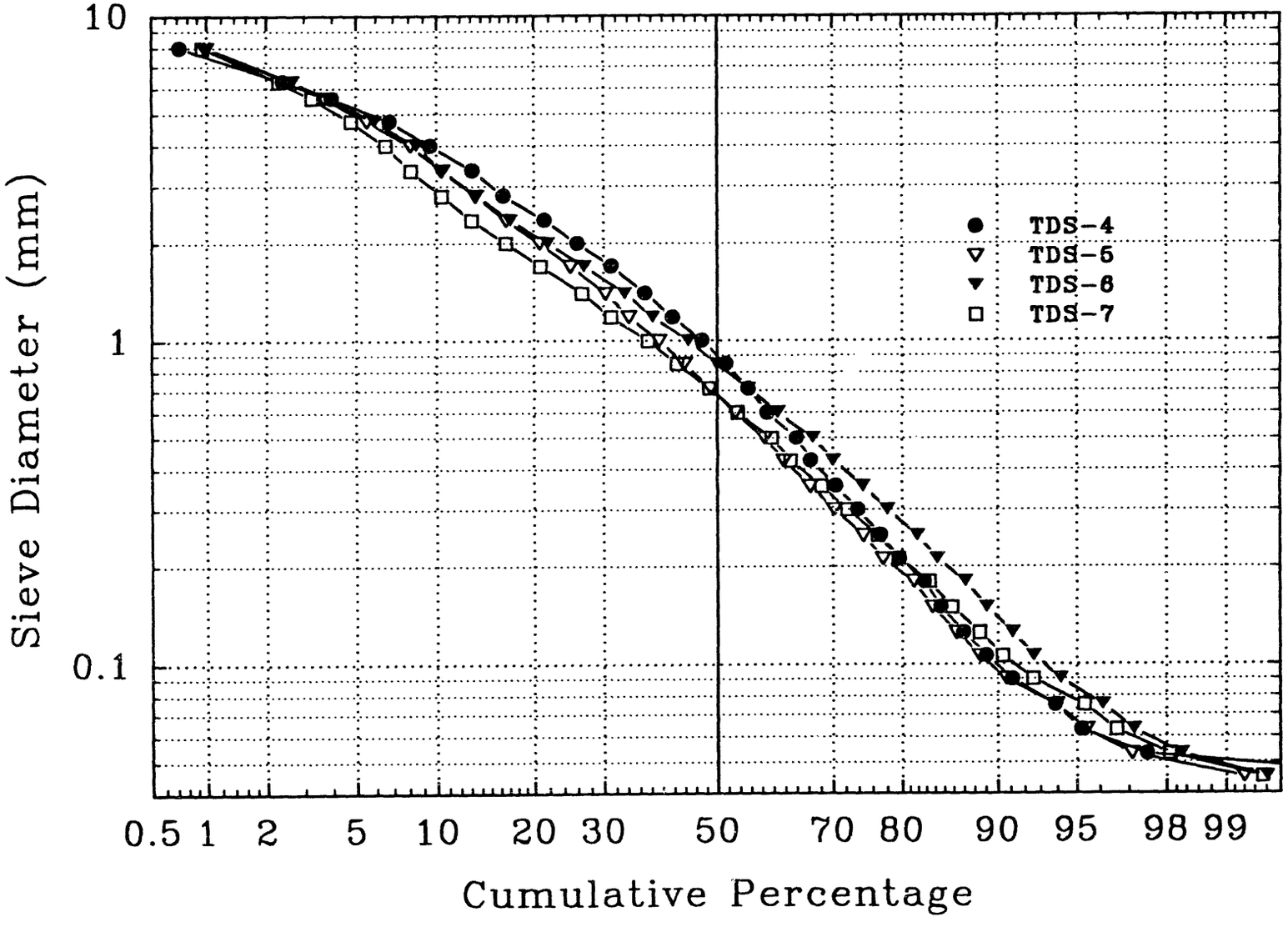

Figure 82. Posttest sieve analysis of debris recovered from the bottom head of the Surtsey vessel in the TDS experiments.

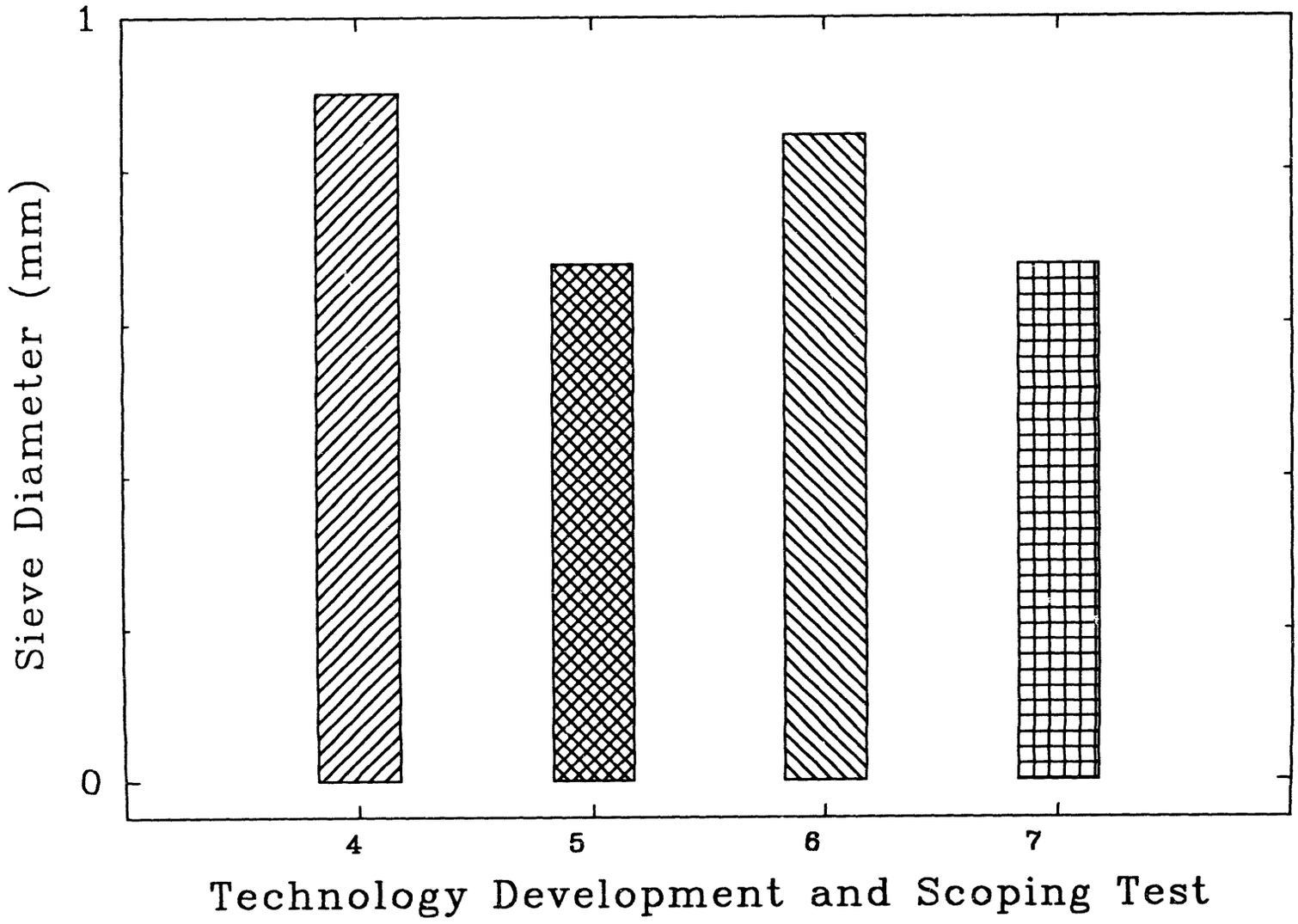

Figure 83. Comparison of the sieve mass median diameter for debris recovered from the bottom head of the Surtsey vessel in the TDS experiments.

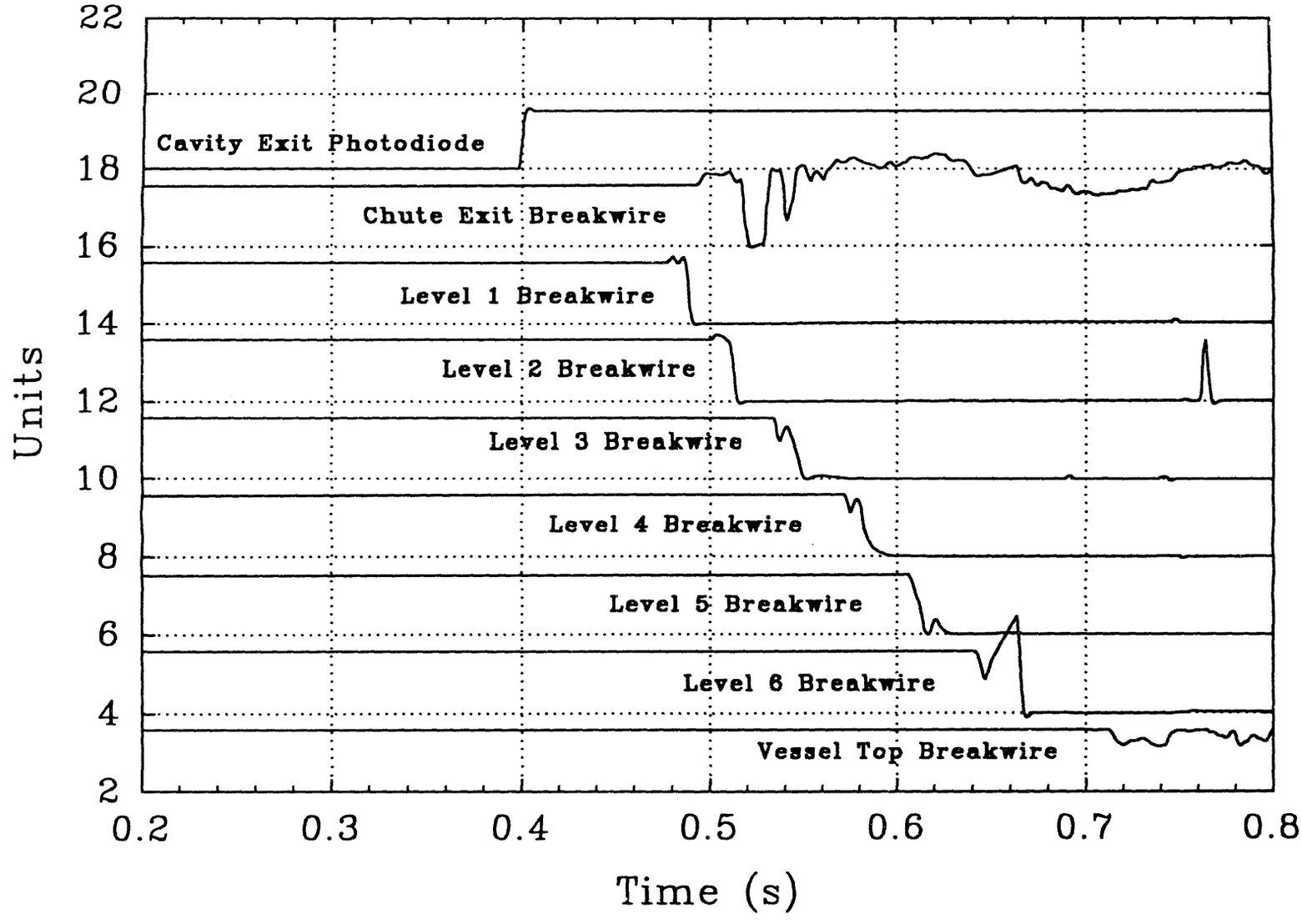

Figure 84. Breakwire signals used to measure debris velocity in the TDS-7 test.

5.0 REFERENCES

Allen, M.D., R.T. Nichols, and M. Pilch, August 1990, A Demonstration Experiment of Steam-Driven, High-Pressure Melt Ejection: The HIPS-10S Test, NUREG/CR-5373, SAND89-1135, Sandia National Laboratories, Albuquerque, NM.

Allen, M.D., et al., 1991a, Test Results on Direct Containment Heating by High-Pressure Melt Ejection into the Surtsey Vessel: The DCH-3 and DCH-4 Experiments, NUREG/CR-5620, SAND90-2138, Sandia National Laboratories, Albuquerque, NM.

Allen, M.D., M. Pilch, R.O. Griffith, D.C. Williams, and R.T. Nichols, 1992c, The Third Integral Effects Test (IET-3) in the Surtsey Test Facility, SAND92-0166, Sandia National Laboratories, Albuquerque, NM.

Allen, M.D., T.K. Blanchat, M. Pilch, and R.T. Nichols, 1992d, The Effects of Condensate Levels of Water on Direct Containment Heating (DCH) in Zion-Like Geometry: The Fourth Integral Effects Test (IET-4) Conducted in the Surtsey Test Facility, SAND92-1241, Sandia National Laboratories, Albuquerque, NM.

Allen, M.D., M. Pilch, R.O. Griffith, R.T. Nichols, and T.K. Blanchat, 1992e, Experiments to Investigate the Effects of 1:10 Scale Zion Structures on Direct Containment Heating (DCH) in the Surtsey Test Facility: The IET-1 and IET-1R Tests, SAND92-0255, Sandia National Laboratories, Albuquerque, NM.

Allen, M.D., T.K. Blanchat, M. Pilch, and R.T. Nichols, 1992f, Experimental Results of an Integral Effects Test in a Zion-Like Geometry to Investigate the Effects of a Classically Inert Atmosphere on Direct Containment Heating: The IET-5 Experiment, SAND92-1623, Sandia National Laboratories, Albuquerque, NM.

Allen, M.D., T.K. Blanchat, M. Pilch, and R.T. Nichols, 1992g, An Integral Effects Test in a Zion-Like Geometry to Investigate the Effects of Preexisting Hydrogen on Direct Containment Heating in the Surtsey Test Facility: The IET-6 Experiment, SAND92-1802, Sandia National Laboratories, Albuquerque, NM.

Allen, M.D., T.K. Blanchat, M. Pilch, and R.T. Nichols, 1992h, An Integral Effects Test to Investigate the Effects of Condensate Levels of Water and Preexisting Hydrogen on Direct Containment Heating in the Surtsey Test Facility: The IET-7 Experiment, SAND92-2021, Sandia National Laboratories, Albuquerque, NM.

Allen, M.D., T.K. Blanchat, M. Pilch, and R.T. Nichols, 1993, Experiments to Investigate the Effects of Fuel/Coolant Interactions on Direct Containment Heating - The IET-8A and IET-8B Experiments, SAND92-2849, Sandia National Laboratories, Albuquerque, NM.

Allen, M.D., M. Pilch, T.K. Blanchat, R.O. Griffith, and R.T. Nichols, 1994, Experiments to Investigate Direct Containment Heating Phenomena with Scaled Models of the Zion Nuclear Power Plant in the Surtsey Test Facility, NUREG/CR-6044, SAND93-1049, Sandia National Laboratories, Albuquerque, NM.

Blanchat, T.K., M.D. Allen, M. Pilch, and R.T. Nichols, 1994, Experiments to Investigate Direct Containment Heating Phenomena with Scaled Models of the Surry Nuclear Power Plant, NUREG/CR-6152, SAND93-2519, Sandia National Laboratories, Albuquerque, NM.

Bogolyubov, V.A., 1980, Temperature of an Aluminothermic Process as a Function of Heat Evolved per Kilogram, SAND80-6013, Sandia National Laboratories, Albuquerque, NM, translated from Stal 17, 1957, pp. 531-535.

DISTRIBUTION

U. S. Nuclear Regulatory Commission (4)
Office of Nuclear Regulatory Research
Attn: C. Tinkler, T-10-K-8
R. Lee, T-10-K-8
F. Eltawila, T-10-K-8
W. Hodges, T-10-E-37
Washington, D.C. 20555-0001

Argonne National Laboratory (2)
Attn: J. Binder
B. Spencer
9700 S. Cass Avenue
Argonne, IL 60439

Fauske and Associates, Inc.
Attn: R. Henry
16W070 West 83rd Street
Burr Ridge, IL 60952

Theo Theofanous
University of California
Department of Chemical &
Nuclear Engineering
Santa Barbara, CA 93106

F. J. Moody
G.E. Nuclear Energy
175 Curtner Ave.
San Jose, CA 95125

Mamoru Ishii
Purdue University
Department of Nuclear Engineering
West Lafayette, IN 47907

University of Wisconsin
Nuclear Engineering Department
Attn: M. L. Corradini
1500 Johnson Drive
Madison, WI 53706

SANDIA DISTRIBUTION:
MS0338 D. W. Schaeffer (1703)
MS0736 N. R. Ortiz (6400)
MS0744 D. A. Powers (6404)
MS0748 F. T. Harper (6413)
MS0742 J. E. Kelly (6414)
MS0745 S. L. Thompson (6418)
MS0745 R. M. Summers (6418)
MS1137 M. D. Allen (5) (6422)
MS1137 T. K. Blanchat (5) (6422)
MS1137 M. Pilch (2) (6422)
MS1139 K. O. Reil (6423)
MS0739 R. O. Griffith (6429)
MS0739 D. C. Williams (6429)
MS0899 Technical Library (5) (7141)
MS0619 Technical Publications (7151)
MS0100 Document Processing (7613-2)
for DOE-OSTI (10)
MS9018 Central Technical Files
(8523-2)

DATE
FILMED
10/18/94
END